UNIVERSITA' DEGLI STUDI DI NAPOLI FEDERICO II

DOTTORATO DI RICERCA

IN

BIOLOGIA, PATOLOGIA E IGIENE AMBIENTALE IN MEDICINA VETERINARIA

XVIII CICLO

ANNO ACC. 2002/2003-2004/2005

TESI DI DOTTORATO

MODULATION OF THE INNATE IMMUNE RESPONSE BY *YERSINIA ENTEROCOLITICA* UPON SYSTEMIC INFECTION

"MODULAZIONE DELLA RISPOSTA IMMUNITARIA INNATA NELL'INFEZIONE DA *YERSINIA ENTEROCOLITICA*"

IL COORDINATORE
PROF. G. PAINO

IL TUTOR
PROF. A. FIORETTI

IL CANDIDATO
DOTT. GIANLUCA MATTEOLI

Table of contents

1 Introduction

1.1 Infection and Immunity

Host defence against pathogens is based on the non-specific or innate immune system and the specific or adaptive immune system. The innate immune system is also the first line of defence against a pathogen because it is permanent present. Components of the non-specific defence are skin, epithelial cells, phagocytic cells, and complement. The second line of defence is specific for a particular type of bacterium or virus and is thus called specific immune system.

1.2 Innate immune system

1.2.1 Pattern recognition receptors

The innate immune system uses a variety of pattern recognition receptors (PRRs) that can be expressed on the cell surface, in intracellular compartments, or secreted into the bloodstream and tissue fluids (125). The principal function of PRRs is to detect a limited set of conserved molecular patterns (pathogen-associated molecular patterns, PAMPs) that are unique to microbes and to signal the host the presence of infection. The PRRs include the acute phase proteins mannan-binding lectins, C-reactive protein, and serum amyloid protein as secreted pattern recognition molecules. The macrophage mannose receptor, the macrophage scavenger receptor and MARCO belong to the PRRs expressed on the cell surface.

The Toll-like receptor (TLR) family is the best-characterized class of PRRs in mammalian cells. TLRs detect multiple PAMPs (202), including lipopolysaccharide (LPS) (detected by TLR4), bacterial lipoproteins and lipoteichoic acids (detected by TLR2), flagellin (detected by TLR5), the unmethylated CpG DNA of bacteria and viruses (detected by TLR9), double

stranded RNA (detected by TLR3) and single-stranded viral RNA (detected by TLR7) (80). TLRs 1, 2, 4, 5, 6 are expressed on the cell surface and are specialised to recognize mainly bacterial products. In contrast TLRs 3, 7, 8 and 9 are localized in intracellular compartments (80,120) and detect viral nucleic acids in late endosomes and lysosomes (58,113).

All PRRs sense microbial infection and trigger a multitude of antimicrobial and inflammatory responses like opsonization, activation of complement, phagocytosis, activation of proinflammatory signalling pathways, and induction of apoptosis.

1.2.2 Complement

The complement system is a set of plasma proteins that act together to attack extracellular pathogens. Complement can be activated spontaneously by certain pathogens or by antibody binding to the pathogen. The pathogen becomes coated with complement proteins that facilitate pathogen removal by phagocytes and can also kill the pathogen directly (92).

1.2.3 Inflammatory cytokines

One important function of the innate immune response is the recruitment of phagocytic cells and thereby effector molecules to the site of infection by the release of a number of cytokines and other inflammatory mediators. The cytokines secreted by phagocytes are a structurally diverse group of molecules including interleukin-1 (IL-1), IL-6, IL-8, IL-12, and tumor necrosis factor-α (TNF-α). IL-1 activates vascular endothelium and lymphocytes. IL-6 induces fever and the production of acute-phase proteins (serum amyloid protein, C-reactive protein, fibrinogen, mannan-binding lectin) in the liver. IL-8 is a CXC chemokine involved in neutrophil recruitment and activation. IL-12 activates NK cells and induces the differentiation of CD4 T cells into Th1 cells. TNF-α activates vascular endothelium and increases vascular permeability, which leads to increased entry of IgG, complement, and cells to tissues and increased fluid drainage to lymph nodes.

Cells infected with viruses produce interferons. These slow down viral replication and enhance the presentation of viral peptides to cytotoxic T cells as well as activating NK cells, which can distinguish between infected and uninfected host cells.

1.2.4 Cells of the innate immune system

Host defence against microbial pathogens relies on a concerted action of both antigen-non-specific innate immunity and antigen-specific adaptive immunity (64,84,125). Key features of the innate immune system include the ability to rapidly recognize pathogens and/or tissue injury and the ability to signal the presence of danger to cells of the adaptive immune system (121). The innate immune system comprises phagocytic cells, natural killer (NK) cells, complement and interferons (IFN). Cells of the innate immune system use a variety of receptors to recognize patterns shared between pathogens, e.g. bacterial LPS, carbohydrates, and double-stranded viral RNA (2,32,134). Evolutionary pressure has led to the development of adaptive immunity, the key features of which are the ability to rearrange genes of the immunoglobulin family, permitting creation of a large diversity of antigen-specific clones and immunological memory. However, this highly sophisticated and potent system needs to be instructed and regulated by antigen presenting cells (APCs).

1.2.4.1 Macrophages and monocytes

Originally, monocytes and macrophages were classified as cells of the reticulo-endothelial system - RES (Aschoff, 1924). Van Furth et al. (1972) proposed the mononuclear phagocyte system - MPS, and monocytes and macrophages became basic cell types of this system. Their development takes in the bone marrow and passes through the following steps: stem cell - committed stem cell - monoblast - promonocyte - monocyte (bone marrow) - monocyte (peripheral blood) - macrophage (tissues). Monocyte differention in the bone marrow proceeds rapidly (1.5 to 3 days). During differentiation, granules are formed in monocyte cytoplasma and these can be divided as in neutrophils into at least two types. However, they are fewer and smaller than their neutrophil counterparts (azurophil and specific granules).

The blood monocytes are young cells that already possess migratory, chemotactic, pinocytic and phagocytic activities, as well as receptors for IgG Fc-domains (FcγR) and iC3b complement. Under migration into tissues, monocytes undergo further differentiation to become multifunctional tissue macrophages. Monocytes are generally, therefore, considered to be immature macrophages. However, it can be argued that monocytes

represent the circulating macrophage population and should be considered fully functional for their location, changing phenotype in response to factors encountered in specific tissue after migration.

Tissue macrophages includes macrophages in connective tissue (histiocytes), liver (Kupffer's cells), lung (alveolar macrophages), lymph nodes, spleen, bone marrow, serous fluids (pleural and peritoneal macrophages), skin (histiocytes, Langerhans's cell) and in other tissues. This wide tissue distribution makes these cells well suited to provide an immediate defence against foreign elements prior to leukocyte immigration. Because macrophages participate in both adaptative immunity via antigen presentation and innate immunity against bacterial, viral, fungal, and neoplastic pathogens, it is not surprising that macrophages display a range of functional and morphological phenotypes.

Heterogeneity and activation of macrophages

Macrophage heterogeneity is a well-documented phenomenon. It has also long been recognized that macrophages isolated from different anatomical sites display a diversity of phenotypes and capabilities. Because macrophage function is dependent in part on signals received from the immediate microenvironment, it is suggested that macrophage heterogeneity may arise from unique conditions within specific tissues.

The production of functionally distinct macrophage populations gives the innate immune system added flexibility to respond to different immunological or inflammatory stimuli.

Furthermore, it has been recognized that cells belonging to the myelomonocytic differentiation pathway including macrophages and dendritic cells, have a key role in polarized innate and adaptative responses. They act by promoting the orientation of adaptive responses in a type I or type II direction, as well as by expressing specialized and polarized effector functions.

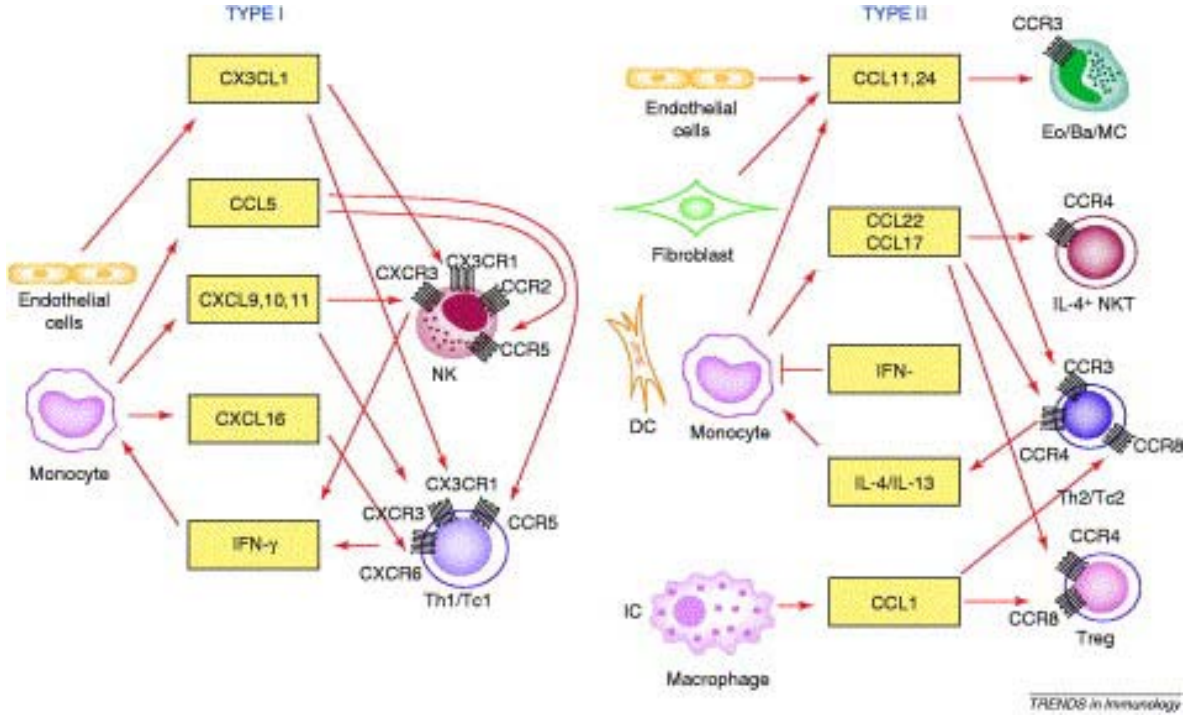

Figure 1.1 Chemokines in polarized T-cell responses (from A. Mantovani, 2004). During type I and type II immune responses, master cytokines regulate chemokine production by stromal and inflammatory cells. Chemokines then support selective recruitment of polarized T cells and specific type I and type II effector cells expressing distinct panels of chemokines receptors. Polarized type I and type II T cells express differential chemokine receptors. Typically, the CC chemokine receptors CCR3, CCR4 and CCR8 have been associated with a type II phenotype, whereas functional CXCR3 and CCR5 are preferentially expressed on polarized type I T cells. CCR3 ligands also attract eosinophils andbasophils, crucial for polarized type II responses. Although differentially expressed, chemokine receptors are not markers for polarized T cells, in that there is no absolute association between chemokine receptor expression and cytokine repertoire of polarized T-cell populations. For instance, CCR4, expressed at much higher levels in polarized type II cells, is also expressed in non-polarized T-cell populations, and it is induced in type I cells following activation.

For this evidences different authors have used a novel nomenclature M1/M2 that has the obvious advantage of reflecting the Th1/Th2 dichotomy.

The M1 phenotype, acquired after the exposition to the classic activation signals like IFN-γ and LPS, is characterized by: high capacity to present antigen, high IL-12 and IL-23 production, high production of toxic intermediates (nitrix oxide, reactive oxygen intermediates) and consequent activation of a polarized type I response.

Instead the M2 phenotype, also indicating as "alternatively activated macrophages", is acquired after the exposition to IL-10, IL-4 and IL-13 or to factors like the immunocomplex and LPS. M2 cells are generally characterized by low production of proinflammatory cytokines (IL-12, IL-1, TNF and IL-6) and high production of IL-10.

With this general caveat, available information suggests that classically activated M1 macrophages are potent effector cells integrated in Th1 responses, which kill

microorganisms and tumor cells and produce copious amounts of proinflammatory cytokines. By contrast, M2 macrophages tune inflammatory responses and adaptive type II immunity, scavenge debris and promote angiogenesis, tissue remodeling and repair. Integration with, and promotion of, type II responses prevail for IL-4- or IL-13-stimulated M2 macrophages, whereas suppression and regulation of inflammation and immunity are predominant in IL-10-stimulated M2 cells.

Therefore, it is probable that the nature of an immune response is dictated in large part by the functional phenotype(s) of the macrophages present within the lesion.

In addition, the orchestration and regulation of cytokine production during inflammatory responses constitute a key determinant of both the resolution of challenge and the limitation of host tissue damage. Hence, the sequential appearance within inflammatory lesions may allow the most appropriate response at a given stage of an immune response. Analysis of temporal production of cytokines during immune responses suggests that different macrophage populations participate at various stages, or that the changing conditions within the lesion differentially affect the functions of distinct macrophage populations.

Biological functions of macrophages

Macrophages are involved at all stages of the immune response. First, as already outlined, they act as rapid protective mechanism which can respond before T cell-mediated amplification has taken place. Activated macrophages play a key role in host defence against intracellular parasitic bacteria, pathogenic protozoa, fungi and helminths as well as against tumours, especially metastasing tumours. After phagocytosis, macrophages prevent intracellularly parasitic organisms from replication at least by three ways:

1. Intracellular environment is unsuitable for microbial reproduction due to low pH and lack of nutrients in a phagolysosome.
2. The toxic reaction may be activated to against dividing organisms. This include ROI, hypochlorite, NO, myeloperoxidase, neutral proteases and lysosomal hydrolases.
3. Macrophages may also produce microbiostatic effector molecules at a steady-state and thus maintain intracellular microorganisms in the non-replicating state. This latent infection is generally observed only in such individuals whose macrophages

cannot be sufficiently activated. Generally, macrophages represent the second line of defence against different agent including pathogenic microorganisms.

In addition, macrophages are important killer cells ; by means of antibody-dependent cell-mediated cytotoxicity (ADCC) they are able to kill or damage extracellular targets. They also take part in the initiation of T cell activation by processing and presenting antigen. Finally they are central effector and regulatory cells of the inflammatory response.

1.2.4.2 Dendritic cells (DCs)

DCs are unique APCs because they are able to induce significant primary immune responses, thus permitting establishment of immunological memory (18,20,78,198).
DCs represent a heterogeneous cell population, residing in most peripheral tissues, particularly at sites of interface with the environment (skin, mucosa) (17). They display a high phagocytic capacity. Following tissue damage, DCs process the captured antigens, load them onto MHC molecules and migrate to the secondary lymphoid organs, where they present the antigenic peptides in the context of MHC molecules to T cells, thereby initiating adaptive immune responses (73,205). DCs activate antigen-specific $CD4^+$ T helper cells, which in turn regulate the immune effectors, including antigen-specific $CD8^+$ cytotoxic T cells (CTL) and B cells, as well as non-antigen-specific macrophages, eosinophils and NK cells. Moreover, DCs induce effector cells to home to the site of infection (17). Four stages of DC development have been delineated: (i) bone marrow progenitors; (ii) precursor DCs that are patrolling through blood and lymphatics as well as lymphoid tissues, and that upon pathogen recognition, release large amounts of cytokines, e.g. IFN-γ; (iii) tissue-residing immature DCs, which possess high endocytic and phagocytic capacity permitting antigen capture; and (iv) mature DCs, present within secondary lymphoid organs, that express high levels of costimulatory molecules permitting antigen presentation and T cell activation (Fig.1.2).

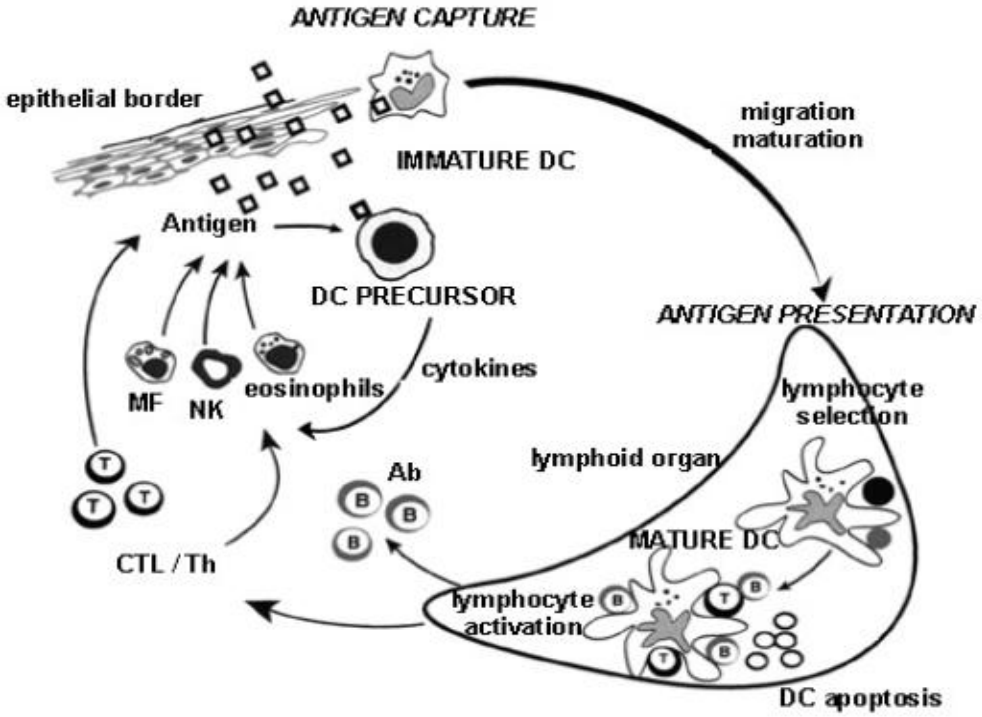

Figure 1.2 The life cycle of dendritic cells (from Banchereau (17)). Circulating precursor DCs enter tissues as immature DCs. They may directly encounter pathogens that induce secretion of cytokines (e.g. IFN-γ). Immature DCs reside at strategically important sites in the periphery to encounter pathogens. After antigen capture, immature DCs migrate to lymphoid organs where, after maturation, they display peptide-MHC complexes, which allows selection of rare circulating antigen-specific lymphocytes. These activated T cells help DCs in terminal maturation, which allows lymphocyte expansion and differentiation. Activated T lymphocytes migrate and reach the injured tissues. Helper T cells secrete cytokines, which permit activation of macrophages (MF), NK cells and eosinophils. Cytotoxic T cells eventually lyse the infected cells. B cells become activated after contact with T cells and DCs and then mature into antibody-producing plasma cells. It is believed that, after interaction with lymphocytes, DCs undergo apoptosis.

In addition to T cell priming, DCs appear to maintain essentially survival of naive $CD4^+$ T cells (33) and immune T cell memory (159). Importantly, DCs are also involved in the tolerization of the T cell repertoire to self-antigen. This occurs in the thymus (central tolerance) by deletion of developing T cells recognising self-antigens (33), and in lymphoid organs (peripheral tolerance) probably by the induction of anergy or deletion of mature T cells.

Dendritic cell activation and maturation

Immature DCs reside in peripheral tissues at sentinel positions where they take up self and non-self antigens. However, they are not able to present the antigens. Immature DCs accumulate MHC molecules intracellularly and present only a small fraction at the cell

surface (37,155). Three types of antigen uptake are known: macropinocytosis, phagocytosis and clathrin-mediated endocytosis (69,172,220,221). Different types of antigens are internalised via these different routes. The constitutive and cytoskeleton-dependent process of macropinocytosis allows rapid and non-specific sampling of large amounts of surrounding fluid and results in the formation of large intracellular vacuoles. Phagocytosis is a receptor-mediated process dependent on actin assembly. In general, the receptors mediating phagocytosis of pathogens are also engaged in clathrin-mediated endocytosis of soluble antigens. The latter allows uptake of macromolecules through specialized regions of the plasma membrane, termed coated pits (194). A large number of endocytic receptors are expressed on immature DCs, namely C-type lectins (93,172,210), receptors for the Fc portion of immunoglobulins (FcRs) (122,152), complement receptors (154), receptors for heat shock proteins (7,21), and scavenger receptors (148).

A signal from pathogens, often referred to as danger signal (67), induces DCs to enter a developmental program, called maturation, which transforms DCs from sentinels into efficient APCs and T cell stimulators (17). The danger signal can be a bacterial or viral product as well as an inflammatory cytokine. Danger signals are recognized through specific pattern-recognition receptors, such as Toll-like receptors, FcR and cytokine receptors (125,152).

Maturation of DCs is accompanied by fundamental morphological and functional changes. Antigen uptake, phagocytosis as well as macropinocytosis is down-regulated (172). In addition, MHC molecules are redistributed from intracellular endocytic compartments to the cell surface (37,155). Antigen processing, peptide loading as well as the half-life of MHC molecules is increased (37,155). Finally, the surface expression of T cell co-stimulatory molecules, such as CD80, CD86 or CD40, also rises (Fig. 1.3).

Simultaneously with the modifications of their antigen presentation abilities, maturation induces migration of DCs out of peripheral tissues (15) to the secondary lymphoid organs. Modifications in the expression of chemokine receptors (e.g. CCR7) and adhesion molecules (e.g. ICAM-I), as well as profound changes of the cytoskeleton organization contribute to the migration of DCs (173).

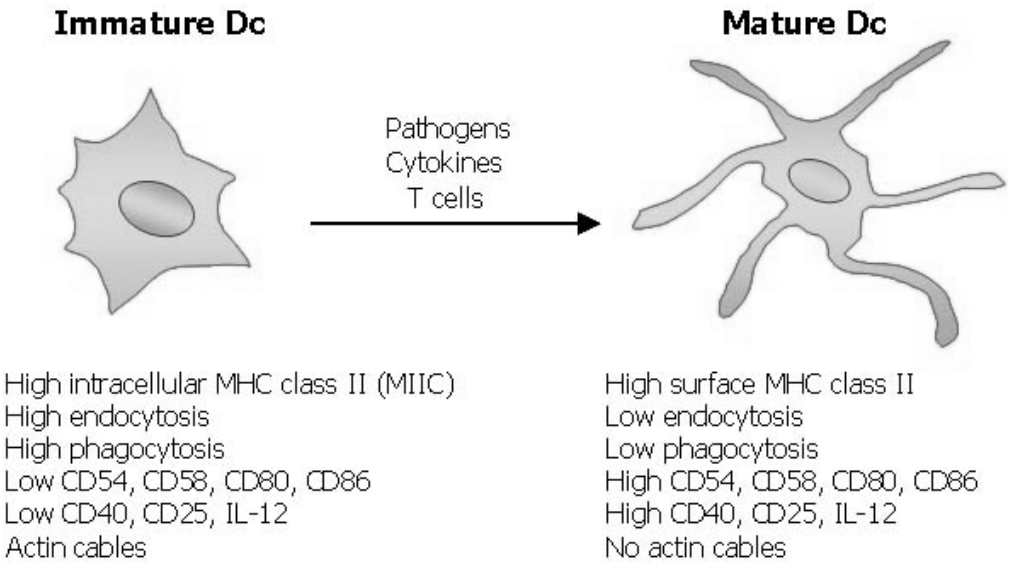

Figure 1.3 Features that change during DC maturation

1.2.4.3 Neutrophils

Neutrophils, which are also known as polymorphonuclear leukocytes (PMN), represent 50 to 60% of the total circulating leukocytes and constitute the "first line of defence" against infectious agents or "non-self" substances that penetrate the body's physical barriers. Once an inflammatory response is initiated, neutrophils are the first cells to be recruited to sites of infection or injury. Their targets include bacteria, fungi, protozoa, viruses, virally infected cells and tumour cells. Their development in the bone marrow takes about two weeks; during this period, they undergo proliferation and differentiation. During maturation, they pass trough six morphological stages: myeloblast, promyeloblast, myelocyte, metamyelocyte, non-segmented (band) neutrophil, segmented neutrophil. The segmented neutrophil is a fully functionally active cell. It contains cytoplasmic granules (primary or azurophil and secondary or specific) and a lobulated chromatin-dense nucleus with no nucleolus. Upon release from the bone marrow to the circulation the cells are in a nonactivated state and have a half-life of only 4 to 10 h before marginating and entering tissue pools, where they survive for 1 to 2 days. Cells of the circulating and marginated pools can exchange with each other. Senescent neutrophils are thought undergo *apoptosis* (programmed cell death) prior to removal by macrophages. The viability is significantly shorter in individuals suffering from infectious or acute inflammatory diseases when the tissue requirement for newly recruited neutrophils increases considerably.

Neutrophil granules

The neutrophil granules are of major importance for neutrophil function. The granules of neutrophils are generated during cell differentiation; they are produced for storage rather than continually. On the basis of function and enzyme content, neutrophil granules can be divided into three main types: azurophil, specific and small storage granules. Their function is not just to provide enzymes for hydrolytic substrate degradation, as in classical lysosomes, but also to kill ingested bacteria and, finally, to secrete their contents to regulate various physiological and pathological processes, including inflammation.

Neutrophils in host defence

The major role of neutrophils is to phagocytose and destroy infectious agents but they also limit the growth of some microbes, thereby buying time for adaptive (specific) immunological responses. With many microbes, however, neutrophil defences are ineffective in the absence of opsonins and various agents that amplify the cytotoxic response.

Opsonization is a process, in which opsonins adsorb to the surface of bacteria or other particles and facilitate their adherence to the phagocyte cytoplasmic membrane through opsonin receptors. Specific binding between the particle and phagocyte which occurs during immune phagocytosis is mediated by immunoadherent receptors. There are two types of immunoadherent receptors: Fc-receptors mainly for IgG antibodies (FcγR) and complement receptors (CR1, CR3). It means that function of opsonins in the first case is realized by antibodies and in the second case by iC3b. Specific binding between the particle and phagocyte may be also performed by lectins and lectin receptors (lectinophagocytosis).

To the phagocytosis itself chemotaxis of phagocytes precede into the site where phagocytosable material occurs. This is regulated by chemotactic factors generated by infectious agents themselves, as well as those release as a result of their initial contact with phagocytes and other components of the immune system.

Phagocytosis is a complex process composed of several morphological and biochemical steps. After recognition and particle binding to the phagocyte surface, ingestion

(engulfment), phagosome origination, phagolysosome formation (fusion of phagosome with lysosomes), killing and degradation of ingested cells or other material proceed. Simultaneously with the recognition and particle binding a dramatic increase in oxygen consumption (the respiratory burst) is observed. During this, oxygen is univalently reduced by NADPH oxidase to superoxide anion or its protonated form, perhydroxyl radical, which then is catalytically converted by action of superoxide dismutase to hydrogen peroxide:

$$O_2 + e^- + H^+ \rightarrow HO_2 = O_2^- + H^+$$

$$O_2^- + O_2^- + 2H^- \rightarrow O_2 + H_2O_2$$

During phagocytosis, cytosolic granules (lysosomes) fuse with the invaginating plasma membrane (around the engulfing microorganism) to form a phagolysosome into which they release their contents, thereby creating a higly toxic microenvironment. This step is of the first importance because during it two categories of cytotoxic substances, present in the preformed state in azurophil and specific granules and synthesized de novo during the respiratory burst, arrive at the same cell compartment. This degranulation normally prevents release of the toxic components into the extracellular milieu. However, some target may be too large to be fully phagocytosed or they avoid engulfment, resulting in frustrated phagocytosis in which no phagosome is formed. These may be killed extracellularly. However, tissue damage occurs when neutrophil microbicidal products are released extracellularly to such an extent that host defences (antioxidant and antiprotease screens) in the immediate vicinity are overwhelmed.

The importance of neutrophils in fighting bacterial and fungal infections is well recognized. Recently, it has been shown that neutrophils are in abundance also in virally induced lesions. Neutrophils bind to opsonized viruses and virally infected cells via antibody (Fc) and complement (iC3b) receptors. Viruses such as influenza can be inactivated by neutrophils trough damage to viral proteins (e.g. hemagglutinin and neuraminidase) mediated by the myeloperoxidase released during degranulation. In contrast to these acute diseases, chronic influenza infections can diminish or exhaust the microbicidal potency of neutrophils.

Regulation of neutrophil function

Under normal conditions, neutrophils roll along microvascular walls via low affinity interaction of selectins with specific endothelial carbohydrate ligands. During the inflammatory response, chemotactic factors of different origin and proinflammatory cytokines signal the recruitment of neutrophils to sites of infection and/or injury. This leads to the activation of neutrophil β_2-integrins and subsequent high-affinity binding to intercellular adhesion molecules on the surface of activated endothelial cells in postcapillary venules. Under the influence of a chemotactic gradient, generated locally and by diffusion of chemoattractants from the infection site, neutrophils penetrate the endothelial layer and migrate through connective tissue to sites of infection (*diapedesis*), where they finally congregate and adhere to extracellular matrix components such as laminin and fibronectin.

Cytokines are basic regulators of all neutrophil functions. Many of them including hematopoietic growth factors and pyrogens have shown to be potent neutrophil priming agents.

Historically, PMNs have not been considered capable of responding to stimuli via gene expression and protein synthesis. It was thought that neutrophils reacted entirely via the secretion of preformed proteins contained within the cytoplasm and granules at the time of cell migration from bone marrow into the blood stream. While recent investigations demonstrated a range of gene products whose expression is modulated by signals sensed in the environment.

PMNs can synthesize and secrete small amounts of some cytokines including IL-1, IL-6, CXCLl1, TNF-α, and GM-CSF; they may act in an autocrine or paracrine manner. A great number of inflammatory cytokines in synergy with IL-1, TNF-α, IL-6 and IFN-γ, can act as priming agents. The term "priming" refers to a stimulus that prepares PMNs for enhanced activity upon secondary stimulation. A variety of traditional PMN functions may be primed, including increase of oxidative metabolism, surface receptor expression, degranulation and various neutrophil cytotoxic functions like the neutrophil antibody-dependent cellular cytotoxicity (ADCC). In the other hand anti-inflammatory cytokines, IL-4 and IL-10 inhibit the production of Cxcl1 and the release of TNF-α and IL-1 which reflects in the blockade of neutrophil activation.

Furthermore, some cytokines like IFN-γ prolong neutrophil survival. PMNs, as terminally differentiated cells, are short-lived ad readily undergo apoptosis, or programmed death cell. Along to cytokines other mediators, including bioactive lipids, neuroendocrine hormones, histamine, and adenosine, are also involved in the regulation of neutrophil activation.

Although neutrophils are essential to host defence, they have also been implicated in the pathology of many chronic inflammatory conditions and ischemia-reperfussion injury. Hydrolytic enzymes of neutrophil origin and oxidatively inactivated protease inhibitors can be detected in fluid isolated from inflammatory sites. Under normal conditions, neutrophils can migrate to sites of infection without damage host tissues. This damage may occur through several independent mechanisms. These include premature activation during migration, extracellular release of toxic products during the killing of some microbes, removal of infected or damage host cells and debris as a first step in tissue remodeling, or failure to terminate acute inflammatory responses.

1.2.4.4 NK Cells

Natural killer (NK) cells play an instrumental role in the innate immune responses against certain bacterial, parasitic and viral pathogens (156). Furthermore, NK cells have been shown to play an important role in suppressing tumor metastasis and growth (84). Activation of NK cells is primarily achieved by the viral induced interferons α/β and to a lesser extent by IL-12 and IL-18 (44). Once activated, NK cells produce large amounts of IFN-γ and a wide variety of other cytokines, combinations of which are thought to specifically tailor downstream adaptive immune responses against the invading pathogen (44). These important functions place NK cells at the interface between the innate and adaptive immune responses (92).

NK cells develop from pluripotent bone marrow derived hematopoietic stem cells and at one stage in their development share a common progenitor with T cells. However, unlike T cells, NK cells do not require receptor gene rearrangement for successful maturation. The crucial role of IL-15 has been demonstrated in mice that lack the IL-2/15Rβ chain or the IL-15Rα chain. These mice are deficient in NK and NK-T cells. In addition, removal of interferon regulatory factor 1 (IRF-1) results in reduced numbers of NK cells that appear

phenotypically normal but lack cytolytic effector function. IRF-1 is a transcription factor essential for effective expression of IL-15 and perhaps other cytokines whose genes also contain IRF-1 response elements. Further development of NK cells requires the acquisition of inhibitory receptors, a process requiring the expression of MHC class I and as yet unidentified stromal derived factors (149). Terminal differentiation of NK cells into IFN-γ producing cells likely requires the action of IL-12 and IL-18, since loss of either results in significantly decreased NK cell cytotoxicity and IFN-γ production (4). The primary peripheral NK cell subset is present as a mature population of leukocytes, which can be easily identified in several compartments including peripheral blood, spleen and bone marrow.

NK cells receptors

NK cell recognition involves the initial binding to potential target cells, interactions between activating and inhibitory receptors with ligands available on the target, and the integration of signals transmitted by these receptors, which determines whether the NK cell detaches and moves on or stays and responds. NK cells respond by reorganizing and releasing cytotoxic granules and by transcribing and secreting cytokines. Recent studies have demonstrated reorientation of the relevant receptors into an "NK synapse" during NK cell encounters with potential target cells (44, 92), as observed previously in the interaction between T cells and antigen-presenting cells. NK cells differ from naive T cells in that mature NK cells are poised as effector cells for an immediate response. These "ready-to-go" cells express granzymes and perforin, and their lytic response can be triggered within minutes, without requiring transcription, translation, or cell proliferation. Recent studies (149) have shown that NK cells constitutively express prestored transcripts for IFN-γ that are immediately available to initiate cytokine synthesis upon activation. Even at their earliest stages of development, IFN-γ transcripts are present in the NK cell progenitors in the mouse bone marrow (149).

Therefore NK cells activity is strictly regulated by a variety of opposing signals from receptors that can either activate or inhibit effector function (92). Target cell specificity is not provided by the activating receptors that may be stimulated by a variety of signals, but rather by an array of inhibitory receptors that recognize MHC class I. This system is consistent with the "missing-self hypothesis" which postulates that NK cells survey tissues

for normal expression of MHC class I and will become activated when in contact with cells that have down-regulated or do not express MHC class I. The last few years have seen a dramatic increase in the number of inhibitory receptors identified and a concurrent expansion in our understanding of their involvement in NK cell function. In contrast, many of the receptors involved in activation have been known for several years but only recently have their signalling pathways become more defined.

Activating Receptors

Unlike T cells and B cells, which recognize antigen using clonally restricted receptors generated by gene rearrangement, NK cells use a variety of different non-rearranging receptors to initiate cytolytic activity and cytokine production. Many of these receptors are not unique to NK cells, but are also expressed by T cells. Receptors implicated in mouse and rat NK cell activation include CD2, CD16, CD28, Ly-6, CD69, NKR-P1, 2B4 (CD244), NKG2D, and CD94/NKG2A. It is believed that to successfully initiate effector function, signaling through one receptor is not sufficient. Additive or synergistic interactions between multiple activating receptors, is required which perhaps signal through a set of shared adaptor molecules or signalling pathways (88).

Inhibitory Receptors

The inhibitory receptor superfamily (IRS) 9 describes an expanding group of receptors that block activation of a number of different cell types in the immune system. By definition, IRS members must act in *trans*, be able to recruit phosphatases (such as SHP-1) through an ITIM, and must associate directly with an activating receptor (92). NK cell inhibitory receptors fall into two main structural groups, the calcium dependent lectin-like receptors and the immunoglobulin-like receptors. C-type lectin family members include the Ly-49 family identified in rodents, and CD94 and the NKG2 family identified in rodents and humans. These C-type lectins, predominantly expressed on NK cells, are encoded by genes located on distal mouse chromosome 6 and syntenic rat chromosome 4 and human chromosome 12 in a region called the "NK gene complex".
NK cells engage in several kinds of interactions with other cells of the immune system, including dendritic cells and macrophages. Dendritic cells can influence the proliferation

and the activation of NK cells both through release of cytokines including IL-12, and trough cell-surface interaction, including CD40/CD40 ligand, LFA-1/ICAM-1, and CD27/CD70. In return, NK cells provide signals that result in either activation or apoptosis to control the inflammatory response.

1.3 Adaptative immune system

Although the non-specific innate defences are effective, they do not protect against all invading pathogens. Microbes have developed several strategies to evade the innate immune system. Therefore a second defence system has evolved, the adaptive immune system, including antibodies and T cells.

1.3.1 Antibodies

Antibodies are protein complexes produced by B lymphocytes (B cells). There are several types of antibodies with different immunological functions. During infection IgM and IgG1-4 are most important. IgM antibodies are synthesized in the early phase of the immune response and are found mainly in the blood. They are pentameric in structure and specialised to activate complement efficiently upon binding antigen._IgG1 and IgG3 are called opsonizing antibodies because these two subtypes are the most effective in opsonizing microbes. This opsonization facilitates the ingestion of antigens by phagocytes. IgG also mediates the attachment of cytotoxic cells to infected tissue, eventually leading to death of an infected cell (antibody-dependent cell-mediated cytotoxicity). This mechanism serves as a defence against intracellular pathogens. Both IgG and IgM neutralize microbes by binding to the surfaces of bacteria and viruses and prevent them from attaching to and invading host cells. Both types of antibodies are also able to activate complement and neutralize toxins (92).

1.3.2 Cytotoxic T lymphocytes (CTLs)

On their surface, CTLs express a protein called CD8, which is associated with the T cell receptor, by which they recognize pathogen-derived peptides bound to MHC class I molecules (mostly from viruses). CTLs play a role in killing infected host cells similar to that of NK cells and produce proteolytic enzymes (granzymes) that trigger apoptosis in the infected cells. This type of attack kills the infected cells but commonly not the microbes. Microbes, released from infected cells, can be taken up by activated macrophages, which finally kill them. Alternatively, the CTLs might also attack the microbes by perforin and granulysin stored within their granules. First, perforin forms pores into the host cell membrane. By these pores granulysin enters the infected cell and kills the bacteria by creating pores in their membranes.

1.3.3 T helper cells

After activation naive CD4 T cells differentiate into either Th1 cells or Th2 cells. IL-12 produced by macrophages or DCs stimulates NK cells to produce IFN-γ, which in turn stimulates CD4 T cells to differentiate into Th1 cells. IL-4 stimulates $CD4^+$ T cells to develop into Th2 cells. Th1 cells produce IFN-γ, which activates macrophages allowing them to destroy intracellular microorganisms more efficiently. Th1 cells can also stimulate B cells to produce subclasses of antibodies and activate cytotoxic T cells. Th2 cells activate eosinophils and stimulate B cells to produce antibodies of the IgG1 class by secreting IL-4 and IL-5.

1.4 The genus *Yersinia*

The genus *Yersinia* belongs to the family of *Enterobacteriaceae*. They are facultative anaerobe, gram-negative rods with an optimal growth at 27-30°C (45). The genus *Yersinia* includes three species that are pathogenic for rodents and humans: *Y. pestis* is the causative agent of plague, *Y. pseudotuberculosis*, and *Y. enterocolitica* cause acute or chronic enteric disorders such as enteritis, enterocolitis, and mesenteric lymphadenitis, which are normally self-limited. In some cases the infection leads to systemic

manifestations like septicaemia and immunopathological sequelae including reactive arthritis, uveitis, and erythema nodosum (48). While a fleabite generally inoculates *Y. pestis*, *Y. pseudotuberculosis* and *Y. enterocolitica* are food-borne pathogens. In spite of these differences in infection routes, all three have a common tropism for lymphoid tissues and a common capacity to resist non-specific immune response, in particular phagocytosis and killing by macrophages and PMNs. Electron microscopy as well as cell biology examinations revealed that *Y. enterocolitica* and *Y. pseudotuberculosis* are largely located extracellularly (14,55,77,188,191).

1.4.1 Pathogenicity factors of *Y. enterocolitica*

Yersinia possesses several virulence factors encoded either by genes of the bacterial chromosome (157) or by genes located on the 70-kb virulence plasmid pYV (*plasmid Yersinia Virulence*) (47,87,145,195) which enables *Yersinia spp.* to survive and multiply in the lymphoid tissues of their host. Table 1.1 gives an overview of the pathogenicity factors of *Yersinia spp.*.

Table 1.1 Overview of the most important virulence factors of enteropathogenic *Yersinia*

a) Chromosomally-encoded factors

Factor	Function	Literature
Ail	Mediates adhesion to and invasion in epithelial cells as well as serum resistance.	(25,129,147)
Inv	Invasin, an adhesin. Initiates by binding to β1-integrins transport of *Yersinia* across the M cells, internalisation in epithelial cells and secretion of IL-8.	(6,31,60,91,95,114,144, 181,184)
Myf	Fibrillae possibly acts as a colonization factor and leads together with Yst to diarrhea.	(90)
SodA	Super oxide dismutate (Sod), enzyme for detoxification of exogenous oxygen radicals produced by phagocytes. Mediates virulence for colonization of liver and spleen, but not of Peyer's patches.	(161)
Yst	Heat-stable enterotoxin, stimulates the activity of guanylate cyclase of intestinal epithelial cells and leads to diarrhea.	(52,151,160)
HPI (High	The HPI encodes the extracellular siderophore Yersiniabactin (Ybt) that enables the bacteria to multiply under iron-depleted conditions.	(11,15,75)

Patho-genicity Island)	Genes involved in Ybt synthesis, transport and regulation are clustered in the HPI. Ybt possibly acts immunosuppressive on T and B cells, macrophages and PMNs.

b) Plasmid-encoded factors

Factor	Function	Literature
YopE	Cytotoxin, works as GAP (GTPase activating protein) for Rho-family proteins, blocks phagocytosis, disrupts actin filaments.	(1,23,165,215)
YopH	Phosphotyrosine phosphatase, which dephosphorylates proteins of focal adhesions therefore responsible for up to 50% of the antiphagocytic activity of yersiniae towards neutrophiles and macrophages. Suppression of oxidative burst in macrophages, inhibition of T and B lymphocyte activation.	(22,24,72,170,175,223)
YopO (YpkA)	Serine-threonine kinase activated by G-actin causing autophosphorylation of serine residues. Disruption of actin filaments. Interacts with RhoA and Rac1.	(19,68,94)
YopM	Strongly acidic protein containing leucine-rich repeats (LRRs). It traffics to the cell's nucleus by means of a vesicle-associated pathway.	(111,112,123,193)
YopP	Cysteine protease, interacts with members of the MAPK kinase (MKK) super family and IKK-β thereby disrupting MAPK and NF-κB signalling pathways leading to inhibited release of proinflammatory cytokines as well as induction of apoptosis in macrophages.	(30,53,54,141,142,167)
YopT	Destruction of actin stress fibres by modification of RhoA, which is released from the plasma membrane and accumulates as monomeric protein in the cytosol.	(89,146,224)
YadA	Mediates adherence to epithelial cells and phagocytes. Binds to collagen, fibronectin, and laminins. It protects *Y. enterocolitica* against killing by PMNs and lysis by complement due to the binding of factor H by YadA.	(40,162,163,185)
LcrV	Suppression of TNF-α and IFN-γ. Inhibits the chemotaxis of neutrophils. Induces the production of IL-10 in macrophages.	(135,192,219)

1.4.2 The type III secretion system of *Y. enterocolitica*

By means of its type III secretion system (TTSS) some gram-negative bacteria are able to translocate their effector proteins directly into the cytosol of host cells (66). To date 20 different TTSS are identified in animal and plant pathogens (46). The pYV plasmid encodes the Yop virulon, a system consisting of secreted proteins called Yops and their dedicated type III secretion apparatus called Ysc.

Upon contact with eukaryotic target cells, *Yersinia* bacteria build several syringe-like organelles at their surface (Fig. 1.5). These organelles, called the Ysc injectisome, are protein pumps spanning the peptidoglycan layer and the two bacterial membranes topped by a stiff needle-like structure protruding outside the bacterium. The whole organelle comprises 27 proteins. The internal part contains 10 proteins, which have counterparts in the basal body of the flagellum, indicating that the two organelles have a common evolutionary origin. The external part of the injectisome, which spans the bacterial outer membrane, is a homomultimeric ring-shaped structure with a central pore of ≈50 Å (98). The Ysc injectisome ends with a 60–80 nm long and 6–7 nm wide needle, whereas the length is genetically controlled (130). Effector Yops destined for secretion through the injectisome have no classical signal sequence (128). Nevertheless, a minimum of 15 residues at the NH_2 terminus are necessary for Yop secretion (4,196).

To become secreted some of the Yops need the help of small individual chaperones called Syc proteins. There are two categories of Yop proteins. Some are intracellular effectors, whereas the others are "translocators" which are needed to deliver the effectors across the eukaryotic plasma membrane into the cytosol of eukaryotic cells. The translocators (YopB, YopD, LcrV) form a pore of 16-23 Å in the eukaryotic cell membrane.

Six effector Yops have been characterized: YopE, YopH, YopM, YopJ/P, YopO/YpkA, and YopT. YopH is a powerful phosphotyrosine phosphatase playing an antiphagocytic role by dephosphorylating several focal adhesion proteins. YopE and YopT contribute to antiphagocytic effects by inactivating GTPases controlling cytoskeleton dynamics. YopP plays an anti-inflammatory role by preventing the activation of transcription factor NF-κB. YopP also blocks the MKKs, inhibiting the activation of MAPK, which abrogates activation of CREB, a transcription factor involved in the immune response. YopP induces apoptosis in macrophages, either directly by acting upstream of Bid or indirectly by blocking the

synthesis of NF-κB–dependent antiapoptotic factors. Less is known about the role of the phosphoserine kinase YopO/YpkA and YopM (see also Table1.1).

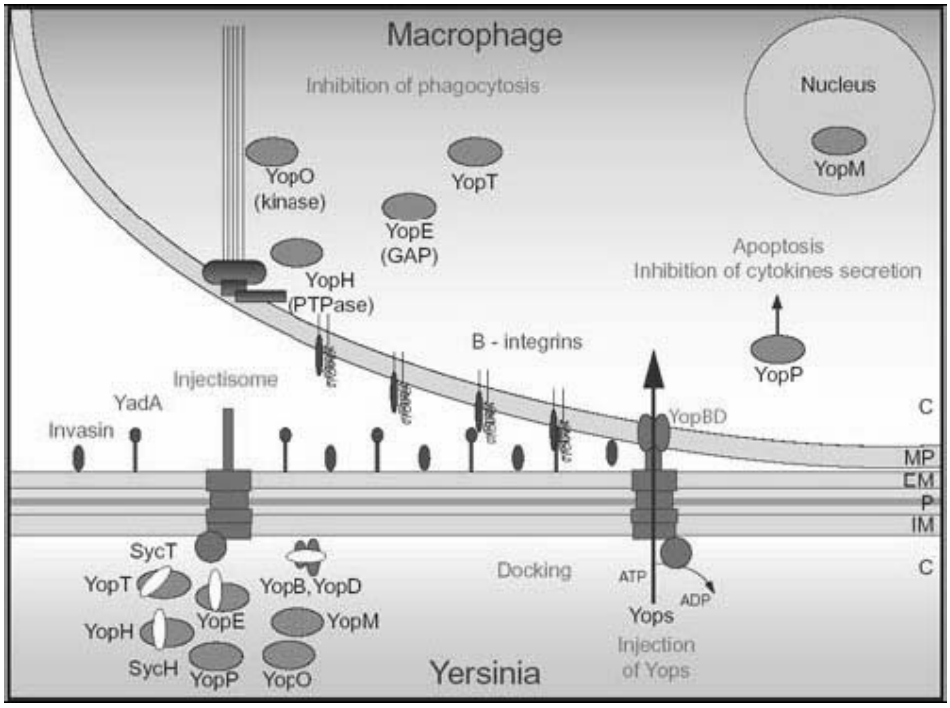

Figure 1.4 **Secretion of Yops by the Ysc injectisome and translocation across the target cell membrane.** (from Cornelis, 2002) When *Yersinia* is placed at 37°C in a rich environment, the Ysc injectisome is installed and a stock of Yop proteins is synthesized. During their intrabacterial stage, some Yops are capped with their specific Syc chaperone. Upon contact with a eukaryotic target cell, the adhesins YadA or Inv interact with integrins and the bacterium docks at the cell's surface. Then, the secretion channel opens and Yops are exported. YopB and YopD form a pore in the target cell plasma membrane (MP), and the effector Yops are translocated across this membrane into the eukaryotic cell cytosol (C). EM, outer membrane; P, peptidoglycan; IM, plasma membrane.

1.4.3 Immune response to *Yersinia*

Enteric *Yersinia spp.* are enteroinvasive pathogens, which are taken up by M cells. M cells are specialized epithelial cells which occur within the follicle-associated epithelium of the Peyer's patches (14,71). M cells expose β1-integrins at their apical ("lumenal") surface, which may bind to the *Yersinia* invasin protein (41,182). The entry of enteric *Yersinia* by this route is an ambiguous process: on the one hand, *Yersinia* may use M cells as a structure of the mucosal immune system for invasion of host tissue, and most likely for subsequent dissemination. On the other hand, the mucosal immune system is stimulated upon entry of *Yersinia* at the very site where efficient immune responses are usually

initiated. One day after M cell invasion by *Y. enterocolitica*, small microabscesses consisting of PMNs and extracellularly located *Yersinia* can be detected in Peyer's patch tissue (14,77).

Yersinia has evolved efficient mechanisms mediated by the outer membrane protein YadA and secreted anti-host effector proteins (Yops) (for references see table 1) to evade host innate defence mechanisms including phagocytosis by PMNs, macrophages and the complement system. In accordance with these *in vivo* observations, *Yersinia* manifests some resistance to phagocytosis *in vitro*, both by macrophages (63,164) and by PMN (40,170,213). After replication in Peyer's patches, enteric *Yersinia* disseminate via the lymphatics and possibly via the blood stream to the mesenteric lymph nodes, spleen, liver, lungs and peripheral lymph nodes (14).

The adaptive immune response plays a crucial role in the clearance of a *Yersinia* infection. It has been clearly demonstrated that *Yersinia* infection leads to a strong T cell responses, including activation and proliferation of CD4 and CD8 T cells, and that these T cells are involved in control of *Yersinia* (15,16,26,29,61,62,137). In fact, mice deficient for T cells are unable to control the pathogen, and therefore develop chronic progressive and fatal infection (15). Adoptive transfer of *Yersinia*-specific $CD4^+$ or $CD8^+$ T cells consistently mediates resistance to a normally lethal challenge of *Yersinia* (16). As protective CD4 or CD8 T cells produce cytokines such as IFN-γ and IL-2, but not IL-4 or IL-10, it can be concluded that Th1 or IFN-γ producing cytotoxic T cells are protective in yersiniosis (14,16,26,28). Th1 cells produce predominantly IFN-γ, and it is established that IFN-γ can activate macrophages which in turn might be able to kill the pathogen.

The role of cytokines in yersiniosis has been extensively studied in mouse strains that are relatively susceptible (e.g., BALB/c) or resistant (e.g., C57BL/6) to *Yersinia* infection. One reason for this differential susceptibility of mice is their different ability to mount Th1 responses and produce IFN-γ upon *Yersinia* infection (15,27). *Yersinia*-resistant C57BL/6 mice can be rendered *Yersinia*-susceptible by neutralizing IFN-γ *in vivo* with monoclonal antibodies (15). Conversely, *Yersinia*-susceptible BALB/c mice can be rendered resistant by treatment with IFN-γ. In keeping with these results, it was found that administration of neutralizing anti-IL-4 antibodies also rendered BALB/c mice resistant to *Yersinia* infection (15). From these data it can be concluded that IFN-γ is a central protective cytokine in *Yersinia* infection. In addition experiments with cytokine- or cytokine receptor-deficient

mice clearly demonstrated that the cytokines TNF-α, IL-12, IL-18 and IFN-γ are all essential for control of *Yersinia* infection (26,28,29,81).
In contrast to T cell responses, protective antibodies recognize the outer membrane protein YadA of *Y. enterocolitica* (214). In *Y. pestis* infections, antibodies against LcrV, F1 antigen and YopD have been demonstrated to be protective. Together, these data suggest that different antigens are possibly involved in protective cellular and humoral immune responses.

1.5 Microarrays technology

Global transcription analysis using microarray technologies provides a new approach to the description of complex biological phenomena.
The development of DNA-microarray technologies, together with the sequencing of genomes from different species, has provided an opportunity to monitor and investigate the complex interactions that regulate biological processes. The availability of such large amounts of information has shifted the attention of scientists towards a non-reductionist approach to biological phenomena. How best to interpret the enormous amount of information that is provided by these new technologies remains a challenging question, not only for bioinformaticians, mathematicians and physicists, but also for immunologists, who have tried to understand how the single constituents of this complex biological system interact.

Understanding how the immune system is regulated and responds to pathogens will require whole-system approaches, because the study of single immunological parameters has, so far, been unable to unlock immune-system complexity.

In the context of immunology, the best interpretation of reality is obtained by the description of altered patterns (perturbations induced by infections).
In this contest microarray approaches, with their large sample capacity, can be used to follow globally altered patterns of gene expression over time. Moreover, microarray technologies allow kinetic studies of gene expression on a global scale to follow the

interactions of different microorganisms with cells of the immune system over the course of infection.

The principle of a microarray experiment, as opposed to the classical northern-blotting analysis, is that mRNA from a given cell line or tissue is used to generate a labelled sample, which is hybridized in parallel to a large number of DNA sequences, immobilized on a solid surface in an ordered array. Tens of thousands of transcript species can be detected and quantified simultaneously.

During recent years, DNA microarray technology has been advancing rapidly. The development of more powerful robots for arraying, new surface technology for glass slides, and new labelling protocols and dyes, together with increasing genome-sequence information for different organisms will enable us to extend the quality and complexity of microarray experiments.

1.5.1 Different Array platforms

Although many different microarray systems have been developed by academic groups and commercial suppliers, the most commonly used systems today can be divided into two groups, according to the arrayed material: complementary DNA (cDNA) and oligonucleotide microarrays.

The arrayed material has generally been termed the probe since it is equivalent to the probe used in a northern blot analysis.

Probes for cDNA arrays are usually products of the polymerase chain reaction (PCR) generated from cDNA libraries or clone collections, using either vector-specific or gene-specific primers, and are printed onto glass slides or nylon membranes as spots at defined locations. Spots are typically 100–300 μm in size and are spaced about the same distance apart. Using this technique, arrays consisting of more than 30,000 cDNAs can be fitted onto the surface of a conventional microscope slide Fig.a.

For oligonucleotide arrays, short 20-25mers are synthesized *in situ*, either by photolithography onto silicon wafers (high-density-oligonucleotide arrays from Affymetrix, http:// www.affymetrix.com) or by ink-jet technology (developed by Rosetta Inpharmatics, http://www.rii.com, and licensed to Agilent Technologies). Alternatively, presynthesized oligonucleotides can be printed onto glass slides Fig.b.

Methods based on synthetic oligonucleotides offer the advantage that because sequence information alone is sufficient to generate the DNA to be arrayed, no time-consuming handling of cDNA resources is required. Also, probes can be designed to represent the most unique part of a given transcript, making the detection of closely related genes or splice variants possible.

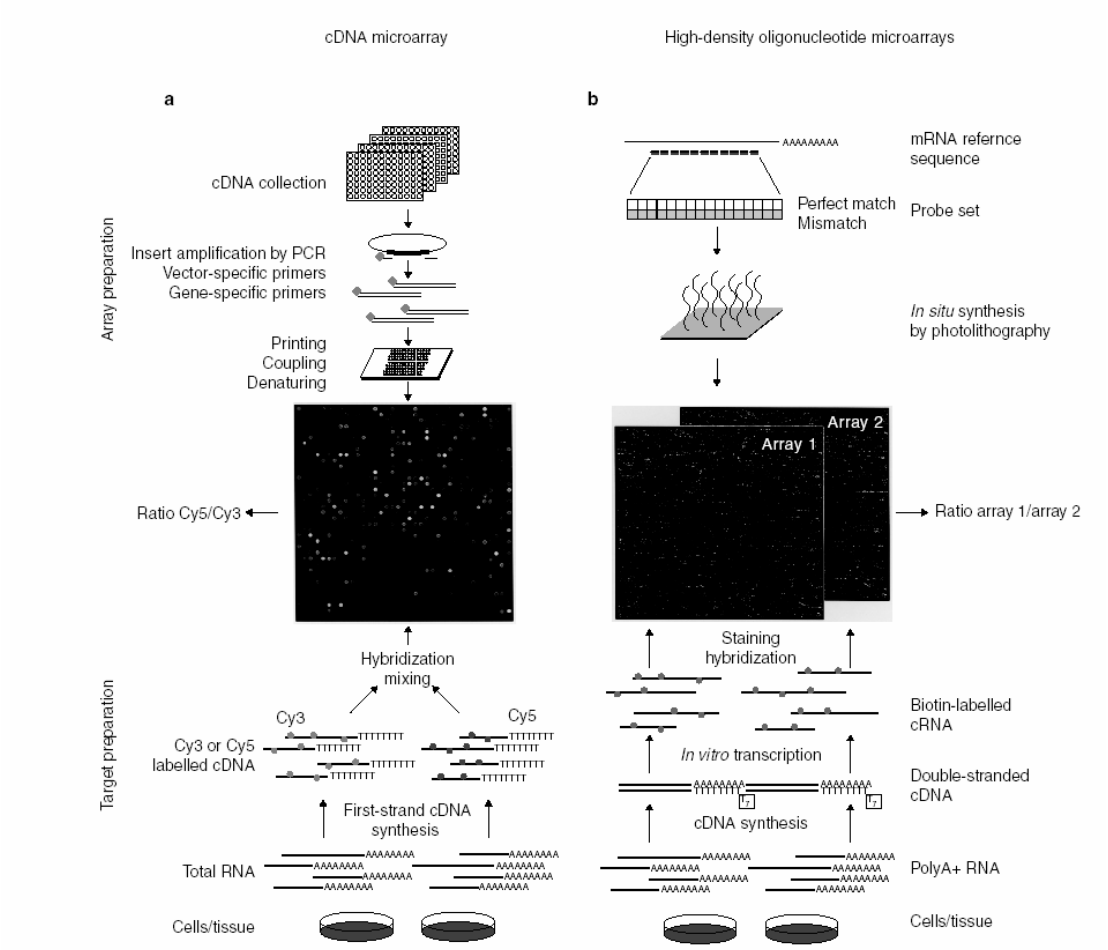

Figure 1.5 Schematic overview of probe array and target preparation for spotted cDNA microarrays and high-density oligonucleotide microarrays. (From A. Schulze and J. Downward, 2001) Fig.A, cDNA microarrays. Array preparation: inserts from cDNA collections or libraries are amplified and printed at specified sites on glass slides. Target preparation: RNA from two different tissues or cell populations is used to synthesize single-stranded cDNA in the presence of nucleotides labelled with two different fluorescent dyes. Both samples are mixed in a small volume of hybridization buffer and hybridized to the array surface resulting in competitive binding of differentially labelled cDNAs to the corresponding array elements. Fig.B, High-density oligonucleotide microarrays. Array preparation: sequences of 16–20 short oligonucleotides are chosen from the mRNA reference sequence of each gene. Target preparation: polyA+ RNA from different tissues or cell populations is used to generate double-stranded cDNA carrying a transcriptional start site for T7 DNA polymerase. During *in vitro* transcription, biotin-labelled nucleotides are incorporated into the synthesized cRNA molecules. Each target sample is hybridized to a separate probe array and target binding is detected by staining with a fluorescent dye coupled to streptavidin.

1.5.2 Target preparation

Another important difference between *in situ* synthesized, high-density oligonucleotide arrays and spotted arrays lies in target preparation. In both cases, mRNA from cells or tissue is extracted, converted to DNA and labelled, hybridized to the DNA elements on the array surface of the array, and detected by phospho-imaging or fluorescence scanning. The high reproducibility of *in situ* synthesis of oligonucleotide chips allows accurate comparison of signals generated by samples hybridized to separate arrays. In the case of spotted arrays, the process of gridding is not accurate enough to allow comparison between different arrays. The use of different fluorescent dyes (such as Cy3 and Cy5) allows mRNAs from two different cell populations or tissues to be labelled in different colours, mixed and hybridised to the same array, which results in competitive binding of the target to the arrayed sequences. After hybridization and washing, the slide is scanned using two different wavelengths, corresponding to the dyes used, and the intensity of the same spot in both channels is compared. This results in a measurement of the ratio of transcript levels for each gene represented on the array.

For those reasons in our experimental setting we use an oligonucleotide chips system. In particular for the analysis of the changing in the transcriptional response in our experiments we had used the GeneChip® technology from Affymetrix (Affymetrix, High Wycombe, UK).

The GeneChip® technology platform consists of high-density microarrays and tools to help process and analyze those arrays, including standardized assays and reagents, instrumentation, and data management and analysis tools.

GeneChip microarrays consist of small DNA fragments (referred to here as probes), chemically synthesized at specific locations on a coated quartz surface. The precise location where each probe is synthesized is called a feature, and millions of features can be contained on one array. By extracting, amplifying, and labeling nucleic acids from experimental samples, and then hybridizing those prepared samples to the array, the amount of label can be monitored at each feature, enabling either the precise identification of hundreds of thousands of target sequence (DNA Analysis) or the simultaneous relative quantitation of the tens of thousands of different RNA transcripts, representing gene activity (Expression Analysis).

The integration of semiconductor fabrication techniques, solid phase chemistry, random access combinatorial chemistry, molecular biology, and sophisticated robotics results in a unique photolithographic manufacturing process capable of producing GeneChip® arrays with millions of probes on a small glass chip.

The photolithographic process begins by coating a 5"x 5" quartz wafer with a light-sensitive chemical compound that prevents coupling between the wafer and the first nucleotide of the DNA probe being created. Lithographic masks are used to either block or transmit light onto specific locations of the wafer surface. The surface is then flooded with a solution containing either adenine, thymine, cytosine, or guanine, and coupling occurs only in those regions on the glass that have been deprotected through illumination. The coupled nucleotide also bears a light-sensitive protecting group, so the cycle can be repeated. In this way, the microarray is built as the probes are synthesized through repeated cycles of random access combinatorial chemistry where combinations of probes are simultaneously synthesized. Commercially available arrays are typically manufactured at a density of over 100 million probes each 25 nucleotides in length per wafer.

1.5.3 Probe Design

Every probe on an Affymetrix microarray is designed to determine whether or not the complementary sequence of RNA is present in the sample. Because of their 25 nucleotide length (25mer), the probes have high specificity and are designed to reject targets that are not identical. This level of specificity is essential when measuring the expression of two very similar gene sequences. The high density of those microarrays affords the ability to use multiple probes for each expression measurement made. Just as the 25mer probe length confers high specificity, the use of multiple probes provides for high sensitivity and reproducibility; 22 probes are routinely used for each expression measurement. For each probe on the array that perfectly matches its target sequence, Affymetrix also builds a paired "mismatch" probe. The mismatch probe contains a single mismatch located directly in the middle of the 25-base probe sequence. While the perfect match probe provides measurable fluorescence when sample binds to it, the paired mismatch probe is used to detect and eliminate any false or contaminating fluorescence within that measurement. The mismatch probe serves as an internal control for its perfect match partner because it hybridizes to nonspecific sequences about as effectively as its counterpart, allowing

spurious signals, from cross hybridization for example, to be efficiently quantified and subtracted from a gene expression measurement or genotype call.

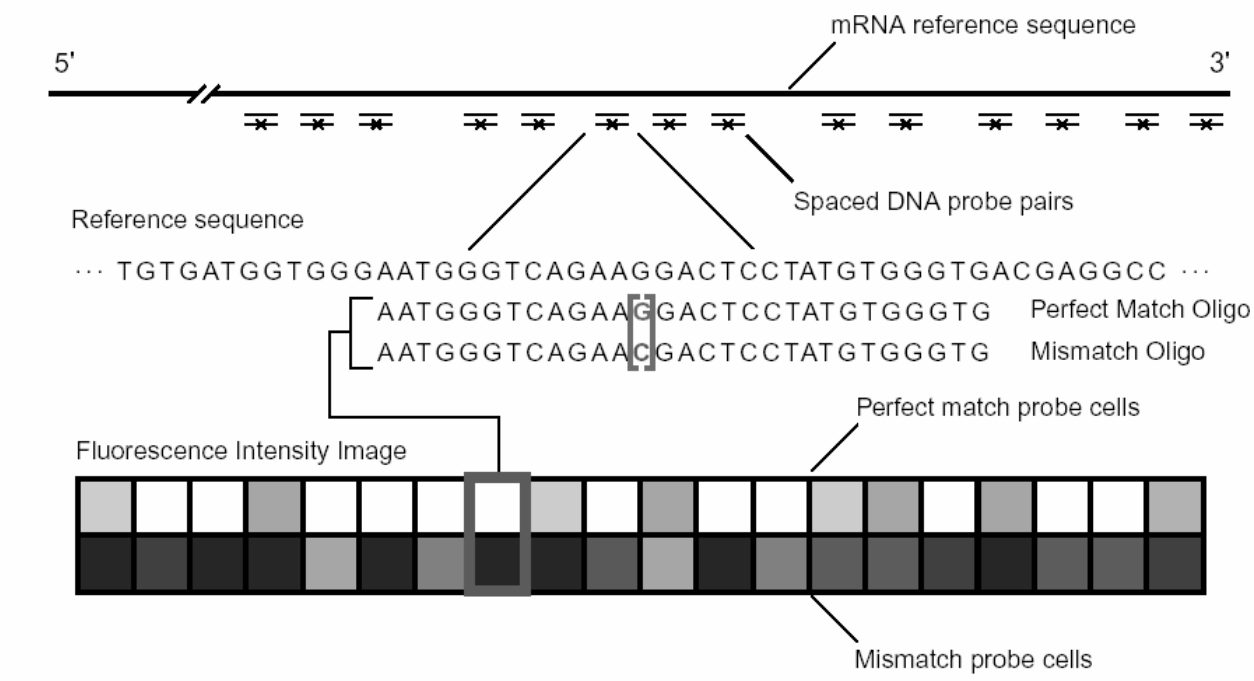

Figure 8 **Expression probe and array design.** (from Affymetrix web site, www.affymetrix.com) Oligonucleotide probes are chosen based on uniqueness criteria and composition design rules. For eukaryotic organisms, probes are chosen typically from the 3´ end of the gene or transcript (nearer to the poly(A) tail) to reduce problems that may arise from the use of partially degraded mRNA. The use of the PM minus MM differences averaged across a set of probes greatly reduces the contribution of background and cross-hybridization and increases the quantitative accuracy and reproducibility of the measurements.

2 Material and methods

2.1 Bacterial strains and plasmids

The bacterial strains used in the present study are listed in Table 2.1

Designation	Description	References
pYV$^+$	Serotype O:8, *Y.enterocolitica* WA-314; clinical isolate; contains virulence plasmid pYV; Nal^r	(79)
pYV$^-$	Serotype O:8, virulence plasmid cured derivative of *Y.enterocolitica* WA-314; Nal^r	(79)
pYV$^+$ Δ*yopH*	pYV$^-$ harbouring pYV *yopH* Δ17-203; Nal^r, Kana^r	(97)
pYV$^+$ Δ*yopP*	*yopP*-negative mutant, derivative of *Y.enterocolitica* WA-314, insertional inactivation of *yopP*; Nal^r, Cm^r	(167)

Table 2.1 Bacterial strains used in the present study

The bacteria were precultured to stationary phase in Luria Bertani medium (LB) at 27°C. In dependency of the used strain the medium was supplemented with specific antibiotics (nalidixic acid 10 μg/ml, kanamicin 25 μg/ml and chloramphenicol 20 μg/ml). For mouse experiments, a 1:20 dilution of the overnight *Yersinia* preculture was incubated for additional 5 h at 37°C and frozen in liquid nitrogen in LB medium with 20% glycerol. The stock suspensions were stored at -80 °C until further use.

For in vitro experiments, a 1:20 dilution of the overnight *Yersinia* culture was incubated for additional 2 h at 37°C. The bacteria were washed with phosphate-buffered-saline (PBS; Invitrogen, Karlsruhe, Germany) and the optical density at 600 nm was determined. Heat-killed pYV$^+$ cells were generated by heating the bacteria at 60°C for 4 h.

2.2 Mouse infections

C57BL/6 mice were purchased from Harlan Winkelmann (Borchen, Germany). IFN-γR$^{-/-}$ from The Jackson Laboratory (Bar Harbor, Maine, USA). The mice were maintained under specific pathogen-free conditions in the breeding facility of the Medical Microbiology Institute of the University Clinic of Tübingen, Germany. The experiments were performed using 6 to 10-week-old female mice.

The animals were housed in plastic cages with wood shavings in a high-efficiency particulate air-filtered barrier unit maintained at 25°C with alternating 12-h periods of light and dark. The mice had drinking water at all times and were fed ad libitum with an autoclaved rodent pellet diet.

The mice were infected intravenously with different doses of *Y. enterocolitica* pYV^{+}, *Y. enterocolitica* pYV^{+}Δ*yopH* and *Y. enterocolitica* pYV^{+}Δ*yopP* mutants after thawing the frozen stock suspensions. A volume of 200 µl of bacterial suspensions in PBS with different doses of bacteria was injected into the lateral tail vein of the mice. The actual injected dose of the bacteria (CFU/ml; colony forming units/ml) was verified by plating out serial dilutions on Mueller-Hinton agar after incubation at 27°C for 36 h.

For kinetic analysis, mice were sacrificed by CO_2 asphyxiation at different timepoints post infection. Spleen was aseptically removed and homogenized in 5 ml HBSS-buffer (Ca^{2+} and Mg^{2+} free Hank's balance solution supplemented, Biochrom, Berlin, Germany; with 2% v/v Fetal Calve Serum, FCS, Sigma, Taufkirchen, Germany and 10mM HEPES, Biochrom, Berlin, Germany). Determining the concentration of the bacteria per organ (CFU/organ), serial dilutions of homogenated organs were plated out on *Yersinia* selective CIN agar and incubated at 27°C for 36 hours.

For survival experiments, five to six mice from each genetic background were infected i.v. with different doses of each different bacterial strain. Animal survival was monitored twice a day over a period of 14 days. This analysis was performed in triplicate in three independent experiments for each mouse strain.

2.3 Immunohistochemistry

C57BL/6 and IFN-γR1$^{-/-}$ mice were intravenously infected with 5x10^{4} CFU of a *Y. enterocolitica* wild type strain (pYV^{+}) or with the Δ*yopH* or the Δ*yopP* mutants. After 1 or 3 days the mice were sacrificed by CO_2 asphyxiation. The spleens were removed and frozen

in liquid nitrogen and stored at -80°C. Sections of 6µm were prepared and fixed in acetone. The endogen peroxidases were blocked with 3% H_2O_2 in PBS for 10 min and subsequently to prevent unspecific antibody binding the sections were incubated with 1% bovine serum albumin in PBS. The tissues were stained with a polyclonal rabbit anti-Inv 3.1 antibody. After one hour at room temperature, the sections were washed with PBS and covered with the secondary antibody HRP-conjugated goat anti-rabbit immunoglobulins (Dianova, Hamburg, Germany). Staining was completed by a five-minute incubation with 1% (v/v) DAB (3,3 diaminobenzidine tetrahydrochloride; Sigma, Taufkirchen, Germany) plus 0.1% H_2O_2 in PBS, which results in a brown precipitate at the antigen site. After washing the sections were counterstained with hematoxylin. Several sections for each spleen were analyzed to detect abscess formation, inflammatory infiltrates, necrosis, and bacterial colonization. In the picture the bacteria appear brown and the nuclei were colored blue.

2.4 Selection of splenic CD11b positive cells

A number of five to ten mice from each infection were sacrificed by CO_2 asphyxiation on day 0, day 1 and day 3 post infection and their spleens were surgically removed and placed in ice-cold HBSS-buffer. The spleens were crushed and forced with a 5 ml syringe pestle through a 40 µm-pore nylon mesh cell strainer (Falcon; BD Biosciences).

The cell suspensions were washed twice with ice-cold HBSS-buffer. Red blood cells were lysed by incubating the cell suspensions at room temperature in lysis buffer (170 mM Tris, 160 mM NH_4Cl, pH 7,4) for 5 min followed by two washes in ice-cold HBSS. Cells were resuspended in MACS Buffer (Ca^{2+} and Mg^{2+} free PBS supplemented with 0,5% Bovine Serum Albumin and 2mM EDTA) at a concentration of $1x10^7$ cells for 90 µl. The cells suspensions were incubated with 10 µl of CD11b antibody conjugated beads (MACS® MicroBeads; Miltenyi Biotec, Bergisch Gladbach, Germany) followed by an incubation at +4°C for 15 min. The mixture of cells and beads was then applied to the MACS column (MACS Columns LS, Miltenyi Biotec, Bergisch Gladbach, Germany) for positive selection, the non-binding cells were allowed to flow through, and the column was washed three times with MACS buffer. To recover bound cells, the column was removed from the magnet and the cells were eluted with 5 ml of Macs buffer using the plunger supplied with the column. To ensure enrichment values of 96-98% purity, the magnetic separation was

repeated using a second column under the same conditions. Cell viability and number were assessed by trypan blue exclusion staining.

2.5 Flow cytometry

A suspension of splenic single cells was resuspended in PBS with 1% (v/v) FCS, 0,01% sodium azide and 2mM EDTA (FACS buffer) and labeled with fluorophore-conjugated antibodies (Abs) targeted against surface markers.
In order to avoid non-specific labeling, FcγII/III receptors were blocked using rat anti-mouse CD16/CD32 antibodies (Ab) (BD Pharmingen, Heidelberg, Germany) at 4 °C for 15 min. The cells were resuspended in FACS buffer at a concentration of $1x10^7$ cells/ml and stained with marker-specific fluorophore-conjugated antibodies (Abs) (fluorescein-5-isothiocyanate [FITC], phycoerythrin [PE], allophycocyanin [APC] and biotin-conjugated Abs, or the appropriate isotype control Abs for 30 min on ice. Then cellular suspensions were then washed twice in FACS buffer and, if necessary, stained with fluorophore-conjugated secondary Abs, streptavidin-PE, or streptavidin- FITC for 30 min on ice. The cells were washed twice as described above and fixed with 1% (v/v) paraformaldehyde in PBS. The subsequent flow cytometric analysis was performed on a four-laser flow cytometer (FACS calibur; BD Biosciences, Heidelberg, Germany). The data were analysed with the Cell Quest Pro software (BD Biosciences, Heidelberg, Germany). For the analysis 100.000 cells of the propidium iodide negative population were analyzed. The following Abs and secondary staining reagents were used for flow cytometric studies: FITC-conjugated rat anti-mouse Ly-6G (Gr-1: RB6-8C5), PE-conjugated rat anti-mouse CD19 (1D3), PE-conjugated hamster anti-mouse CD11c (HL3), FITC-conjugated rat anti-mouse CD4 (RM4-5), FITC-conjugated rat anti-mouse CD8a (53-6.7), PE-conjugated rat anti mouse Pan-NK-cell (DX5), FITC-conjugated rat anti-mouse CD45R/B220 (RA3-6B2), APC-conjugated rat anti-mouse CD11b (M1/70), PE-conjugated hamster anti-mouse CD3ε chain (145-2C11), PE-conjugated rat anti-mouse α-I-A/I-E (2G9) and FITC-conjugated rat anti-mouse α-CD80 (16-10A1), rat anti-mouse α-CD86 (GL1) or α-CD40 (3/23) , and appropriate isotype control Abs, streptavidin-FITC, streptavidin-PE (all from BD Pharmingen, Heidelberg, Germany), and FITC and PE-conjugated rat anti-mouse F4/80

(CI:A3-1) and PE-conjugated rat anti-mouse MARCO (ED31; Serotec, Oxford, UK). The specificity of the staining was verified by the use of isotype control mAbs.

2.6 Bone marrow-derived macrophages

Bone marrow derived macrophages (BMDM) were generated from total bone marrow cells. Marrow cells flushed from the femurs and tibias of mice, were seeded in 100 mm Petri dishes (Greiner, Wemmel, Belgium) with 40 ml of Dulbecco modified Eagle medium (DMEM) (Invitrogen, Karlsruhe, Germany), containing 10% v/v FCS (Sigma, Taufkirchen, Germany), 5% horse serum (Invitrogen, Karlsruhe, Germany), and 15% L929 mouse myeloma strain culture supernatant as a source of M-CSF and supplemented with Na-pyruvate at 1 mM (Biochrom, Berlin, Germany), 2 mM L-glutamine (Invitrogen, Karlsruhe, Germany), 100 U of penicillin per ml (Invitrogen, Karlsruhe, Germany), and 100 μg of streptomycin (Invitrogen, Karlsruhe, Germany), per ml. At day 8 the slightly attached cells were washed out with warm PBS. Subsequently the cells were harvested by incubation for 10 min with cold PBS (4°C). BMDM resuspended in DMEM medium without horse serum, L929 culture supernatant and antibiotics and used for infection experiments.

2.7 Phagocytosis assay

Twenty hours before infection, $3x10^5$ BMDM were seeded into 1 cm diameter tissue culture plates (Greiner, Wemmel, Belgium) on glass coverslips. Two hours before infection, the cells were washed twice and covered with Dulbecco modified Eagle medium lacking FBS, horse serum, L929 culture supernatant and antibiotic.

For some experiments BMDM were primed for 24 hours with a recombinant IFN-γ 50 ηg/ml (R&D Systems, Abingdom, UK).

Before infection, overnight cultures of different *Y. enterocolitica* strains were inoculated in LB medium at an optical density at 600 nm of 0.2 and grown for 2 h at 37°C with shaking. After washing in prewarmed phosphate-buffered saline (PBS), bacteria were added to the cells at a multiplicity of infection (MOI) of 50:1. The bacteria were sedimented onto the cells at 400 x *g* for 5 min. After an infection period of 30 min, bacteria associated with the target cells in intra- and extracellular locations were distinguished by the double-

immunofluorescence method as described previously (1, 2). To stain extracellularly located bacteria, the coverslips were first washed with PBS and incubated for 30 min with 1% BSA in PBS to prevent unspecific antibody binding. Then the coversplips were incubated for 45 min at RT with a polyclonal rabbit anti-Inv 3.1 antibody (diluted 1:100). Thereafter, the excess antiserum was removed by four washes in PBS and the coverslips were covered with FITC-conjugated goat anti-rabbit immunoglobulins (Dianova, Hamburg, Germany). After incubation for 30 min at room temperature, cells were washed four times in PBS. The cells were permeabilized by treatment with 2% Triton X-100 in PBS for 4 min, and washed again with PBS. To stain the intracellular and extracellular bacteria, the coverslips were incubated again with a polyclonal rabbit anti-Inv 3.1 antibody (diluted 1:100) for 45min at room temperature. The coverslips were then washed four times in PBS, overlaid with carbocyanin 5-conjugated goat anti-rabbit immunoglobulins (Dianova, Hamburg, Germany) and with tetramethyl rhodamine isothiocyanate-conjugated phalloidin (Sigma, Taufkirchen, Germany) to stain F-actin and incubated for 30 min at room temperature. Finally, after another washing, the coverslips were mounted in Fluroprep (bioMerieux, Marcy l´Etoile France) containing polyvinylic alcohol and glycerin and examined by fluorescence microscopy. Under these conditions, the extracellular bacteria were stained with both FITC and Cy5 and appeared green or blue, depending on the filter used, while intracellular bacteria were stained only with Cy5 and appeared only blue. The fluorescence images were obtained with a Leica DMRE HC fluorescence microscope (Leica, Wetzlar, Germany).

At least 100 cells were examined, and the number of extracellularly located bacteria and the total number of cell-associated bacteria was counted. For each condition, the experiments were done three times each in duplicate. The phagocytosis percentage represents the ratio of the number of intracellular bacteria to the total number of cell-associated bacteria.

2.8 Isolation of total RNA

The total RNA was isolated from the selected $CD11b^+$ cells from uninfected or infected mice using the Rneasy Mini-Kit following the manufacturer's instructions (Qiagen, Hilden, Germany).

In order to reduce the biological variability, the quality and the quantity of all of the RNA samples were assessed to ensure the highest reproducibility in the microarray experiments.
The absorbance was measured at 260/280 nm for both total RNA and biotinylated cRNA. Exclusively the samples with acceptable 260/280 nm ratios in the range of 1.9 to 2.1 were used for further microarray hybridization or for real time-PCR experiments.
Moreover, the quality of the RNA samples prepared for the microarray hybridization was measured by the Agilent 2100 Bioanalyzer - Bio Sizing. Exclusively the samples with optimal quality given by a low baseline, sharp 18S and 28S ribosomal peaks and with a ratio (28S:18S) of 2:1 were used for further analysis.

2.9 Reverse transcription real-time PCR

For independent confirmation of gene expression results, total cellular RNA was isolated by using Rneasy mini kits (Qiagen) at the indicated time points from CD11b positive cells from the spleens of infected and uninfected mice as described above. For reverse transcription, 1 µg of total RNA was mixed with 0.5 µg of oligo $(dT)_{12\text{-}18}$ primers (New England Biolabs, Frankfurt am Main, Germany), and DEPC-treated water was added to a final volume of 10 µl, followed by incubation at 65°C for 10 min. After adding 10 µl of a solution containing 5x First-Strand Buffer (Invitrogen, Karlsruhe, Germany) [250 mM Tris-HCl, 375 mM KCL, 15 mM $MgCl_2$], 20 mM dithiothreitol, 200 U SuperScript III (Invitrogen, Karlsruhe, Germany), 40 U RNaseOut (Invitrogen, Karlsruhe, Germany) and 2 mM dNTPs (Invitrogen, Karlsruhe, Germany), the mixture was incubated at 42°C for 60 min. Finally, the cDNA samples were heated at 90°C for 5 min, diluted 1:10 with DEPC-treated water and stored at –20°C until further use.
RNA preparations for RT-PCR were independent from those used for array hybridisations.
Real-time RT-PCR was carried out in duplicate in 96-well format on a GeneAmp 5700 Sequence Detection System (Applied Biosystems, Darmstadt, Germany). Each 20-µl reaction contained 10 µl Platinum Quantitative PCR SupeMix-UDG (Invitrogen, Karlsruhe, Germany), 0.4 µl ROX Reference Dye (Invitrogen, Karlsruhe, Germany), 3.6 µl PCR grade water, 1 µl target gene specific Assay-on-Demand Gene Expression Assay Mix (including primers and dye-labeled hybridization probes; Applied Biosystems, Darmstadt, Germany),

and 5 µl cDNA. Thermal cycling conditions for all reactions were as follows: 2 min at 50°C, 10 min at 95 °C, then 40 cycles of 15 s at 95°C and 1 min at 60°C.

Gene expression levels were recorded relative to the expression of the gene Ribosomal protein L8 (Rpl8) as: $E=2^{-\Delta\Delta CT}$ (E = gene expression value, $\Delta\Delta$CT = (Crossing point of gene of interest – Crossing point housekeeping) condition x – (Crossing point of gene of interest – Crossing point housekeeping) control. All PCR experiments were performed in duplicate, and standard deviations were calculated and displayed as error bars.

The unpaired, two-tailed Student t test was used (to compare differences between mean of semiquantitative real-time RT-PCR data.

2.10 Microarray experiments

2.10.1 One-cycle cDNA synthesis

Double-stranded cDNA was synthesized from the total RNA samples using a Superscript choice kit (Invitrogen, Karlsruhe, Germany) with a T7- (dT) 24 primer (Metabion, Planegg-Martinsried, Germany) incorporating a T7RNA polymerase promoter.

Poly-A RNA controls were used to monitor the entire target labeling process. *Dap, lys, phe, thr*, and *trp* are *B. subtilis* genes that have been modified by the addition of poly-A tails, and then cloned into pBluescript vectors, which contain T3 promoter sequences (GeneChip® PolyAControl Kit, Affymetrix, High Wycombe, UK). These poly-A controls spiked into the RNA sample, are carried through the sample preparation process, and evaluated like internal control genes. The final concentrations of these controls, relative to the total RNA population, were: 1:100000; 1:50000; 1:25000; 1:7500, respectively.

After purification, cDNA was used as templates to generate biotinylated cRNAs by *in vitro* transcription reactions with a Bio-Array High-Yield RNA transcript labeling kit (Enzo Diagnostics Inc., Farmingdale, N.Y.). Labeled cRNAs were subsequently fragmented by incubation at 94°C for 35 min in the presence of 40 mM Tris-OAc (pH 8.1), 100mM KOAc, and 30mM MgOAc.

At this step in order to improve the confidence of the hybridization procedure same biotinylated oligonucleotide were added to the hybridization cocktail (GeneChip® Eukaryotic Hybridization Control Kit, Affymetrix, High Wycombe, UK). This oligonucleotide

represent the genes *bioB, bioC, bioD,* present in the biotin synthesis pathway of *E. coli*, and *cre* a recombinase gene from P1 bacteriophage.
This biotin-labeled cRNA transcripts were included in staggered concentrations (1.5 pM, 5 pM, 25 pM, and 100 pM final concentrations for *bioB, bioC, bioD*, and *cre*, respectively) to evaluate sample hybridization efficiency. Moreover, one other oligonucleotide called B2 was included as a positive hybridization control to allow the analysis software to place a grid over the microarray image and to define the single probes position on the array.
The labeled, fragmented cRNA (15 µg) was hybridized for 16 h at 45 °C to a murine genome GeneChip® probe arrays MG-U74Av2 from Affymetrix (Affymetrix, High Wycombe, UK), comprising approximately 12600 mRNA transcripts from mouse genes and expressed sequence tags (ESTs).
After hybridization, arrays were automatically washed and stained with streptavidin–phycoerythrin using a Fluidics Station 400 (Affymetrix, High Wycombe, UK). The probe arrays were scanned at 3-µm resolution using a GeneChip Scanner 2500 (Affymetrix, High Wycombe, UK).
The Microarray Suite software (version 5.0), MicroDB and Data Mining Tool were used to scan and analyze the relative abundance of each gene based on the intensity of the signal from each probe set. Analysis parameters used by the software were set to values corresponding to moderate stringency (statistical difference threshold = 30, statistical ratio threshold = 1.5).

2.10.2 Microarray data analysis

Analysis of microarray data was performed using the Affymetrix Microarray Suite 5.0, Affymetrix MicroDB 3.0 and Affymetrix Data Mining Tool 3.0 (Affymetrix, High Wycombe, UK).

2.10.2.1 Assessing Data Quality

All of the probe arrays were carefully inspected to allow presence of image artifacts like: high/low intensity spots, scratches, high regional or overall background.

The hybridization efficiency was measured by analyzing the level of the assay sensitivity for the control *bioB, bioC, bioD*, and *cre*, prior mentioned. *BioB* is at the level of assay sensitivity (1:100000 complexity ratio) and should be called "Present" at least 50% of the time. *BioC, bioD*, and *cre* should always be called "Present" with increasing Signal values, reflecting their relative concentrations.
Furthermore the oligonucleotide B2 was used as a positive hybridization control and to place a grid over the images.
Furthermore to avoid incorrect analysis the Average Background and Noise (Raw Q) had been estimated. Exclusively arrays with an Average Background values range from 20 to 100 were used for further analysis.

2.10.2.2 Affymetrix Statistical Algorithms

The GeneChip® probe arrays analysis was performed using the Affymetrix Statistical Algorithms implemented in the Affymetrix® Microarray Suite Version 5.0 (Affymetrix, High Wycombe, UK).

2.10.2.3 Single Array Analysis

Signal Algorithm

The signal was calculated for each probe set, which represents the relative level of expression of a transcript. The signal was calculated using the One-Step Tukey's Biweight. Each probe pair in a probe set was considered as having a potential vote in determining the Signal value. The vote, in this case, was defined as an estimate of the real signal due to hybridization of the target. The mismatch intensity was used to estimate stray signal. The real signal was estimated by taking the log of the Perfect Match intensity after subtracting the stray signal estimate. The probe pair vote was weighted more strongly if this probe pair Signal value was closer to the median value for a probe set. Once the weight of each probe pair was determined, the mean of the weighted intensity values for a probe set was identified. This mean value was corrected back to linear scale and was output as Signal.

Detection algorithm

This analysis generates a Detection *p*-value, which was evaluated against user-definable cut-offs to determine the Detection call. This call indicates whether a transcript was reliably detected (Present) or not detected (Absent).
The Detection algorithm uses probe pair intensities to generate a Detection *p*-value and assign a Present, Marginal, or Absent call. Each probe pair in a probe set was considered as having a potential vote in determining whether the measured transcript was detected (Present) or not detected (Absent). The vote was described by a value called the Discrimination score [R]. The score was calculated for each probe pair and was compared to a predefined threshold Tau. Tau is a small positive number that can be adjusted to increase or decrease the sensitivity of the analysis (used value: 0.015). Probe pairs with scores higher than Tau vote for the *presence* of the transcript. Probe pairs with scores lower than Tau vote for the *absence* of the transcript. The voting result was summarized as a *p*-value. The greater the number of discrimination scores calculated for a given probe set that are above Tau, the smaller the *p*-value and the more likely the given transcript was truly Present in the sample.

Detection *p*-value

To calculate the statistical significance of the Detection we used the Discrimination score (R). This was a basic property of a probe pair that describes its ability to detect its intended target. It measures the target-specific intensity difference of the probe pair (Perfect Match-Mis Match) relative to its overall hybridization intensity (PM+MM):

$$\mathbf{R = (PM - MM) / (PM + MM)}$$

For example, if the PM is much larger than the MM, the Discrimination score for that probe pair will be close to 1.0. If the Discrimination scores are close to 1.0 for the majority of the probe pairs, the calculated Detection *p*-value will be lower (more significant). A lower *p*-value is a reliable indicator that the result is valid and that the probability of error in the calculation is small. Conversely, if the MM is larger than or equal to the PM, then the Discrimination score for that probe pair will be negative or zero. If the Discrimination

scores are low for the majority of the probe pairs, the calculated Detection *p*-value will be higher (less significant). The next step toward the calculation of a Detection *p*-value is the comparison of each Discrimination score to the threshold Tau. The One-Sided Wilcoxon's Signed Rank test was the statistical method employed to generate the Detection *p*-value. It assigns each probe pair a rank based on how far the probe pair Discrimination score is from Tau. The modifiable Detection *p*-value cut-offs, provide boundaries for defining Present, Marginal, or Absent calls. In our experimental setting the detection p-value of ≤0.04 was considered as present (P), a detection p-value of >0.04 and ≤0.06 was considered marginal (M) and a detection p-value >0.06 was considered absent (A).

2.10.2.4 Comparison Analysis (Experiment versus Baseline arrays)

In the second part of the analysis, two samples were compared against each other in order to detect and quantify changes in gene expression. Usually the array hybridized with RNA from uninfected samples was designated as the baseline and the other as an experiment. The analysis compares the difference values (PM-MM) of each probe pair in the baseline array to its matching probe pair on the experiment array. Two sets of algorithms were used to generate a change significance and change quantity metrics for every probe set. A change algorithm generates a Change *p*-value and an associated Change. A second algorithm produces a quantitative estimate of the change in gene expression in the form of Signal Log Ratio.

Before comparing two arrays we had scaled to the same target intensity the arrays in order to correct the possible variations between two arrays (used value: 150).

In this way the intensity of the probe sets from the experiment array were normalized to the intensity of the probe sets on the baseline array. When scaling is applied, the intensity of the probe sets (or selected probe sets) from the experimental array and that from the baseline array are scaled to the defined target intensity.

Change Algorithm

As in the Single Array Analysis, the Wilcoxon's Signed Rank test was used in Comparison Analysis to derive biologically meaningful results from the raw probe cell intensities on expression arrays. During a Comparison Analysis, each probe set on the experiment array

was compared to its counterpart on the baseline array, and a Change *p*-value was calculated indicating an increase, decrease, or no change in gene expression. Cut-offs were subsequently applied to generate discrete Change calls (Increase, Marginal Increase, No Change, Marginal Decrease, or Decrease).

Change *p*-value

The Wilcoxon's Signed Rank test uses the differences between Perfect Match and Mismatch intensities, as well as the differences between Perfect Match intensities and background to compute each Change *p*-value.
From Wilcoxon's Signed Rank test, a total of three, one-sided *p*-values are computed for each probe set. The most conservative value was chosen to determine the change call. That is the value that is closest to 0.5 which signifies that no change is detected. These are combined to give one final *p*-value which is provided in the data analysis output .
The *p*-value ranges in scale from 0.0 to 1.0 and provides a measure of the likelihood of change and direction. Values close to 0.0 indicate likelihood for an increase in transcript expression level in the experiment array compared to the baseline, whereas values close to 1.0 indicate likelihood for a decrease in transcript expression level. Values near 0.5 indicate a weak likelihood for change in either direction. Hence, the *p*-value scale is used to generate discrete change calls using thresholds.

Change Call

The final Change *p*-value described above is categorized by cutoff values. These cut-offs provide boundaries for the Change calls: Increase (I), Marginal Increase (MI), No Change (NC), Marginal Decrease (MD), or Decrease (D).
A change call of increase (I) was assigned with a median change p-value of ≤ 0.0025 and a change call of marginal increase (MI) was assigned at a median change p-value >0.0025 to 0.003. Change calls of marginal decrease (MD) were assigned at a median change p-value of ≥ 0.997 to <0.998 and a change call of decrease (D) was assigned at a p-value ≥ 0.998. All others were assigned no change (NC). Only those probe sets that had a change call other than NC in comparison to uninfected and were not absent in both

compared groups were retained. Probe sets with an increase but a detection call of A in the infected cells were also discarded.

Signal Log Ratio Algorithm

To estimate the magnitude and direction of change of a transcript when two arrays were compared (experiment versus baseline) the Signal Log Ratio (SLR) was used. The SLR is calculated by comparing each probe pair on the experiment array to the corresponding probe pair on the baseline array. This strategy cancels out differences due to different probe binding coefficients and is, therefore, more accurate than a single array analysis. As with Signal, this number was computed using a one-step Tukey's Biweight method by taking a mean of the log ratios of probe pair intensities across the two arrays.
The log scale used was base 2, making it intuitive to interpret the SLR in terms of multiples of two. Thus, a SLR of 1.0 indicates an increase of the transcript level by 2 fold and -1.0 indicates a decrease by 2 fold. A SLR of zero would indicate no change.
In our analysis setting the filtering of the results was performed as follows: signal $\log_2$ ratios (SLR) was calculated compared the expression of the infected experiments to the corresponding uninfected control for each time point. A median SLR greater than 1.5 or less than –1.5 was considered as significant change.
Since we use $\log_2$, the following formulas were used for calculation of the fold change:

$$\text{Fold Change} \begin{cases} 2^{\text{Signal Log Ratio}} & \text{SLR} \geq 0 \\ (-1) * 2^{-(\text{Signal Log Ratio})} & \text{SLR} \leq 0 \end{cases}$$

2.10.2.5 Gene cluster analysis

Output from the microarray analysis was merged with the Unigene or GenBank descriptor and saved as an Excel data spreadsheet.
For Cluster analysis the Genesis software was used, release 1.6.0 (Institute for Genomics and Bioinformatics, University of Technology, Graz, http://genome.tugraz.at). To analyze the relationships between the expression profiles in different conditions we performed hierarchical clustering by using average linkage clustering for the experiments. However, to analyze the eventual presence of gene groups with a similar expression profile the k-

means algorithmic had been used with a define number of clusters 10 and a maximum of 200 iterations.

The functional analysis and the categorization of the genes were based on the NetAffx database (http://www.NetAffx.com) and on the Gene Ontology database (http://www.geneontology.org) (9).

2.11 Statistical analyses

The significance of the differences among different groups was determined by the unpaired two-tailed Student's *t* test. *P* values < 0.05 were considered statistically significant.

Aim of the study

The first line of defence is innate immunity, which is composed of cells that engulf pathogens as well as cells that release potent signalling molecules to activate an inflammatory response and the adaptive immune system. Pathogenic bacteria have evolved a set of weapons, or effectors, to ensure survival in the host. *Yersinia spp*. use a type III secretion system to translocate some effector proteins, called Yops, into the host.
The aim of this study was to investigate how the *Yersinia outer proteins* influence the transcriptional response in cells of the innate immunity. In order to gain insight these complex interactions, CD11b positive cells were selected from spleen of C57BL/6 mice infected intravenously with a *Yersinia enterocolitica* wild type strain (pYV^+) and from mice infected with two different deletion mutants Δ*yopH* and Δ*yopP* strains.
We came to the decision to use the $CD11b^+$ cells as a model because this population has an essential role in the innate immune responses and furthermore as recently shown it is primarily affected by *Y. enterocolitica* during the early stage of infection by the direct injection of the Yops.
The CD11b, also called integrin alpha M, is a member of the integrin family, plays a role as transmembrane receptors for cell-adhesion. The CD11b molecule is part of the CD11b/CD18 heterodimer which is strongly expressed on myeloid cells (macrophages/monocytes, granulocytes and dendritic cells) and only weakly on NK cells and on a subset of B lymphocytes. It functions as a receptor for the complement component 3 (C3), the fibrinogen or for the clotting factor X.

The $CD11b^+$ cells can be efficiently selected via an anti-CD11b monoclonal antibody conjugated with magnetic particles. The cells are subsequently isolated from a heterogeneous cell suspension as a highly pure population via binding to a magnetic column. The use of this model gives us the possibility to analyze the actual influence of *Y. enterocolitica* infection on cells of the innate immune system directly in their natural microenvironment.
It has been clearly demonstrated that *Yersinia* infection leads to strong T cell responses, including activation and proliferation of CD4 and CD8 T cells, and that these T cells are involved in control of *Yersinia* (Autenrieth et al*.,* 1992a; Autenrieth et al*.,* 1993; Bohn et al*.,* 1996; 1998b; Noll and Autenrieth, 1996; Falgarone et al*.,* 1999a; Falgarone et al*.,*

1999b). These cells produced predominantly IFN-γ, and it seems that IFN-γ can activate macrophages which in turn might be able to kill pathogen. Moreover, it is not fully clear yet which of the IFN-γ-mediated antimicrobial mechanism are playing a role in cells of the innate immune during *Yersinia enterocolitica* infection.

To address these questions we performed a transcriptional analysis in splenic $CD11b^+$ cells isolated from *Y. enterocolitica* -infected IFN-γ receptor deficient mice.

Result and discussion

3.1 Virulence of Δ*yopP* and Δ*yopH* mutants after intravenous infection

To evaluate the role of YopP and YopH during the course of a *Y. enterocolitica* infection, groups of C57BL/6 female mice were intravenously infected with $5x10^4$ CFU of the *Y. enterocolitica* wild type strain O:8 pYV^+ or with a Δ*yopH* or Δ*yopP* mutants. The progression of the disease was pursued by counting the bacterial CFU number in the spleen 24 h and 72 h post infection.

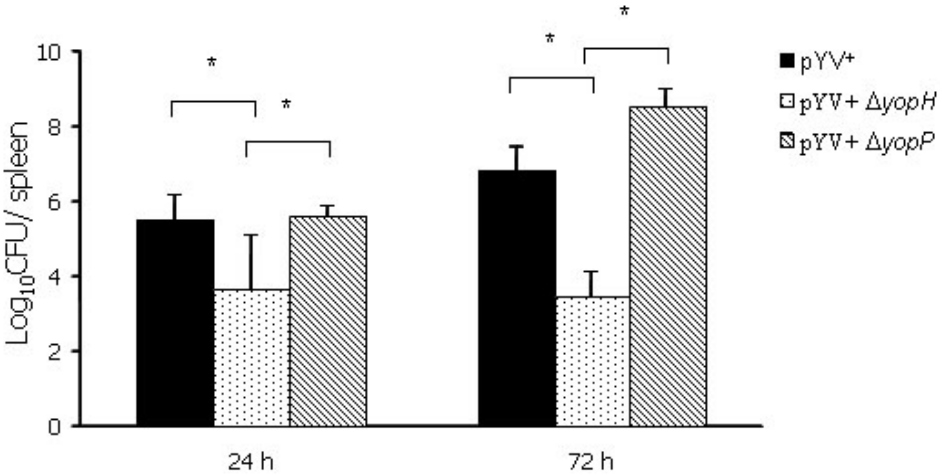

Figure 3.1 **Evaluation of the role of YopP and YopH in a *Y. enterocolitica* systemic infection.** C57BL/6 female mice 6-8 week-old were infected intravenously with $5x10^4$ CFU of a *Y. enterocolitica* wild type strain (pYV^+) or with a Δ*yopH* or Δ*yopP* mutants. The course of infection was monitored by counting the bacterial CFU number in homogenized spleens after 24 h and 72 h post infection. Values represent the average log_{10} CFU per spleen for fifteen mice with the standard errors of the means indicated by error bars. Asterisks indicate significant differences when compared CFU in C57BL/6 infected with the pYV^+ and Δ*yopP* strain vs Δ*yopH* infection ($p \leq 0.05$).

The wild type *Y. enterocolitica* pYV^+ showed high colonization rate of the spleen (5.52±0.62 log CFU) 24 h p.i. with a significant increase of the bacterial number in the organs after 72 h p.i. (6.83±0.65 log CFU).

Surprisingly, the deletion of YopP does not seem to attenuate the virulence of the bacteria. In contrast, the colony counts of the Δ*yopH* strain showed high virulence attenuation with more then 100-fold reduction in CFU compared to the wild type *Y.*

enterocolitica strain already after 24 h (3.67±1.38 log CFU) with a further clearance of the bacteria in the spleen after 72 h (3.47±0.65 log CFU).

In order to investigate the pathology further, the effects of the different *Y. enterocolitica* strains were compared by a detailed histopathologic analysis. The mice were sacrificed on day one and three post infection, and the spleens were removed for histological analysis. Consistent with the results obtained during the kinetic analysis, the microscopic pathology of the spleen showed significant difference between the diverse bacteria strains. Indeed, the mice infected with the wild type *Y. enterocolitica* and with the YopP deletion mutant showed the presence of high percentage of bacteria aggregate that appeared to be delimitate by inflammatory cells. This led to the formation of disseminated abscesses in the spleen with a complete disorganization of the tissue morphology 72 h p.i.. In contrast, the infection with Δ*yopH* strain displayed a complete different outcome. Rarely, and if so, only smaller amounts of aggregated bacteria were found in the spleen 24 hours post infection. Furthermore, the bacteria were rapidly cleared as shown by the histological analysis of the spleen 72 h p.i..

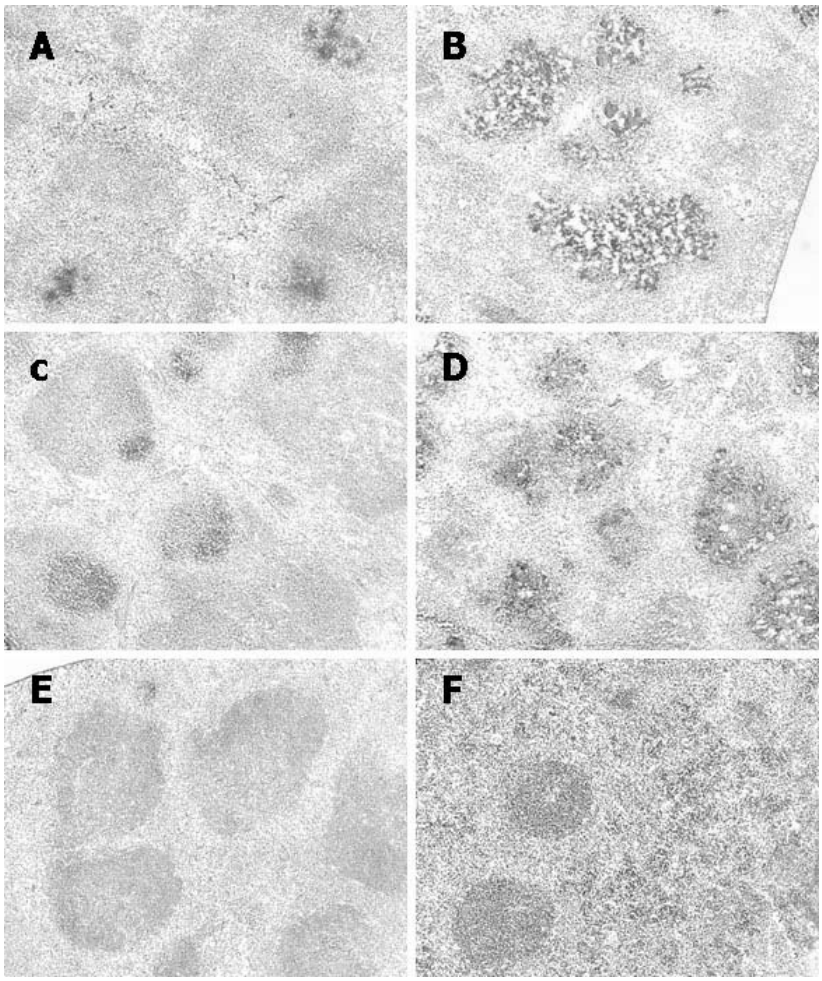

Figure 3.2 **Abscesses formation in a *Y. enterocolitica* systemic infection.** C57BL/6 female mice 6-8 week-old were infected intravenously with $5x10^4$ CFU of a *Y. enterocolitica* wild type strain (pYV^+) (Fig. A and B) or with the Δ*yopP* (Fig. C and D) or the Δ*yopH* mutants (Fig. E and F). The spleens were removed 24 h (Fig. A, C and E) and 72 h (Fig. B, D and F) post infection. Tissue sections were stained with an anti-*Y. enterocolitica* monoclonal antibody and with hematoxylin. The bacteria appear brown and the nuclei blue.

Surprisingly, these results suggest that the virulence factor YopP does not play a key role at the early stage of *Y. enterocolitica* infection. The high efficiency of YopP in gene silencing and in inducing apoptosis, demonstrated by several *in vitro* experiments, does not deliver a similar outcome *in vivo*.

On the contrary, the presence of YopH seems to be essential for a successful colonization of the host by *Y. enterocolitica* and to exhibit its entire virulent strength.

3.2 Composition of the splenic $CD11b^+$ cell population upon *Y. enterocolitica* infection

In order to gain insight into the complex gene expression pattern of the innate immune system upon *Y. enterocolitica* systemic infection, and to characterize the effects mediated by the injection of the *Yersinia outer proteins* YopP and YopH, microarrays representing 12000 genes were hybridized with labeled RNA isolated from CD11b positive cells immuno-magnetically enriched from spleens 24 h and 72 h p.i. and compared to the expression level of CD11b positive cells selected from spleen of uninfected control mice of the same age and sex.

For this aim, groups of six C57BL/6 female mice 6-8 week-old were infected intravenously with $5x10^4$ CFU of a *Y. enterocolitica* pYV^+ or with Δ*yopH* or Δ*yopP* mutants. The $CD11b^+$ cells were selected from the spleen cell suspensions (Fig. 3.2) of uninfected and infected mice. The purity and the composition of the isolated cell population was characterized by flow cytometry analysis (Table 1).

Figure 3.2A depict dot plots representing the CD11b positive fraction out of the total splenic cells population stained with an anti-CD11b antibody prior selection and after selection with the CD11b-conjugated magnetic beads. The purity of the isolated cells was analyzed by staining with APC-labelled anti-CD11b antibody and it is presented as histogram in the figure 3.3B.

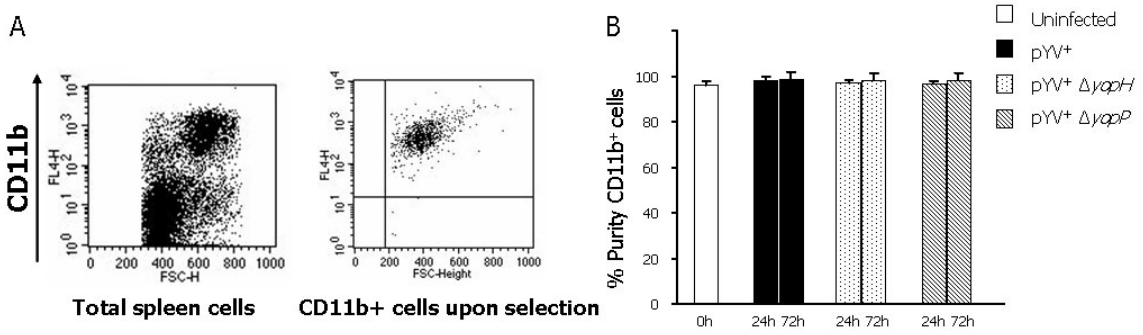

Figure 3.3 **CD11b$^+$ cells purity upon selection.** Fig.A Splenic single cells suspensions were prepared from uninfected and infected mice as reported in materials and methods. CD11b positive cells were positively selected by using magnetic beads conjugated with a monoclonal antibody against the surface marker CD11b. the CD11b$^+$ cells fraction prior and upon selection. Fig.B The purity of the cells was assessed by flow cytometry analysis. Values represent the average of the purity per samples with the standard errors of the means indicated by error bars.

The composition of each CD11b$^+$ cell population was characterized by double staining with APC-labeled anti-CD11b antibody and PE-labeled anti-DX5, anti-B220, anti-GR1, anti-CD11c or anti-F4/80 antibodies (Table 3.1). The main population of CD11b$^+$ cells comprised CD11b$^+$/F4/80$^+$ cells, CD11b$^+$/GR1$^+$ and CD11b$^+$/CD11c$^+$ cells representing macrophages, granulocytes and a subset of dendritic cells. Low amounts of CD11b$^+$/B220$^+$, CD11b$^+$/DX5$^+$ and CD11b$^+$/CD3$^+$ cells representing mainly B cells, NK cells and T cells were found. One day after infection with pYV$^+$ and with the Δ*yopP* strain, the amount of CD11b$^+$/GR1$^+$ as well as CD11b$^+$/DX5$^+$ cells increased in comparison with uninfected mice (approximately 1.5 fold) whereas the amount of CD11b$^+$/F4/80$^+$ and CD11b$^+$/CD11c$^+$ was still comparable to control CD11b$^+$ cells. Three days after the cell coposition was still similar in the infection with the wild type *Y. enterocolitica* and Δ*yopP* mutant strain Indeed, the amount of CD11b$^+$/GR1$^+$ cells was slightly lower compared to uninfected cells, while the amount of CD11b$^+$/F4/80$^+$ cells was significantly increased.

Interestingly, the CD11b$^+$ cells isolated upon infection with the Δ*yopH* strain showed a complete different composition. In total the amount of the CD11b$^+$/GR1$^+$ cells was significantly lower compared to wild type infection with an increasing tendency though out the timecours of infection. By contrast, there was never found a significant increase of CD11b$^+$/F4/80$^+$ cells upon 72 h p.i.. This finding seems to be in agreement with the different bacterial load in the spleen of mice infected with Δ*yopH*. The lower virulence of this strain leads to a lower amount of bacteria. This correlates with a lower influx of

$CD11b^+/GR1^+$ cells usually considered as neutrophils, the first defense line during a bacteria infection.

A total number of more than 100% cells is reached due to the existence of subsets of cell populations which are positive for more then two surface markers.

$CD11b^+$	DX5	CD3	B220	CD11c	F4/80	GR1
Uninfected	0.81±0.2	0.59±0.1	1.83±0.5	6.68±2.0	45.01±13.4	43.17±12.8
pYV^+						
24 h	1.26±0.1	1.62±0.2	1.50±0.1	6.89±2.6	43.46±4.0	69.33±9.0
72 h	2.42±2.3	2.10±1.6	2.86±1.3	14.37±11.2	59.38±1.7	36.67±3.1
Δ*yopP*						
24 h	5.5±0.8	1.77±2.1	2.29±0.1	11.57±2.6	33.4±4.8	60.89±2.7
72 h	1.56±1.5	1.1±1.1	3.94±0.9	8.55±1.4	49.61±11.4	30.78±19.1
Δ*yopH*						
24 h	1.56±0.1	1.40±1.5	2.49±0.07	16.75±2.7	51.57±28.5	44.94±13.4
72 h	1.85±0.4	1.55±0.5	3.62±1.6	7.78±5.0	45.19±25.30	65.61±1.07

Table 3.1 **Composition of the splenic $CD11b^+$ population after selection from mice prior and upon infection with *Y. enterocolitica*.** $CD11b^+$ cells selected from the spleen were stained with fluorophore-conjugated antibodies anti-CD11b, DX5, CD3, CD45R, CD11c, F4/80 and Ly6G. The cell composition was analyzed by flow cytometry. The percentage of the $CD11b^+$ cells positive for the indicated markers is shown in the table with the correspondent standard error.

3.3 Reprogramming of the $CD11b^+$ cells transcriptome in response to *Y. enterocolitica*

To characterize the effect on the transcriptional response in the innate immune system during a *Y. enterocolitica* infection, the $CD11b^+$ cells were isolated from the spleen of mice infected with the wild type bacteria strain pYV^+ and the total mRNA was hybridized on oligo-microarrays.

In order to minimize determinations of "false positive" or "false negative" results, exclusively, probe sets with an expression difference of at least of 3-fold (Signal Log Ratio

of ±1.5) between infected and uninfected mice were considered as significantly regulated (see materials and methods).

The expression signal analysis revealed the presence of 822 probe sets representative of 769 genes detected as differentially regulated, according to the applied filters, upon infection with *Y. enterocolitica* pYV^+ at least at one of the two time points investigated (Fig. 3.4; supplementary table 1). The 85.64% (704 probe sets) of the probe sets were significant regulated 24 h post infection. In particular, the 47.68% of the probe sets (392 probe sets) were significant induced in comparison with uninfected samples. Rather than the 37.95% (312 probe sets) was suppressed. The number of the modulated genes decreased significantly 72 h p.i. (410 probe sets). In detail, only the 31.02% (255 probe sets) of the total regulated probe sets were still significantly induced and the 18.85% (155 probe sets) still suppressed.

Presumably, this is the consequence of immune regulatory mechanisms, essential to control and to prevent an overreacting response. On other hand, the high number of regulated genes clearly indicates the efficient and prompt response of the innate immune system to *Yersinia* infection.

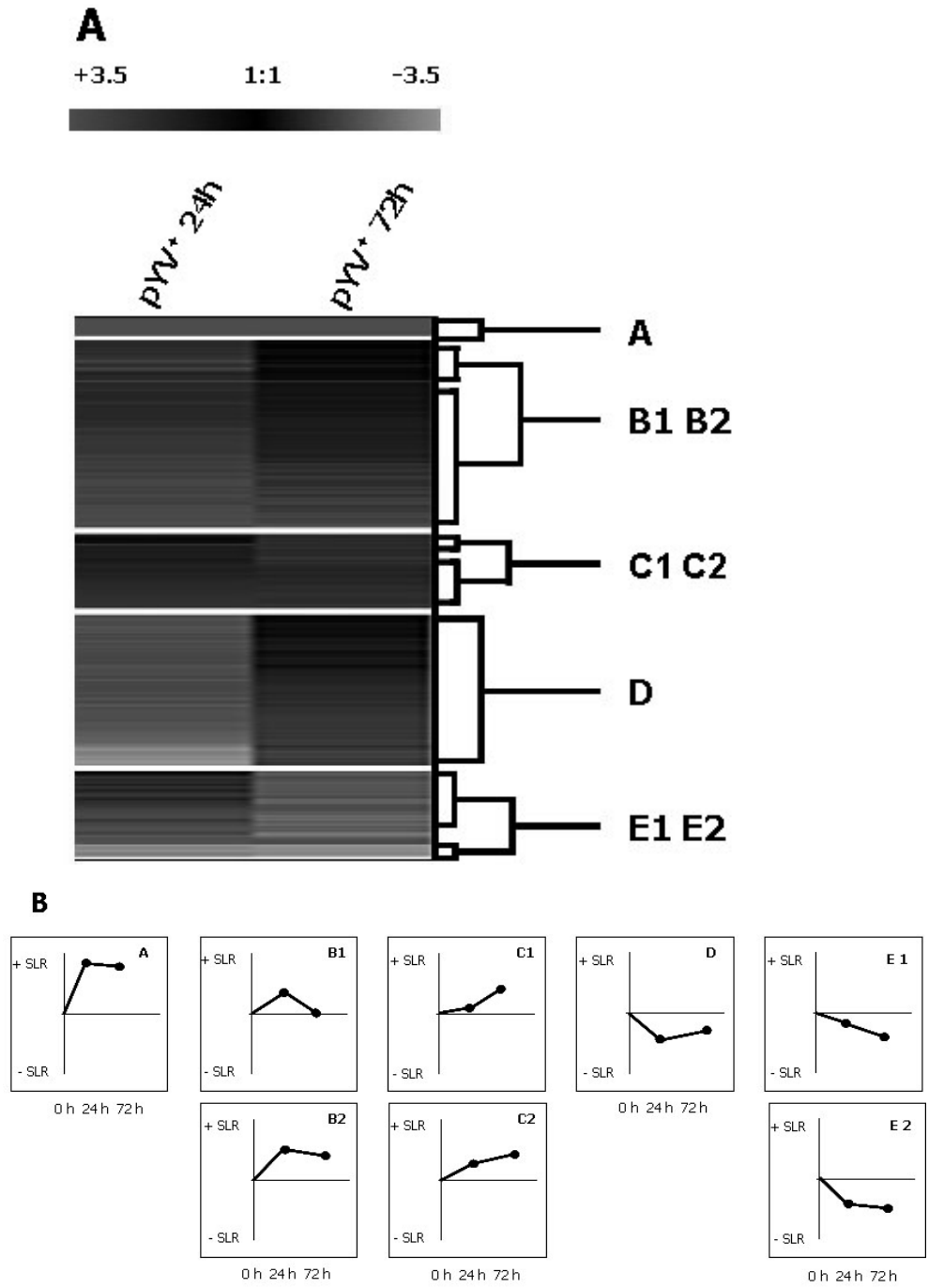

Figure 3.4 **K-means cluster diagram of 822 differentially expressed genes in splenic CD11b$^+$ cells upon systemic infection with *Y. enterocolitica* pYV$^+$.** Group of six C57BL/6 mice were intravenously infected with 5x10^4 CFU of *Y. e.* pYV$^+$. After 24 h and 72 h p.i. the CD11b$^+$ cell population was isolated from the spleen. The total RNA was hybridized on a murine genome GeneChip® probe arrays MG-U74Av2 (Affymetrix, High Wycombe, UK), comprising approximately 12600 mRNA transcripts from mouse genes and expressed sequence tags (ESTs). A group of 822 genes was differentially regulated at least at one of the indicated time points in comparison with the expression profile in splenic CD11b$^+$ cells selected from uninfected control mice. Fig. A The K-means algorithm was applied to the differentially regulated genes according to the signal log ratios to cluster co-expressed genes. Expression levels are colour coded, red indicates expression level above and green below the expression level of uninfected control mice. Group of co-expressed genes are indicated by letters. Fig. B Centroid view of the gene clusters (24 h p.i. and 72 h p.i.).

The K-mean algorithm was applied to the differentially regulated genes to identify genes with a common regulation profile (Genesis 1.6.0, Institute for Genomics and Bioinformatics, Graz University of Technology, Austria). This analysis revealed the presence of 5 major groups of commonly regulated genes (Fig.3.4).

Group A contains the strongest induced genes after *Y. enterocolitica* infection with a high expression at both time points investigated.

Considering the Gene Ontology categorization of all genes on the probe array used in our experiments, the number of genes involved in the inflammatory and immune response was remarkably high in this group. Indeed, several genes with cytokines activity ($p<4.4x10^{-15}$) like IL-1α, CXCL1 and a group of genes involved in the chemotaxis process ($p<7.8x10^{-14}$) like CXCL10, CXCL2 and CCL4 were represented by this group.

The majority of the induced genes could be clustered in the group B. This cluster contains genes that were highly induced after 24 h and consequently not longer (B1) or only weakly regulated (B2) 72 h post infection (Fig. 3.4 B).

This group is also significantly enriched with genes involved in the immune response ($p<2.1x10^{-38}$) and the inflammatory process ($p<2.9x10^{-14}$). Still significant is the presence of genes with chemokines activity ($p<7.2x10^{-9}$) and with chemokines receptor activity ($p<7.2x10^{-9}$). Notably, there are several cytokines in this cluster (TNF, IL-12, IFN-γ, IL-6) known to be essential for clearance a *Yersinia spp.* Infection (11, 13, 27, 28, 30, 50).

In the last few years it has been recognized that cells included in the myelomonocytic cells, including macrophages and dendritic cells (DCs), have a key role in polarized innate and adaptive responses. They can act by promoting the orientation of adaptive responses in a type I or type II direction, as well as by expressing specialized and polarized effector functions.

Intriguingly, several of the genes (CCL5, CXCL9, CXCL10, IL-12 and IFN-γ) that we found to be strongly induced upon *Y. enterocolitica* infection are known to trigger a polarization in a type I response. Furthermore, this evidence was supported by the observation that mRNAs encoding for several surface markers contributing to the formation of the "immunological synapse" (MHC class II, CD86, ITGAL, ICAM-1 and CD40) were significantly up regulated in our model. The expression of these molecules suggests that the $CD11b^+$ cells are implicated in the antigen presentation process, first step for the development of a specific adaptive immune response.

We could also demonstrate for the first time that the murine homolog of the human B7-H3, so called CD256, which is involved in the activation of T cells and in the induction of a potent IFN-γ production was expressed during *Yersinia* infection.

Intriguingly, this is a confirmation of our hypothesis that IFN-γ seems to play a crucial role in the modulation of the gene expression during *Y. enterocolitica* systemic infection. Proofing the hypothesis, several genes of the most important antimicrobial pathways triggered by IFN-γ signaling were induced upon *Yersinia* infection in the splenic $CD11b^+$ cell population. Factors such as the 2'-5' oligoadenylate synthetase 1G (OAS1), the adenosine deaminase, the RNA-specific (ADAR), protein kinase, the interferon-inducible double stranded RNA dependent (PRKR) and the nitric oxide synthase 2 (NOS2) were significantly induced upon infection.

Furthermore, the highly expression also of the cytoplasmic transcription factor STAT-1 is a good example of this process. STAT-1, if it is phosphorylated in response to the activation of the interferon gamma receptors, forms homodimer that is translocated to the nucleus, and binds on the GAS (gamma activation site) elements present in the promoter of the IFN-γ-responsive genes. This leads to the transcription of several genes that are responsible for the antimicrobial activity of interferon gamma.

Recently, a new family of IFN-γ-induced genes has been discovered that includes important mediators of host resistance to intracellular bacteria (39, 96, 153). This family is called IFN-responsive GTPase and includes the p47 and the p65 guanylate-binding protein (GBP), the myxovirus resistance GTPase and the very large inducible GTPase (VLIG). These proteins are highly expressed in a variety of hematopoietic and non-hematopoietic cells following infection with intracellular-bacteria and parasite in an IFN-dependent manner. Intriguingly, we demonstrated that all of the six characterized murine p47 family members [IGTP (interferon gamma induced GTPase), LRG-47 (interferon inducible protein 1, IFI1), IRG-47 (interferon gamma inducible protein 47, IFI47), TGTP (T-cell specific GTPase), IIGP1 (interferon inducible GTPase 1), and GTPI (interferon inducible GTPase 2, IIGP2)], two of the p65 family members [GBP2 (guanylate nucleotide binding protein 2) and GBP3 (guanylate nucleotide binding protein 3)] and the Mx1 (myxovirus resistance 1) were induced in our *Y. enterocolitica* infection moldel. While their precise function is unknown, each encodes for a protein with a guanosine 5’ triphoshatase activity that has a potent antimicrobial activity. All these gene products can bind to subcellular membranes,

including the endoplasmic reticulum (ER) and the Golgi apparatus and probably they play a role in the host cell trafficking and in promoting the phagosome maturation.

Furthermore, also some genes (SOCS1, SOCS3 and CISH) know to act as regulatory factors of the IFN-γ response were up-regulated by *Yersinia* infection. Recent studies had demonstrated that the expression of these proteins results in the inhibition of JAK/STAT-mediated cytokine signaling. Probably the activation of this classic negative feedback loop is necessary to avoid an over activation of the host response.

Interestingly, the group B is also highly enriched for genes of the apoptosis pathway ($p<2.2x10^{-13}$); in particular a group of them show caspase activity ($p<1.1x10^{-11}$) (Casp1, Casp7, Casp8 and Casp11). Furthermore, several of these genes are involved in the Caspase 8-mediated apoptosis pathway, in particular FAS (TNF receptor superfamily member), Daxx (Fas death domain-associated protein), TNFSF10 (tumor necrosis factor ligand superfamily, member 10, old name TRAIL) APAF1 (apoptotic protease activating factor 1) RIPK1 (Rip) receptor (TNFRSF)-interacting serine-threonine kinase and TRAF1 (Tnf receptor-associated factor 1). This apoptosis pathway seems to be directly activated by *Y. enterocolitica* via the injection of the virulence proteins Yops to counteract the response of the host cells.

On the other hand, some anti-inflammatory factors like IL-6, IL-1RA (interleukin 1 receptor antagonist) were also highly induced. Probably the play a role in regulate the activation of the cell host response The exact role of IL-6 in innate immunity remains unclear but, as previous studies demonstrated in a *Y. enterocolitica* infection, the regulation of the inflammatory responses before serious tissue damage seems to be required for a correct immune response (50). Indeed, the reduction of the IL-1-mediated inflammatory responses at the site of infection by means of induction of IL-1RA (interleukin 1 receptor antagonist) in response to *Y. enterocolitica* infection may be a key role of IL-6 (50, 87, 97, 151).

The third group of induced genes (cluster C) includes genes that are higher expressed at day 3 p.i. rather than at day 1 p.i.. This group includes mostly surface receptors such as colony stimulating factor 2 receptor beta 1, LIFR, CCR5 or FcR or the scavenger receptor SCARBP as well as genes encoding transcription factors or genes involved in signaling such as NF-IL, MEKK1, and JAK3.

The infection with *Y. enterocolitica* leads also to suppression of a great number of genes in splenic $CD11b^+$ cells. As shown in figure 3.4, these genes are clustered in the group D

and E. Genes with metabolic function and general cellular process are predominant in these groups. In particular lipid metabolism ($p<4.7x10^{-3}$), fatty acid metabolism ($p<3.4x10^{-5}$) and sterol biosynthesis ($p<1.0x10^{-7}$) are the most represented functional pathways. Taken together these data show a remarkable shift of expressed genes during an immune response in dependency of their functions. The expression of genes with general cellular and metabolic function was significantly reduced in favor of mediators of the immune response.

Interestingly, the expression of the mRNA encoding for interleukin 4 was strongly suppressed in our systems. IL-4 is a potent inducer of Th2 responses. Probably, the suppression of IL-4 and the induction of genes such as IL-12 and IFN-γ might facilitate a polarization towards a Th1 response, essential in *Y. enterocolitica* infection.

3.4 Modulation of the gene expression by YopH and YopP in *Y. enterocolitica* infection

The main focus of this study was to investigate if and how the lack of certain Yops can modulate the gene expression of cells of the innate immune system *in vivo*. For this aim C57BL/6 mice were infected intravenously with $5x10^4$ CFU of two *Y. enterocolitica* strain pYV$^+\Delta$*yopP* and pYV$^+\Delta$*yopH* lacking the virulence factors YopP and YopH, respectively.
The gene expression analysis was performed as reported in material and methods. To define the differentially regulated genes the expression levels obtained with the deletion mutant strains was compared to the expression levels upon wild type infection.
Average linkage hierarchical clustering was applied to the regulated genes (more than 3-fold regulated in comparison with uninfected mice) for each bacteria strain at each time point investigated (Figure 3.5).

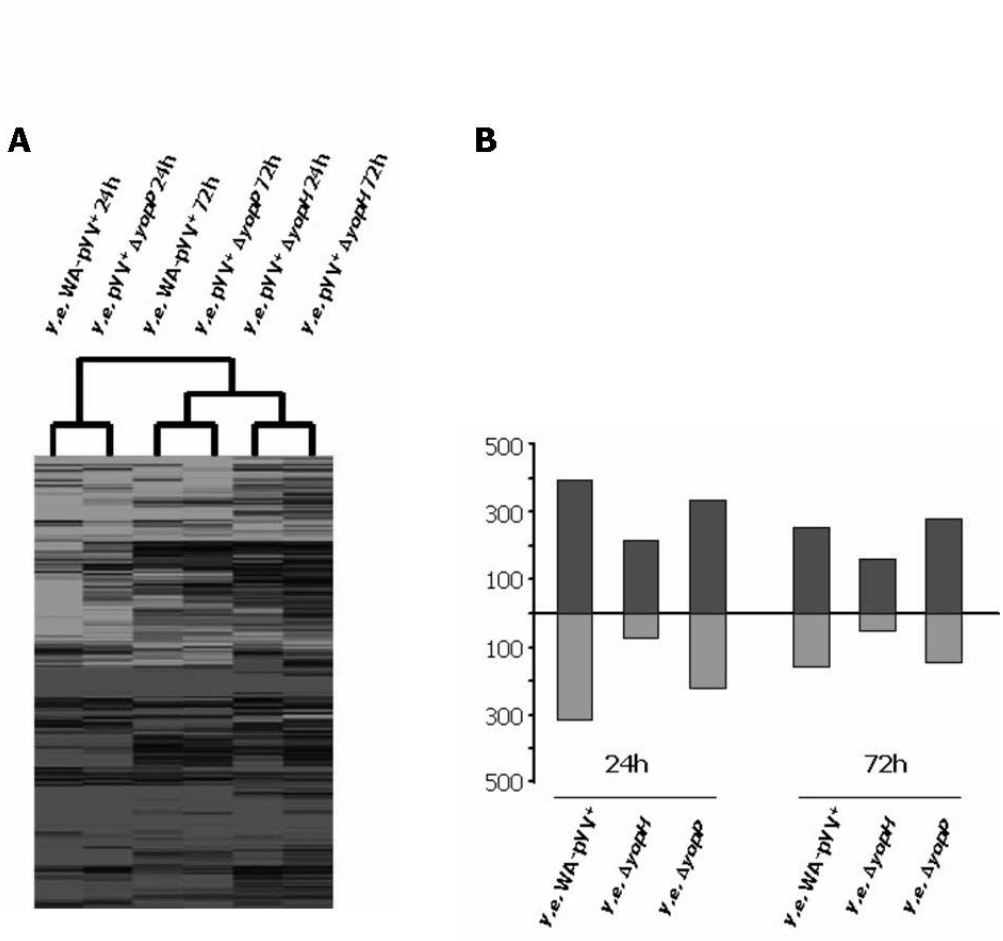

Figure 3.5 **Modulation of gene expression by the *Y. enterocolitica* virulence factors YopH and YopP.** Groups of six C57BL/6 mice were intravenously infected with $5x10^4$ CFU of *Y. e.* pYV$^+$ or pYV$^+\Delta$*yopH* or pYV$^+\Delta$*yopP*. 24 h and 72 h p.i. the CD11b$^+$ cells population was selected from the spleen. The total RNA was hybridized on a murine genome GeneChip® probe arrays MG-U74Av2 (Affymetrix, High Wycombe, UK). Fig.A Probesets which are

displayed fulfilled the following criteria: for at least one of the indicated groups the change in gene expression as shown as Signal log_2 ratio (SLR) was >1.5 or < -1.5 compared to gene expression in uninfected control mice. The hierarchical algorithm was applied to the differentially regulated genes according to the signal log ratios to cluster co-expressed genes. Expression levels are colour coded, red indicates expression level above and green below the expression level of uninfected control mice.Fig. B The bars represent the numbers of the differentially expressed probe sets between the infected mice and uninfected control mice.

This algorithm, applied according to the signal log ratio of all differentially expressed genes, revealed that the transcriptional responses after infection with pYV^+ and $pYV^+\Delta$*yopP* are closely related whereas the profile of the bacteria that lack YopH is clearly segregated suggesting that this virulence factor may play an essential role during *Yersinia* infection (Fig. 3.5 A). In line with these finding the numbers of the regulated probe sets at day 1 (289 probe sets) and at day 3 p.i. (211 probe sets) with $pYV^+\Delta$*yopH* versus uninfected are much lower compared to the amount of probe sets regulated upon infection with pYV^+ (day 1, 704 and day 3,501) or with Δ*yopP* (day 1, 558 and day 3, 433) as shown in figure 3.5 B.

Probe sets regulated		**24 h**			**72 h**		
		pYV^+	**Δ*yopH***	**Δ*yopP***	**pYV^+**	**Δ*yopH***	**Δ*yopP***
1	**Induced**	392	218	336	255	159	281
	Suppressed	312	71	222	155	52	142
	Tot	704	289	558	410	211	433

Table 3.2 Probe sets more than 3-fold regulated in splenic $CD11b^+$ cells compared to uninfected control mice.

3.4.1 Modulation of gene expression by YopP

A detailed analysis revealed the presence of 66 probe sets that were found to be differentially expressed during the infection with the Δ*yopP* strain compared to the infection with the wild type *Yersinia* strain (supplementary table 2). Interestingly, we did not find genes indicating suppression of a pro-inflammatory response and no genes indicating apoptotic processes known to be influenced by YopP *in vitro*.

The lacking of apoptosis occurrence correlates with the finding that in the presence of YopP high expression of the cell cycle inhibitors p21WAF1 (CDKN1A) and p27 KIP1

(CDKN1B) was found *in vivo*, while the expression of these genes is lower in the absence of YopP. Like other cells of the immune system, macrophages are produced in large amounts during the course of an infection. To prevent an accumulation and to fine regulate their activity most of them die through apoptosis if not functionally activated. Recently, Xaus et al. had proved that IFN-γ is one of the most powerful soluble factors in protecting macrophages from apoptosis via induction of the cyclin-dependent kinase (cdk) inhibitor, p21WAF1 (167, 21). Probably the strong activation that macrophages received at the inflammatory loci, during *Y. enterocolitica* infection is sufficient to overcome the activation of the apoptosis process mediated by YopP. However, further studies are necessary to clearly understand this process and to define the real role of this virulence factor *in vivo*.

3.4.2 Modulation of gene expression by YopH

These findings clearly suggest that the absence of the bacterial factor YopH leads to a complete different transcriptional response in cells of the innate immune response. This is probably correlated with the diminished virulence of the bacteria strain lacking YopH that may facilitate the clearance of the bacteria at the site of infection.

To follow up more specifically these differences, we compared directly the gene expression profile obtained upon infection with YopH deletion mutant to the expression level of the wild type strain infection. Thus a group of 354 probe sets representing 343 genes were more than 2-fold differential expressed in *Y.e.* pYV^+ versus $pYV^+\Delta yopH$ infected mice.

Interestingly, this group was significantly enriched of genes involved in the immune response ($p=<7.1x10^{-11}$) and in the inflammatory response ($p=<2.1x10^{-13}$), with a significant presence of genes with chemokine activity ($P=<2.1x10^{-9}$) and chemokine receptor activity ($P=<2.7x10^{-14}$).

The expression of the mRNA encoding for several cytokines (IL-6, IL-1α, IL-12a, IFN-γ, IL-15, TNF, CCL5, CXCL1 and CXCL9) and for pro-inflammatory factors such as CD14, COX2, NOS2 was much weaker upon infection with Δ*yopH* compared to infection with pYV^+.

To confirm these array-based gene expression data independently, we performed Real-Time quantitative PCR (RT-qPCR) for some representative genes (IL-1α, TNFα, IFN-γ and

IL-12a). RNA preparations for RT-PCR were independent from those used for array hybridizations. As shown in Figure 3.6, the overall expression pattern could be confirmed for every gene. There were, however, some negligible differences in the extent of increase in mRNA levels between RT-qPCR and array data.

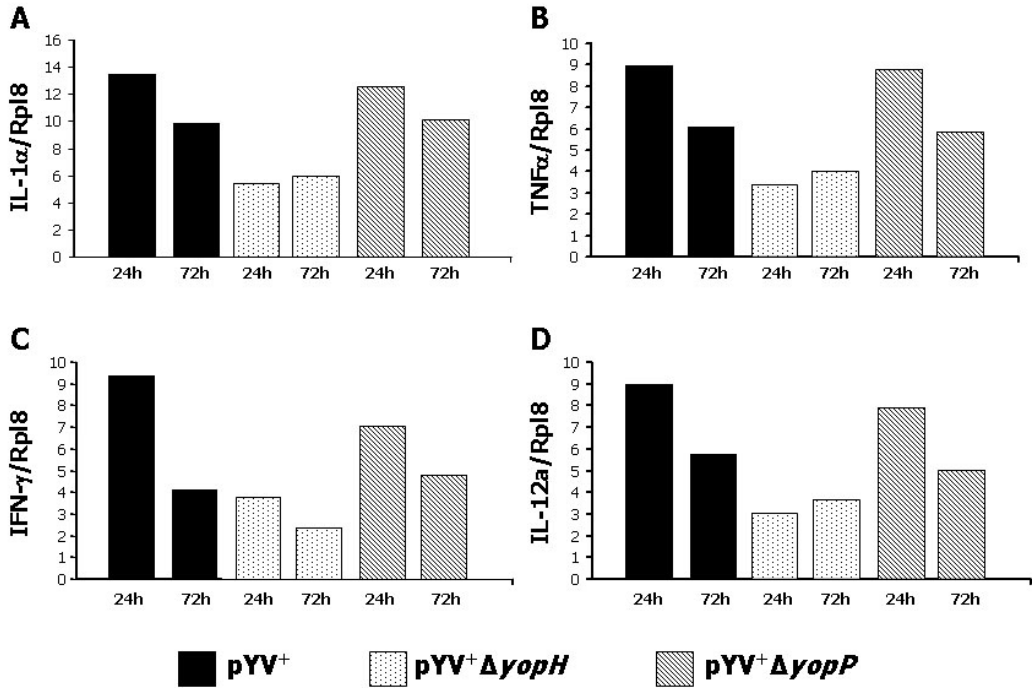

Figure 3.6 **Quantification of mRNA expression by Real time-PCR.** The mRNA expression of IL-1α, TNFα, IFN-γ and IL-12a in splenic CD11b$^+$ cells isolated from C57BL/6 mice upon intravenous infection with 5x10^4 CFU of *Y. e.* pYV$^+$ or pYV$^+$Δ*yopH* or pYV$^+$Δ*yopP*. 24 h and 72 h p.i. the CD11b$^+$ cells population was selected from the spleen. The mRNA expression of the indicated genes was analyzed by semiquantitative RT-qPCR. The bars represent mean values of the $\log_2$ of the fold difference between infected and control mice normalized to the expression level of the control gene RPL8.

Furthermore, several genes encoding for receptors and costimulatory molecules involved in the formation of the immunological synapses were significantly lower expressed upon Δ*yopH* infection. In order to verify these data, the expression of some surface markers known to be induced on activated dendritic cells and macrophages (antigen presenting cells APCs) was evaluated. Single cell suspension isolated from spleen of mice infected with 5x10^4 CFU of *Y. e.* pYV$^+$ or with pYV$^+$Δ*yopH* at 24 h p.i. were stained with fluorophore-conjugated antibodies anti-MHCII, CD40, CD80 and CD86, and the presence of these surface molecules was examined by flow cytometry.

The expression levels of the MHC class II receptors and of the co-stimulatory molecules CD86, CD80 and CD40 increased on both macrophages and dendritic cells upon wild type

Y.e. infection (Fig. 3.7). Therefore we could conclude that the systemic infection with the wild type *Y. enterocolitica* strain induced a strong activation of the antigen presenting cells (APCs). The increased expression of these latter molecules suggests that the APCs might be competent to interact with T cells to activate an adaptative immune response.

Conversely, the Δ*yopH* infection induced just a moderate increase of these surface molecules, revealing an incomplete activation of the innate immune response

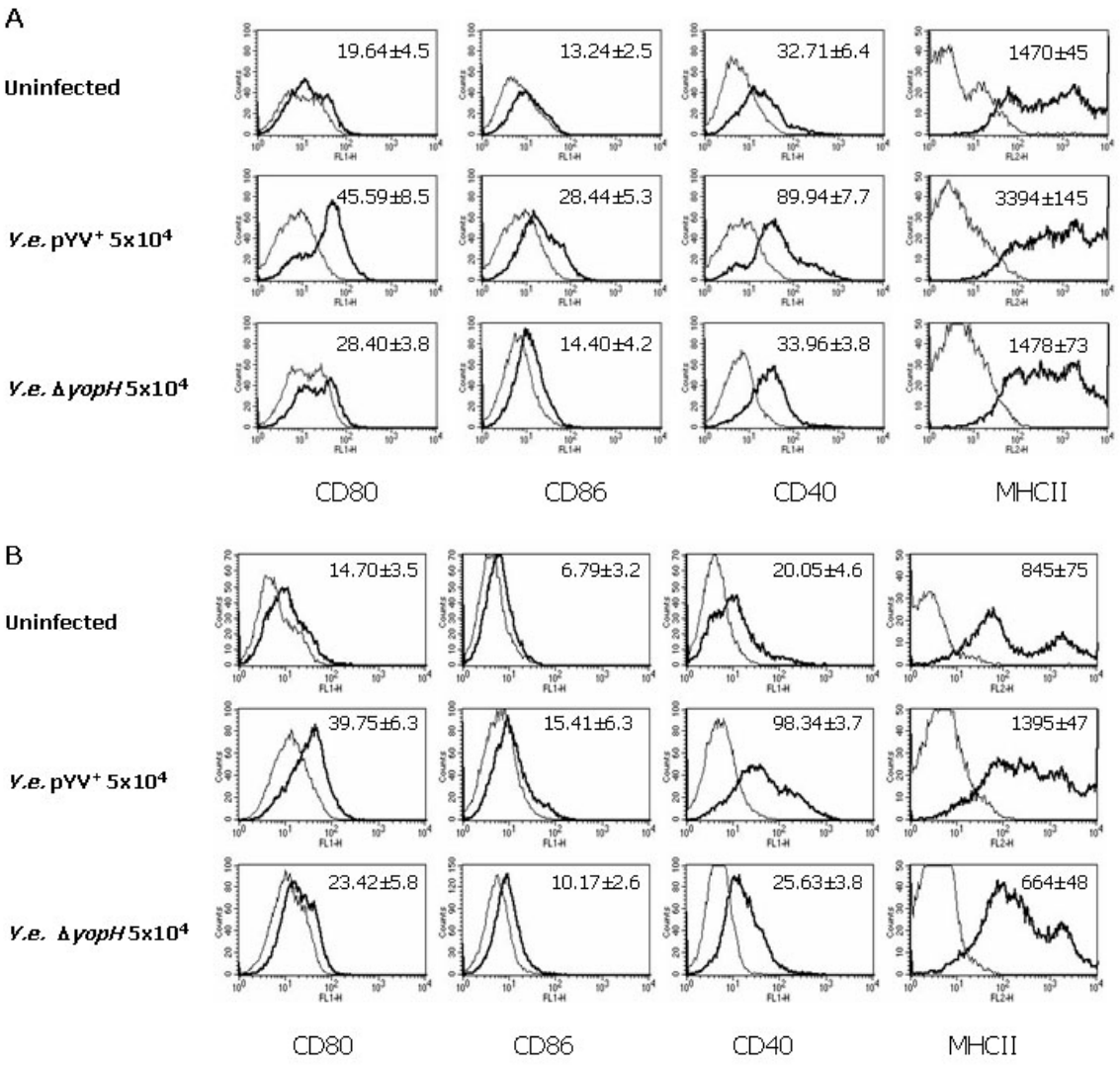

Figure 3.7 **Expression of MHC class II and co-stimulatory molecules by splenic dendritic cells and macrophages after infection with *Y. enterocolitica*.** Splenocytes were isolated upon 24 h p.i. infection with the indicated *Y. enterocolitica* strains. The cells were stained with CD11b, CD11c, F4/80 and Gr-1 to differentiate dendritic cells (Fig.A) and macrophages (Fig.B). Subsequently the expression of surface molecules like MHC class II, CD86, CD80 and CD40 (thick lines) or isotype-matched control IgG (thin lines) was assessed by flow cytometry gating on the propidium iodide negative population. In the histograms the differences between the mean fluorescence intensity (MFI) values of specific antibodies to isotype controls are indicated ± SD of 3 independent experiments.

3.4.2.1 Inflammatory cells influx in the spleen upon *Y. enterocolitica* systemic infection

Once an inflammatory response is initiated, neutrophils and macrophages are the first cells to be recruited to the site of infection. Chemotaxis of phagocytes proceeds into the site where phagocytosable material occurs. This is regulated by chemotactic factors generated by infectious agents themselves, as well as those released as a result of their initial contact with phagocytes and other components of the immune system.

As previously mentioned, our microarray data indicate that the infection with the bacteria lacking the expression of YopH leads to a different modulation of the transcriptional levels of several chemotactic factors. For example, chemokines and interleukins such as CXCL1, CXCL2, CCL2, CCL3, CCL4, CCL5, IFN-γ and IL-6 were significantly lower expressed in the mice infected with Δ*yopH* in comparison to the other two strains expressing this crucial virulent factor.

In order to elucidate whether this different transcriptional response was actually, associated with a discrepant recruitment of inflammatory cells in the spleen upon *Yersinia* infection, analysis of the different cell populations present in this organ was performed by flow cytometry (FACS) (Fig. 3.8 and Fig. 3.9).

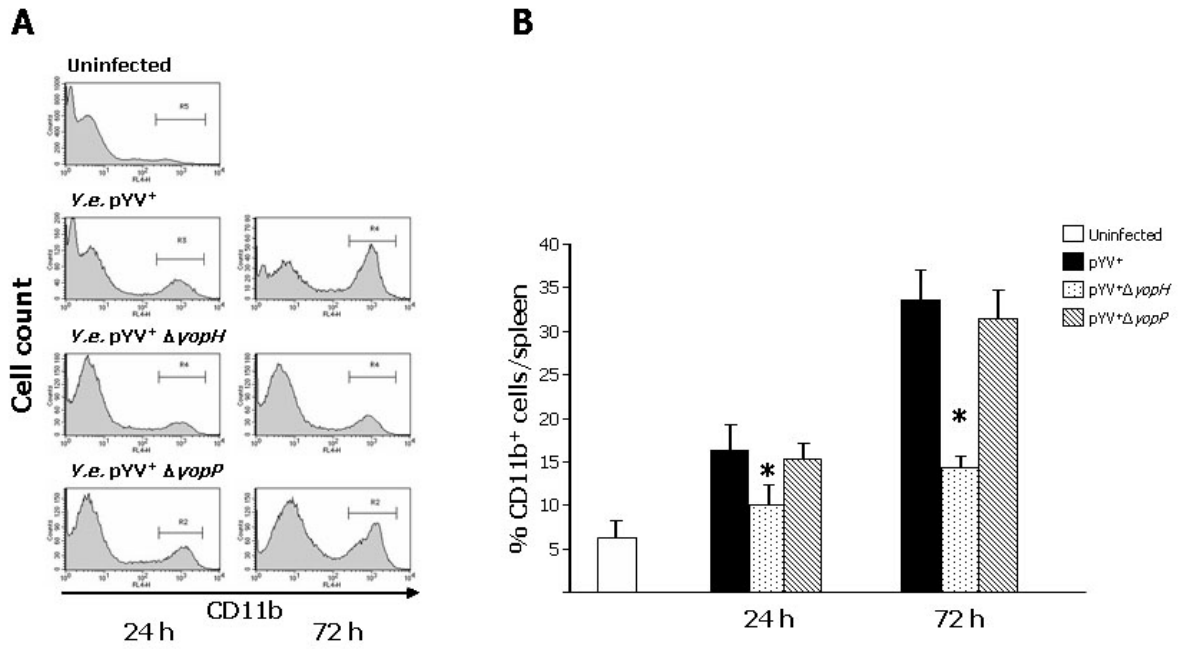

Figure 3.8 **CD11b$^+$ cells influx in the spleen of *Yersinia*-infected mice.** The relative number of the CD11b$^+$ cells from naive mice or mice intravenously infected with 5x10^4 CFU of *Y. enterocolitica* pYV$^+$ or pYV$^+$Δ*yopH* and or pYV$^+$Δ*yopP* was assessed by flow cytometry. FigA. The dot plots are representative of 3 independent experiments. Fig.B The bars represent mean values ±SD from 10 mice. Statistically significant differences compared pYV$^+$Δ*yopH* versus wild type *Yersinia* infection are indicated with an asterisk (p≤ 0.05).

Figure 3.8 shows histograms indicating of the increased amount of CD11b positive cells in the spleen upon infection. In line with the lower induction of chemotactic cytokines, a significant low influx of inflammatory cells in the spleen of mice infected with the bacteria lacking the virulence factors YopH was found. Upon infection with the wild type *Yersinia* and with the bacteria that lack YopP, the CD11b$^+$ cells augment more than three-fold at 24 h post infection with an ongoing influx of cells, that has been constant throughout the progression of the disease and reached 30% of the total splenic cells after 72 hours.

To define which cell type was mainly involved in this process, single-cell suspensions from spleen were stained with marker-specific fluorophore-conjugated antibodies (Abs), and the number of polymorphonuclear leukocytes (CD11b high, Gr-1 high and F4/80 negative) and macrophages (CD11b high, Gr-1 low and F4/80 high) was estimated (Fig. 3.9).

Neutrophils have the earliest detectable change in abundance, whereas changes in macrophages numbers appeared a couple of days thereafter. Neutrophils, which are rare in the spleen of naive mice, undergo a 10-fold increase in absolute number by day one

post infection in both wild type *Y. enterocolitica* and Δ*yopP* infection. A similar increase in the number of macrophages was also observed upon infection with delay in the expansion of the population that increased 3-fold more than neutrophils after 72 h (Fig. 3.9).

In agreement with the gene expression data, the mice infected with the Δ*yopH* strain showed no significant influx of macrophages one day p.i.. Only after 72 h a slightly increase of these cells was observed but still significantly lower in comparison with the two other *Yersinia* strains expressing the virulence factor YopH.

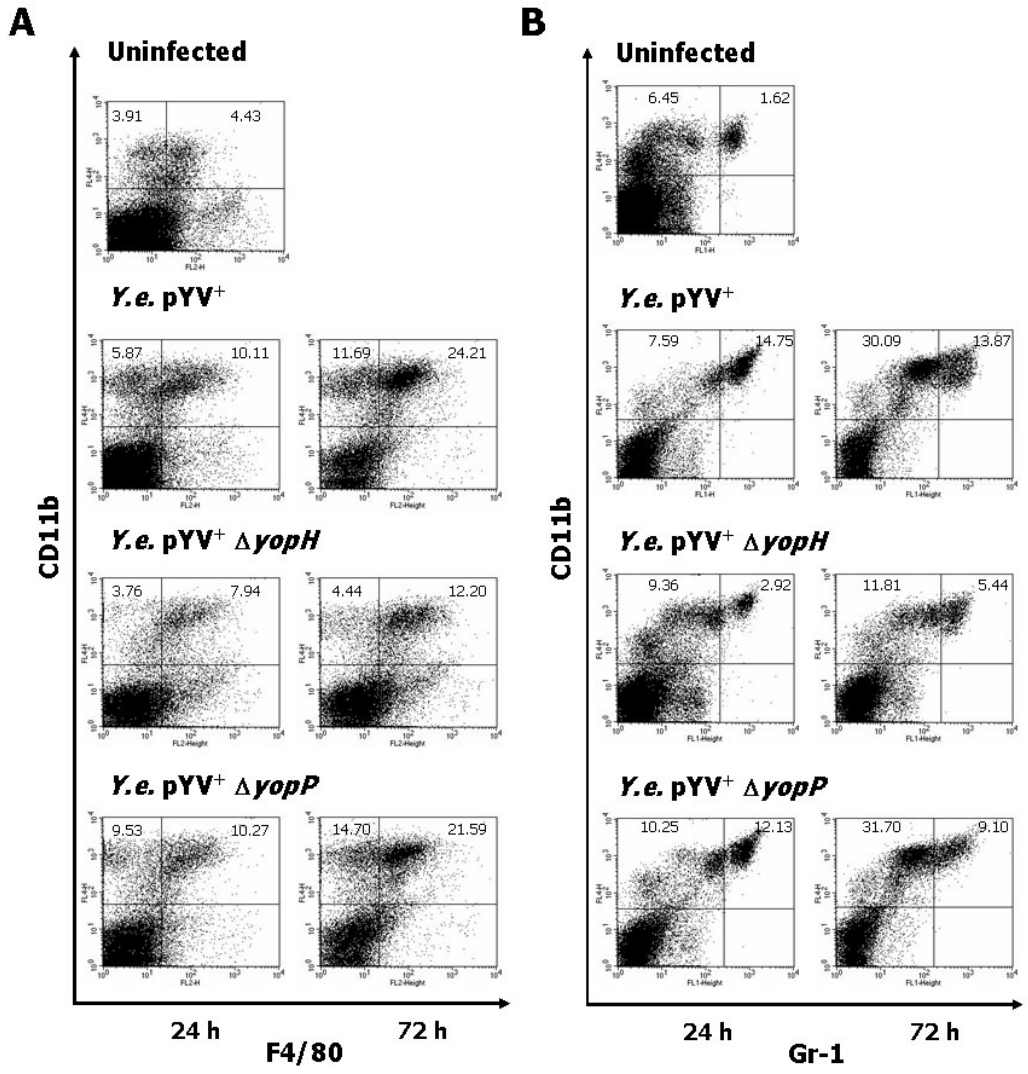

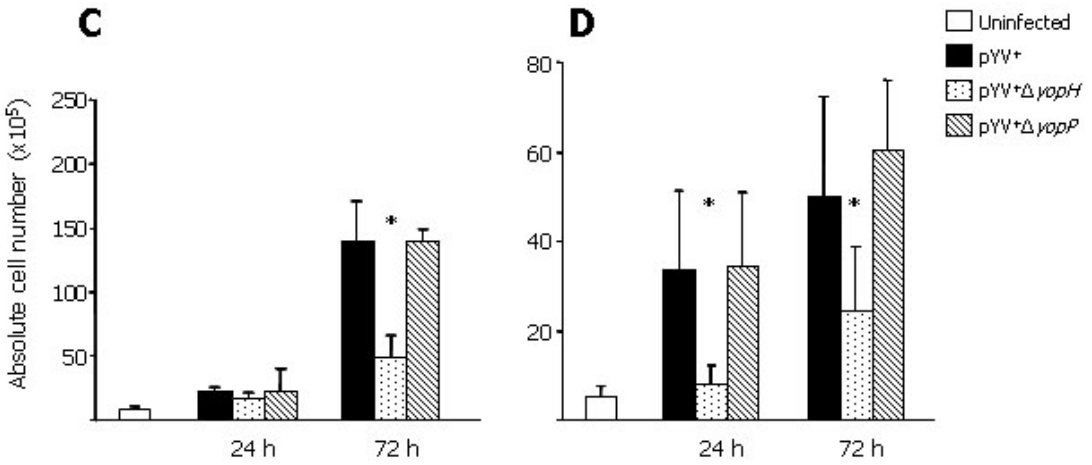

Figure 3.9 **Influx of phagocytic cells in the spleen of naive and of *Yersinia*-infected mice.** The absolute number of the indicated cell populations within total splenocytes from naive mice or mice intravenous infected with $5x10^4$ CFU of *Y. enterocolitica* pYV^+, $pYV^+\Delta yopH$ and $pYV^+\Delta yopP$. The cell populations were defined as follows: neutrophils ($CD11b^{high}$, $Gr\text{-}1^{high}$), and macrophages ($CD11b^{high}$, $F4/80^{high}$, $Gr\text{-}1^{intermediate}$). The bars represent mean values ±SD from 10 mice. Statistically significant differences compared $pYV^+\Delta yopH$ versus wild type *Yersinia* infection are indicated with an asterisk ($p \leq 0.05$).

3.4.2.2 Definition of a YopH specific signature

As a consequence of the reduced virulence of the *Yersinia enterocolitica* Δ*yopH* strain, the bacterial abundance in the spleen already at 24 h p.i. was 100-fold lower compared to that observed in the wild type infection (Fig. 3.1). These findings lead us to the suggestion that the weaker immune response after infection with Δ*yopH* is associated with the lower bacterial load. To investigate whether this is the case, C57BL/6 mice were infected intravenously with $5x10^3$ CFU of the *Y.e.* pYV^+ or $5x10^6$ CFU of the Δ*yopH* mutant strain which resulted in the same bacteria number in the spleen 24 h p.i., respectively (4.5±0.4 and 4.8±0.6) (Fig.3.10).

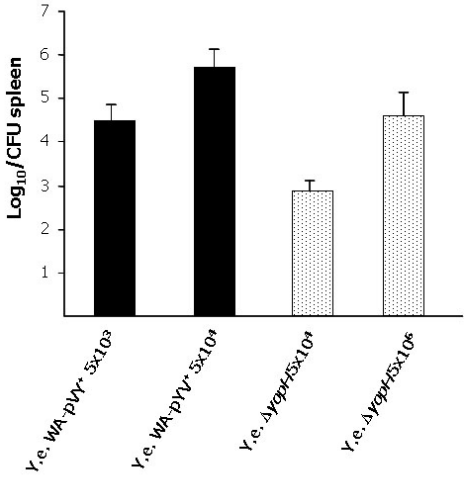

Figure 3.10 **The lack of YopH leads to a significant reduction of the virulence.** C57BL/6 female mice 6-8 week-old were infected intravenously with the indicated doses of a *Y. enterocolitica* pYV^+ or with a pYV^+Δ*yopH*. The bacterial number was assessed in homogenized spleens after 24 h post infection. Values represent the average log_{10} CFU per spleen for ten mice with the standard errors of the means indicated by error bars.

Each spleen was aseptically removed, the $CD11b^+$ cells were selected as prior mentioned and the mRNA of these cells was used for additional microarray experiments.

The expression of the 354 differentially regulated probe sets between the wild type infection and the Δ*yopH* infection was subsequently analyzed to exclude the influence of the different bacterial loads in the spleen (supplementary table 3).

The k-means algorithm was applied to cluster according to the signal log ratio probe sets with a similar expression profile. By this approach genes with similar expression patterns were sorted into 5 major groups of genes (Fig. 3.11; supplementary table 3).

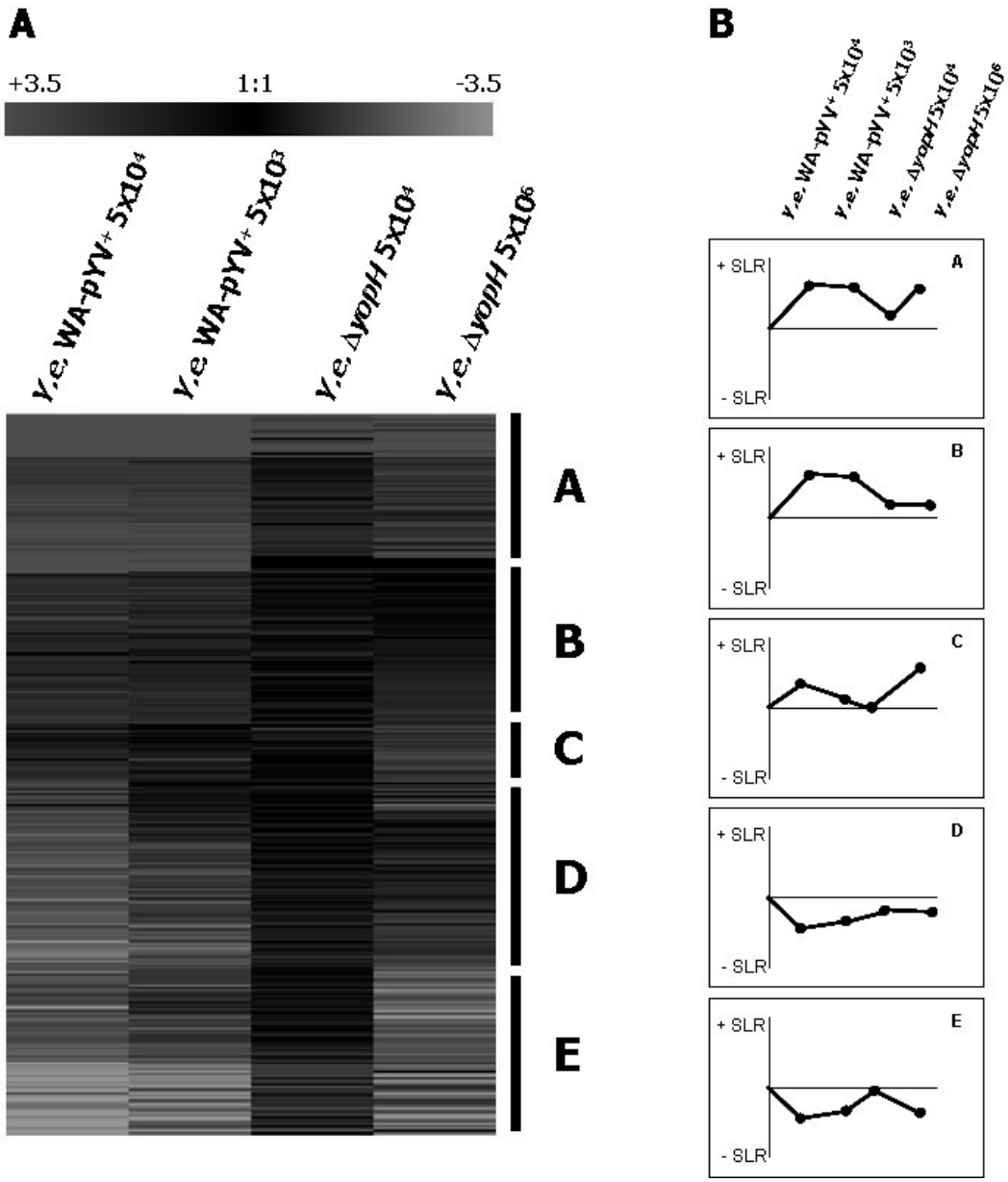

Figure 3.11 **Expression profiles of the differentially regulated genes in Δ*yopH* vs pYV$^+$.** Fig.A The expression profile of the probes sets (354) differentially regulated during the infection with 5x10^4 CFU of *Y. e.* pYV$^+$ versus pYV$^+$Δ*yopH* (more than 2-fold difference) was analyzed during the infection experiments with the doses that had led to the same bacterial load in the spleens. The K-means algorithm was applied to characterize the common expression profiles. Expression levels are colour coded, with red indicating expression level above and green below the expression level of uninfected control mice. Fig.B Expression profile of the different gene clusters over the time course of infection (24 h p.i. and 72 h p.i.).

In details we could group the genes according their expression patterns in the following clusters:

i. **Cluster A:** probe sets directly influenced by the bacterial load in the spleen
ii. **Cluster B:** probe sets induced only when the bacteria produce YopH
iii. **Cluster C:** probe sets induced only when the bacteria lack YopH
iv. **Cluster D:** probe sets suppressed only when the bacteria produce YopH

v. **Cluster E:** probe sets directly influenced by the bacterial load in the spleen.

Intriguingly, we could prove that only the expression level of a small group of genes was completely restored. By contrast, the most part of the genes were still weakly or not induced even upon infection with $5x10^6$ CFU of the Δ*yopH* mutant strain.

The probe sets that were differentially regulated by the bacterial number in the spleen are reunited in the cluster A (75) and in the cluster E (164) (Fig. 3.11) as induced and suppressed genes upon infection, respectively.

Several of these genes are known to be transcriptional regulated via the stimulation of the pattern recognition receptors i.e.Toll like receptors by different bacterial products.

The mRNA ofl genes described to be induced upon LPS stimulation such as the platelet-activating factor receptor, the interleukin 1 receptor antagonist and the LPS receptor CD14 were strongly induced when the infection dose of the Δ*yopH* mutant strain was increased.

In line with these findings is, that the expression of many well-characterized pro-inflammatory cytokines was restored, including TNF, IL-1α, CXCL1, CXCL2, CCL2 and CCL4, when the bacterial load and consequently the stimulation via the pattern recognition receptors on the cells was increased.

Intriguingly, a group of 73 probe sets representing 72 genes (cluster B, Fig. 3.11) was still weakly or not induced upon infection with the *Y. enterocolitica* bacteria strain that do not produce the virulence factor YopH. Out of this cluster, more than 20 genes could be functionally classified under the biological process "immune response".

More strikingly, of these 72 genes, 18 are known to be IFN-γ regulated. This group included several chemokines involved in activation of innate and adaptive immunity (CCL5, IL-12a, IL-15), members of the GTPase family implicated in resistance to intracellular infection (IIGP1), and other proteins such as the protein kinase interferon-inducible double stranded RNA dependent (PRKR), the adenosine deaminase RNA-specific (ADAR) and NOS2 effector factors responsible for IFN-γ-microbicidal activity.

In order to confirm this data we performed quantitative Real time-PCR for IFN-γ and for IL-12a (Fig. 3.13). These genes are lower expressed when the bacteria do not produce the virulence factor YopH, as we could show with the microarray experiments.

Taken together this data demonstrate that there is a specific signature of YopH during *Yersinia* infection. It became evident from different *in vitro* studies that YopH is very efficient in effecting the phagocytosis process in macrophages and neutrophils . Probably

the lack of this virulence factor leads to a better clearance of the infection via a more efficient phagocytosis and to a subsequently reduced host response. Otherwise, to clear the wild type *Yersinia* strain with the full virulence machinery, the phagocytes will require a full activation to overcome the activity of the *Yersinia* outer proteins. IFN-γ seems to be the crucial factor for this activation. Therefore we can conclude that the presence of YopH triggers a much stronger immune response.

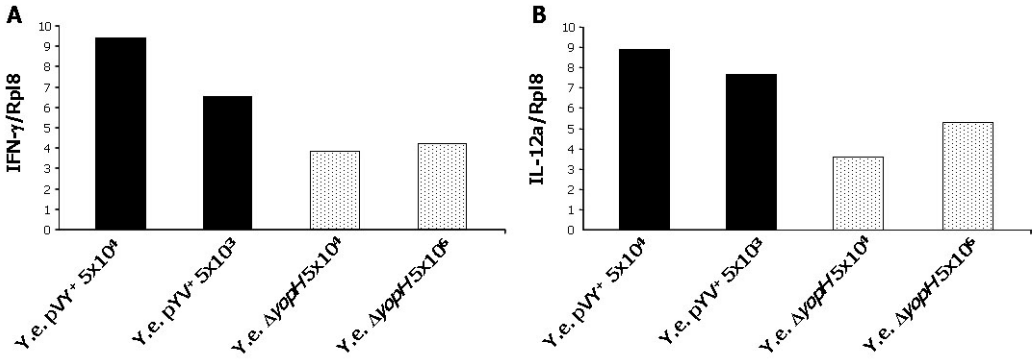

Figure 3.13 Quantification of the mRNA expression of interferon-γ and IL-12a upon *Yersinia* Δ*yopH* infection. The mRNA expression of IFN-γ and IL-12a was assess in splenic $CD11b^+$ cells isolated from C57BL/6 mice upon intravenous infection with *Y. e.* pYV^+ or $pYV^+\Delta yopH$ at the indicated doses. The $CD11b^+$ cells population was selected from the spleen 24 h p.i.. The mRNA expression of the indicated genes was analyzed by semiquantitative RT-PCR. The bars represent mean values of the $\log_2$ of the fold difference between infected and control mice normalized to the expression level of the control gene RPL8.

Unexpectedly, in our experiments there was a group of genes that was strongly induced only during the infection with the bacteria strain that do not produce the virulent factor YopH (Cluster C, Fig. 3.11; supplementary table 3).Probably, its the injection in the host cells cytoplasm of this bacterial protein can directly interfere at the transcriptional level with the expression of mRNAs. Interestingly, none of the known targets of YopH were found by this *in vivo* approach and therefore this may lead to novel effector functions of this virulence factor.

This group comprised mostly genes encoding for cell adhesion molecules (a disintegrin and metalloprotease domain 8, ADAM8; thrombospondin 1, THBS1; selectin platelet, SELP) and factors involved in chemotaxis (formyl peptide receptor 1, FPR1), although these functional groups were not significantly enriched compared to a randomly selected group of genes.

For the first time we could prove that *Y. enterocolitica* infection can induce the expression of the scavenger receptor MARCO (macrophage receptor with collagenous structure), which is a new and interesting finding.

This is a multifunctional trimeric glycoprotein, member of the class A scavenger receptor family. It has been implicated to varying degrees in systemic innate immunity against infections (8, 111, 160). Moreover, MARCO can bind LPS or LTA, as well as intact bacteria *Escherichia coli* and *Staphylococcus aureus* (160).

Real time quantitative-PCR experiments were performed using RNA samples independently isolated from the RNA used for the microarray hybridization in order to verify previous results (Fig. 3.14).

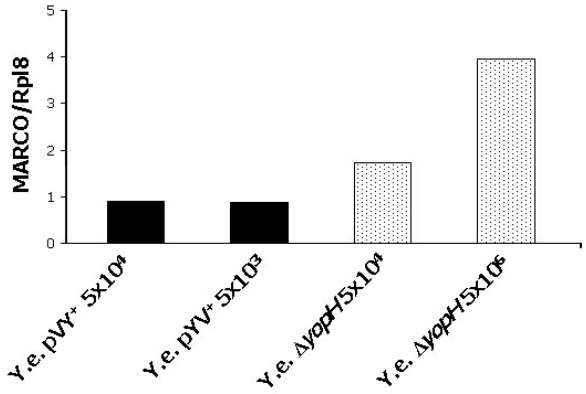

Figure 3.14 **In vivo induction of MARCO expression by Yersinia infection.** The mRNA expression of MARCO was assessed in splenic $CD11b^+$ cells isolated from C57BL/6 mice upon intravenous infection with *Y. e.* pYV^+ or $pYV^+\Delta yopH$ at the indicated doses. The $CD11b^+$ cell population was selected from the spleen 24 h p.i.. The mRNA expression of the indicated genes was analyzed by Real time RT-PCR. The bars represent mean values of the $\log_2$ of the fold difference between infected and control mice normalized to the expression level of the control gene RPL8.

To investigate whether the different expression of MARCO mRNA leads also a different receptor expression on the cell surface, we analyzed freshly isolated splenic cells by flow cytometry analysis. Total splenic cells were stained with different antibody (CD11b, CD11c, F4/80 and Gr-1) to differentiate macrophages and dendritic cell populations and to detect the expression of MARCO on the surface.

The spleen cells from uninfected mice and from intravenously infected mice with different doses of the wild type *Y. enterocolitica* strain and with the Δ*yopH* mutant strain were analyzed 24 h p.i. (Fig. 3.15).

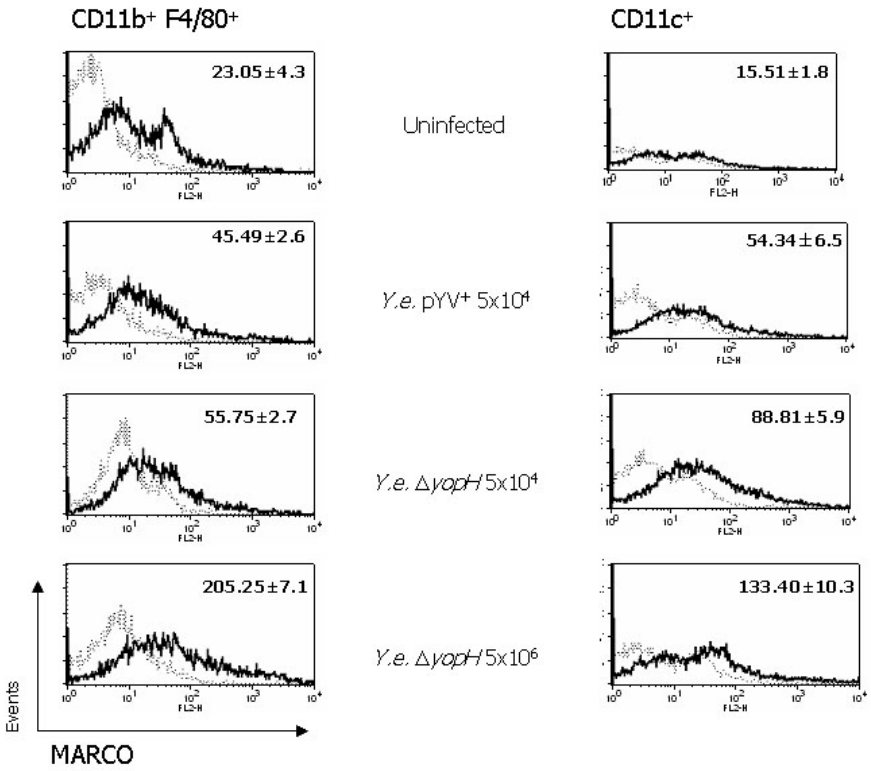

Figure 3.15 Expression of MARCO from splenic macrophages and DCs after infection with Y *.enterocolitica*. C57BL/6 mice were infected intravenous with different doses of different *Y. enterocolitica* strain as indicate in figure. 24 h post infection the splenocytes were stained with fluorophore conjugated antibodies anti-CD11b, F4/80, CD11c and MARCO or with the correspondent isotype controls. The expression of MARCO was evaluated by flow cytometry gating on the CD11b and F4/80 positive population or on the CD11c positive and F4/80 negative population. The fluorescence of the antibody (thick lines) or isotype-matched control IgG (thin lines) is shown. In the histograms the differences between the mean fluorescence intensity (MFI) values of specific antibodies to isotype controls are indicated ± SD. The histograms are representative of 3 independent experiments.

In agreement with previous studies, only a small subset of macrophages and dendritic cells from spleen of specific pathogens free mice express constitutively MARCO receptors on the surface. Upon infection with *Y. enterocolitica* the expression of this receptor was significantly induced in both macrophages and dendritic cells all over the spleen. Moreover, the proteins were never detected on lymphocytes and granulocytes (data not shown). Thus, MARCO expression seems to be dose dependent and restricted to macrophages and dendritic cells. Intriguingly, in confidence with the microarray data we

found a significant higher quantity of the receptor MARCO upon infection with *Y.e.* pYV^{+}Δ*yopH*. It is not clear if this difference can be correlated directly with the effect of YopH at the transcriptional levels in the infected cells or it is an indirect consequence of the different modulation of chemokines and interleukins expression in the spleen. Further *in vitro* experiments will be required to definitively address these questions.

3.4.2.3 Surface molecule expression by dendritic cells and macrophages after *Y. enterocolitica* infection

As previously reported, a group of genes (Cluster B; Figure 3.11) was permanently weakly expressed in splenic CD11b^{+} cells even upon infection with the highest dose of the Δ*yopH* strain (CFU 5x10^{6}) compared to wild type *Y. enterocolitica*. This suggests that the regulation of those genes is rather influenced by other factors than structural bacteria substances. It is very interesting that the gene expression profiles of some surface markers (CD86, CD40) identified to be induced upon infection on antigen presenting cells (APCs) belongs to this group.

Eventually, in order to verify these data we tested splenic macrophages and dendritic cells upon infection by flow cytometry, if the weak expression of the mRNA leads also to a reduced presence of receptors on the cell membrane.

Splenic cell suspensions from mice infected with the *Y.e.* pYV^{+} or with Δ*yopH* strains, were stained to evaluate the expression of MHC class II and of the co-stimulatory molecules CD86, CD80 and CD40.

Twenty-four h after intravenous infection with the wild type *Y. enterocolitica* strain, the expression of MHC class II was remarkably increased compared to uninfected mice in both macrophages and dendritic cells in a dose dependent manner as shown in figure (Fig. 3.16). Increased MHC class II expression was also observed after infection with the YopH deficient mutant, although the expression was significantly lower even with the highest infection dose (CFU 5x10^{6}) compared to the infection with the wild type bacteria. Furthermore, the co-stimulatory molecules CD86, CD80 and CD40 were significantly expressed on the cells only after the wild type infection, whereas significantly less increase was observed after infection with the YopH deficient mutant strain (Fig. 3.16).

Taken together these results indicate that the infection with YopH deficient mutant strain leads to a weaker activation of macrophages and dendritic cells, even when the bacteria load in the organs is comparable. This is probably due to the lower virulence of the pYV$^{+}\Delta$*yopH* strain. The lack of the virulence factor YopH leads to a fast resolution of the infection, and a subsequently lower induction of pro-inflammatory cytokines and activation of the host response.

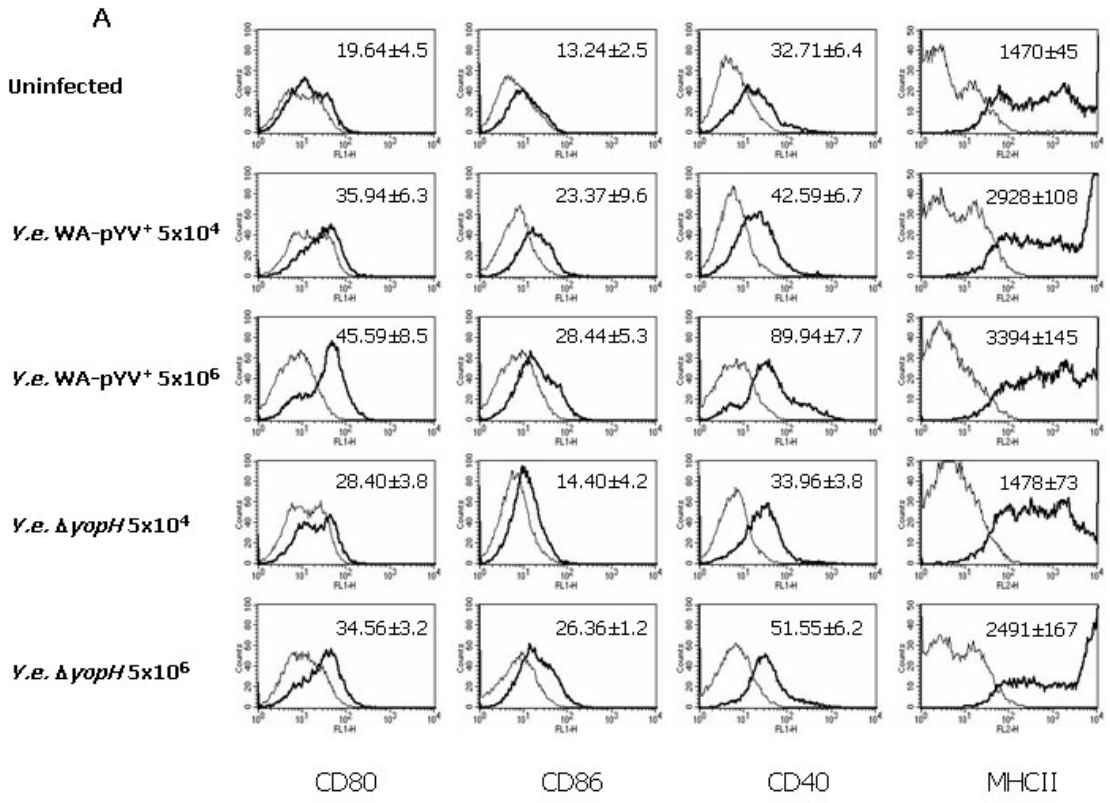

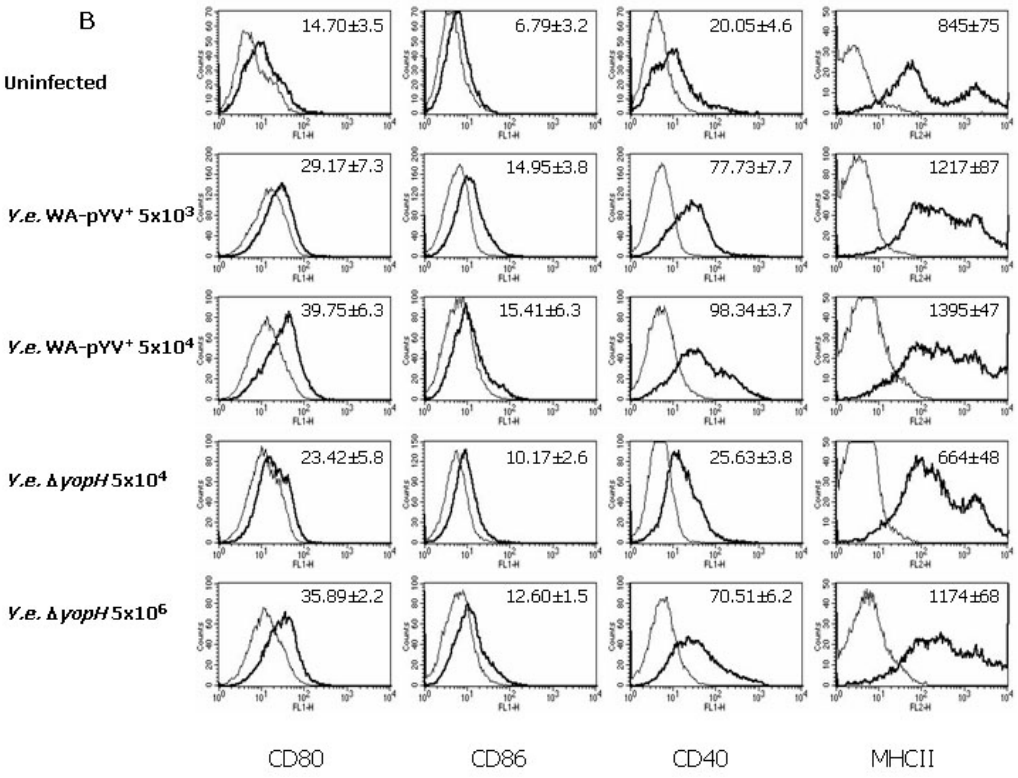

Figure 3.16 **Expression of MHC class II and co-stimulatory molecules by splenic dendritic cells and macrophages after infection with *Y. enterocolitica*.** Slenocytes were isolated upon 24 h p.i. infection with the indicated *Y. enterocolitica* strains. The cells were stained with CD11b, CD11c, F4/80 and Gr-1 to differentiate dendritic cells (Fig. A) and macrophages (Fig. B). Subsequently the expression of surface molecules like MHC class II, CD86, CD80 and CD40 (thick lines) or isotype-matched control IgG (thin lines) was assessed by flow cytometry gating on the propidium iodide negative population. In the histograms the differences between the mean fluorescence intensities (MFI) values of specific antibodies to isotype controls are indicated ± SD of 3 independent experiments.

3.4.2.4 IFN-γ is dispensable if *Y. enterocolitica* lack YopH

The gene expression pattern achieved upon infection with the *Y.e.* Δ*yopH* strain revealed that IFN-γ and some of the most important IFN-γ-regulated genes are weakly induced by the bacteria lacking YopH.

This suggests that IFN-γ might be to some extent dispensable at least in the early phase of infection if the bacteria do not produce this virulence factor. Therefore, we hypothesized that the expression of this cytokine and its mediated microbicidal activity is crucial to overcome the effects of YopH in inhibiting the host cells immune response. To address this hypothesis, IFN-γR1 deficient mice and wild type mice (C57BL/6) were infected with $5x10^4$ CFU of either *Y. enterocolitica* pYV^+ or with the Δ*yopH* strain. While IFN-$\gamma R1^{-/-}$ mice were extremely susceptible to the wild type *Yersinia* strain pYV^+ , they

were able to clear the infection with the YopH deficient mutant as well as the C57BL/6 mice. The evaluation of the bacteria number in the spleen reveals a comparable amount of living bacteria in the spleen of the two mice strains (Fig. 3.17). Furthermore, the IFN-γR deficient mice were enabled to a proper clearance of the infection and fast recovery within some days when infected with the Δ*yopH* bacteria (data not shown).

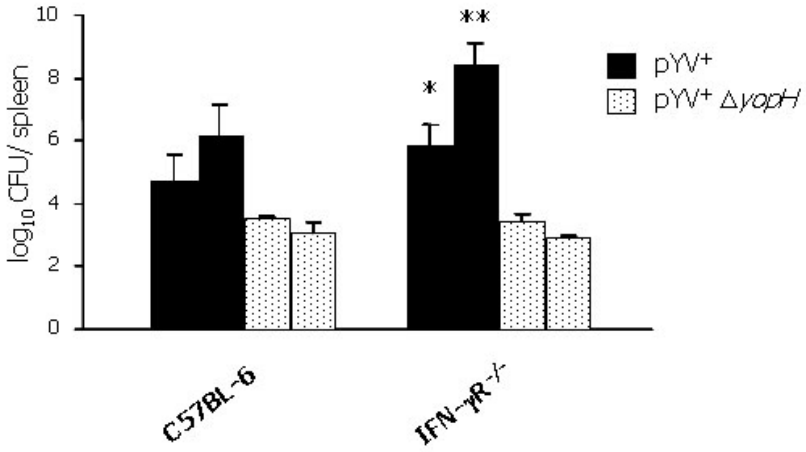

Figure 3.17 **IFN-γ signaling is dispensable if *Y. enterocolitica* lack YopH.** C57BL/6 and IFN-γR1$^{-/-}$ female mice 6-8 week-old were infected intravenously with 5x10^4 CFU of a *Y. enterocolitica* pYV$^+$ or with a pYV$^+$Δ*yopH*. The bacterial number was assessed in homogenized spleens after 24 and 72 p.i.. Values represent the average $\log_{10}$ CFU per spleen for ten mice with the standard errors of the means indicated by error bars.

3.4.2.5 IFN-γ enhances internalization of *Y. enterocolitica* by macrophages

Taking into account that the key effect of YopH is subverting phosphotyrosine signals essential for the phagocytosis in macrophages and neutrophils, we decided to test whether IFN-γ might be able to overcome these effects by enhancing the antimicrobial activity of the macrophages. Bone marrow derived macrophages (BMDMs) primed or not primed with 50ng/ml IFN-γ for 24 h were infected with *Y.e.* pYV$^+$ strain, pYV$^-$ and pYV$^+$Δ*yopH* at MOI of 50 for 30 min (Fig. 3.18). We first monitored the behaviour of *Y. enterocolitica* wild type strain in contact with BMDMs. Thirty min after infection, the number of cell-associated bacteria was counted and the percentage of internalized bacteria was calculated by using the double-immunofluorescence staining. In parallel, we tested wild-type *Y. enterocolitica* and a mutant (pYV$^-$) deprived of the virulence plasmid encoding for the type III secretion machinery. Adherence of both non-opsonized bacteria

to BMDMs was in the same magnitude (data not shown). However, only 16% of the *Y. enterocolitica* pYV^+ bacteria were ingested (Fig. 3.18 A, G), while 86% of the pYV^- bacteria were taken up. This demonstrated that the injection of the Yops allows *Y. enterocolitica* to resist phagocytosis by macrophages. To determine the involvement of YopH effector in resistance to phagocytosis, a $pYV^+\Delta$*yopH* strain was used. For each experiment, we measured the total number of bacteria associated with macrophages and retrieved consistant data for each strain tested (data not shown). In the absence of opsonization the YopH mutant bacteria was internalized by BMDMs at least 5-fold more than wild type bacteria. The percentage of phagocytosis increased from 16% (pYV^+) to 70% ($pYV^+\Delta$*yopH*), confirming that YopH contributes significantly to resistance to phagocytosis. For note, infection of pYV^+ with a lower MOI than 50 lead also to internalization indicating that the effects mediated by YopH are dose dependent (Fig. 3.23).

To investigate whether IFN-γ might be able to enhance *Y. enterocolitica* phagocytosis, BMDMs were primed for 24 h with IFN-γ and subsequently infected with the wild type *Y. enterocolitica* and with the YopH deletion mutant. 30 min after infection intracellular and extracellular located bacteria were determined. As reported previously, the wild type *Yersinia* were predominantly extracellularly located, while after priming with IFN-γ the internalization of pYV^+ was significantly increased up to 73% (Fig. 3.18 B, G). These data clearly indicate that IFN-γ can overcome the inhibitory effect of YopH on phagocytosis.

The mechanisms by which IFN-γ priming of BMDMs increased the number of internalized *Yersinia* bacteria is not clear, but our data suggest that IFN-γ increased the opportunity for bacterial-macrophage interaction, perhaps by an increase in the size of the cells as shown in the figure 3.19. Such morphological changes have previously been described following IFN-γ priming of human macrophages (107).

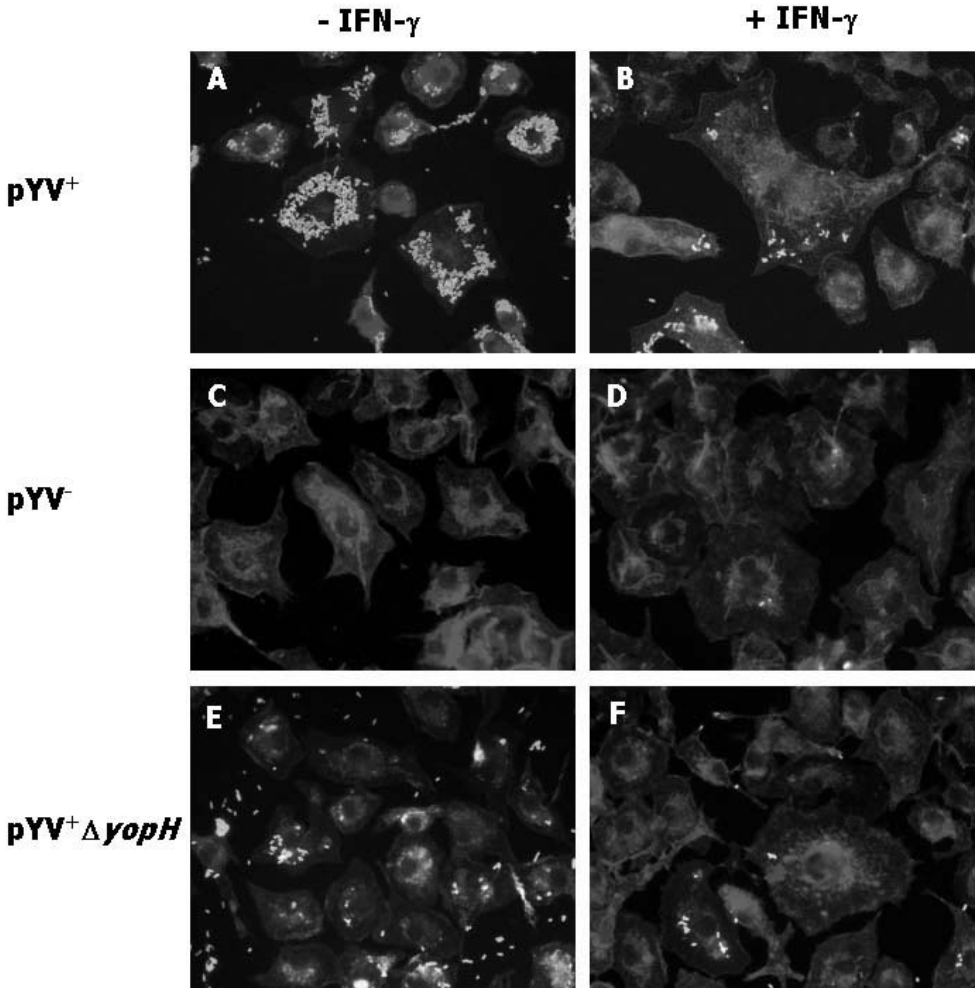

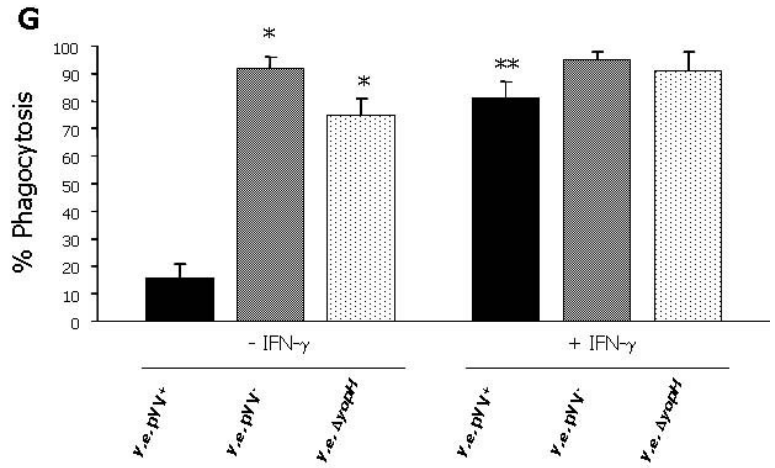

Figure 3.18 **IFN-γ priming enhances internalization of *Y. enterocolitica* by macrophages.** Bone marrow-derived macrophages from C57BL/6 mice primed (B, D and F) or not (A, C and E) with IFN-γ 50ηg/ml for 24 h were infected with MOI 50:1 of different *Y. enterocolitica* strains: pYV^+ (A and B), pYV^- (C and D) or $pYV^+\Delta yopH$ (E and F) cultivated at 37°C. The number of adherent bacteria and intracellular bacteria were determined by the double-immunofluorescence staining. The extracellular bacteria appear green and the intracellular

blue in the figure. Phagocytosis results are given as percentages of phagocytosed bacteria normalized to the total number of cell-associated bacteria (*, $p \leq 0.05$ compared to the WT; **, $p \leq 0.05$ compared to the WT primed with IFN-γ). The values are the mean plus the standard error of three independent experiments. For each experiment, at least 100 cells were counted.

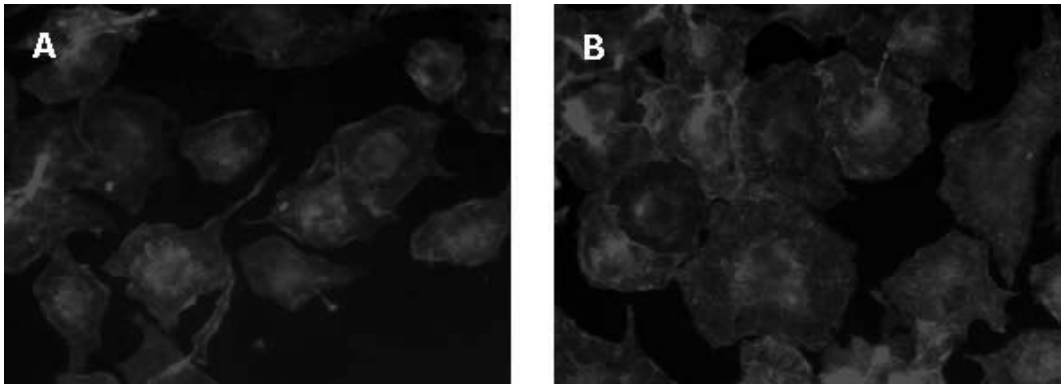

Figure 3.19 **IFN-γ priming increases the size of macrophages.** Bone marrow-derived macrophages from C57BL/6 mice primed (B) or not primed (A) with IFN-γ 50ηg/ml for 24 h were stained with tetramethyl rhodamine isothiocyanate-conjugated phalloidin for 30 min and analyzed by fluorescence microscopy. The pictures were taken at the same magnification.

3.5 Interferon-γ-dependent immunity to *Y. enterocolitica*

Historically, the role of IFN-γ has been only considered as necessary in infection with intracellular pathogens, including *Mycobacterium tuberculosis*, *Salmonella typhimurium*, *Leishmania major* and *Listeria monocytogenes*.

Intriguingly, also in *Y. enterocolitica* infection IFN-γ seems to be crucial for protection. Furthermore, it has been shown that this cytokine is critical for the development of a Th1 cell mediating resistance that is essential to successfully clear the infection. Usually IFN-γ is secreted by natural killer (NK) cells and T cells upon stimulation with IL-12 and IL-18 considered the most powerful IFN-γ-inducing cytokines. These interleukins are abundantly secreted by antigen presenting cells following *Yersinia* infection. On the contrary, not much is known about the molecular mechanisms of the IFN-γ-induced-microbicidal capacity, and furthermore which cell types are the effectors of this process in a *Yersinia* infection. Several *in vitro* and *in vivo* studies with other bacteria had shown that IFN-γ-priming of phagocytes (neutrophils and macrophages) can significantly enhance their antimicrobial capacity by inducing several genes. Intriguingly, our microarray data had shown that several IFN-γ-regulated genes were highly induced in splenic $CD11b^+$ cells upon *Y. enterocolitica* infection (supplementary table 1). Therefore, in order to address what is the actual influence of this cytokines on the transcriptome of cells of the host innate immune response during a *Y. enterocolitica* infection, we decide to characterize the whole gene expression in splenic $CD11b^+$ cells isolated from mice deficient for the IFN-γ receptor during the course of *Y. enterocolitica* in fection. These mice are unable to initiate signaling in response to IFN-γ and they may be useful to understand which pathways are involved in the host immune response against *Y. enterocolitica*.

First of all IFN-γ$R1^{-/-}$ mice on C57BL/6 background and correspondent C57BL/6 wild type mice were intravenously infected with $5x10^4$ CFU of *Y. enterocolitica* pYV^+ to analyze their response to the infection. The mice were sacrificed one and three days after infection, and the number of bacteria in their spleens was assessed. We could prove that the bacterial number increased significantly in the organs of the interferon-γ receptor deficient mice (Fig. 3.20 A). Moreover, 72 h p.i. the dramatic boost of the bacteria in the spleen (200-fold increase) was associated with obvious clinical manifestations (anorexia, loss of body weight, lethargy) never evident in normal mice that end 4-6 days p.i. to death.

To further evaluate the role of IFN-γ in the progression of infection, we infected the interferon-γ receptor deficient mice with an infection dose of *Y. enterocolitica* ($5x10^3$ CFU/mouse) that was usually well tolerated by the wild type mice. As shown in figure 3.20 B, the IFN-γR1$^{-/-}$ mice revealed a significant greater mortality in comparison to wild type mice. Indeed they displayed 100% mortality around day 8 and day 9 as confirmed in three different experiments, whereas the majority of the wild type mice were able to recover.
These data reveal a severe defect in the control of *Yersinia* infection. Furthermore, our data clearly indicate that IFN-γ is crucial already at the early stage of infection suggesting that its antimicrobial effects are probably achieved by cells of the innate immune system.

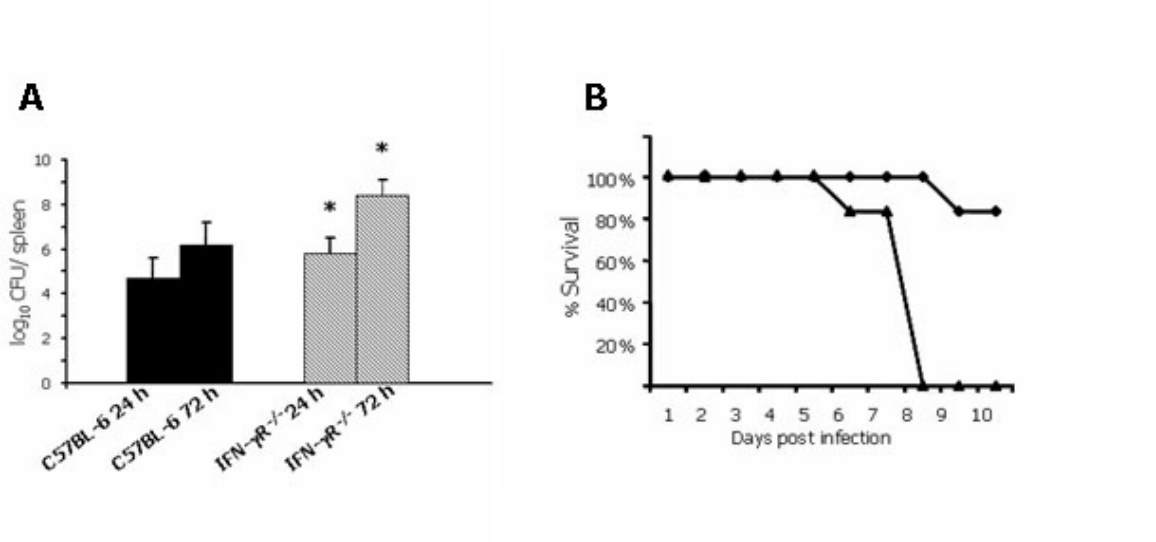

Figure 3.20 **IFN-γR1 deficiency increases the susceptibility to *Y. enterocolitica* infection.** Fig.A C57BL/6 and IFN-γR$^{-/-}$ mice were infected intravenously with $5x10^4$ cfu/mouse of *Y. enterocolitica* pYV$^+$. Values represent the average $\log_{10}$ CFU per spleen for six mice with the standard errors of the means indicated by error bars. Asterisks indicate significant differences when compared CFU in C57BL/6 vs IFN-γR$^{-/-}$ mice ($p \leq 0.05$). Fig.B C57BL/6 (◆) and IFN-γR$^{-/-}$ (▲) mice (6 per group) were infected intravenous with $5x10^3$ cfu/mouse of *Y. enterocolitica* pYV$^+$. The mice were monitored daily for survival. Data presented are representative of 3 independent experiments.

3.5.1 Gene expression profile in *Y. enterocolitica*-infected IFN-γR1$^{-/-}$ mice

As previously described, the splenic CD11b$^+$ cells were selected from IFN-γR1$^{-/-}$ mice and C57BL/6 wild type mice day one and three upon intravenously infection with $5x10^4$ CFU of *Y. enterocolitica* pYV$^+$. The total mRNA was extracted from those cells and the gene expression profile was characterized by oligonucleotide microarray experiments as described in materials and methods.

3.5.1.1 Gene expression level in CD11b$^+$ cells from spleen of uninfected IFN-γR1$^{-/-}$ mice

First of all, we investigated whether the lack of interferon-γ signaling leads to a different modulation of the gene expression already in CD11b$^+$ cells selected from uninfected mice. Exclusively, probe sets whether the signal log ratio between uninfected CD11b$^+$ cells from C57BL/6 and IFN-γR1$^{-/-}$ was >1.5 or <-1.5 (approximately 3-fold difference) were analyzed. Surprisingly, 211 probe sets were differentially regulated in uninfected CD11b$^+$ C57BL/6 to IFN-γR1$^{-/-}$ spleen cells. Indeed, 88 probe sets were lower and 123 higher expressed suggesting that IFN-γ modulates the basal expression of a high number of genes. For example, several receptors (insulin-like growth factor I receptor, interleukin 1 receptor type II, IL-8 receptor, IL-6 receptor, integrin-β7), and genes involved in apoptosis (Dead box polypeptide 6, Caspase 8 and FADD-like apoptosis regulator) are lower expressed in uninfected CD11b$^+$ IFN-γR1$^{-/-}$ cells. In contrast, some genes involved in antigen presentation and processing e.g. IMUC class II genes, ATP binding family subtype b (Tap/MDR), were found to be expressed higher in CD11b$^+$ IFN-γR deficient cells.
In order to investigate whether these differences in basal expression can affect the expression levels during infection, the expression profile of those cells isolated 24 h and 72 h p.i. from the spleen of IFN-γR deficient mice was compared to the expression profile in wild type mice C57BL/6. As mentioned before we considered as differentially regulated probe sets with a difference of more than 3-fold. Indeed, 97 probe sets after 24 and 229 after 72 h p.i. are within this threshold.

3.5.1.2 Interferon–γ regulated genes induced in *Y. enterocolitica* infection

Comparison of the gene expression profiles between IFN-γR deficient mice to C57BL/6 wild type mice revealed the presence of nearly 300 probe sets representing 271 different genes (supplementary table 5).

Probe sets regulated	24 h	72 h
	IFN-γR1$^{-/-}$ vs C57BL/6	IFN-γR1$^{-/-}$ vs C57BL/6
Higher expressed	66	133
Lower expressed	31	96
Tot	97	229

Table 3.3 Probe sets more than 3-fold regulated in *Yersinia*-infected IFN-γR1$^{-/-}$ mice compared to C57BL/6 infected mice.

In contrast, with the severe immunological defects in response to *Yersinia* infection showed by the interferon-γ receptor deficient mice several genes involved in the immune and inflammatory response were higher compared to wild type mice. The higher expression of these genes seems to be a consequence of the great bacteria load in the spleen of the IFN-γR1$^{-/-}$ mice that led to a deregulation of the inflammatory response. The high number of bacteria was responsible of an increase stimulation of the host response proved also by the high recruitment of inflammatory cells in the spleen. In fact, a significant boost of the spleen weight in these mice was detected (Fig. 3.21). Surprisingly, the relative number of the CD11b^{+} cells was apparently lower in the IFN-γR1$^{-/-}$ mice 72 h p.i., but a further analysis revealed that this was a consequence of the dramatic decline of live cells isolated 3 days post infection in the spleen of the *Yersinia*-infected IFN-γR1$^{-/-}$ mice.

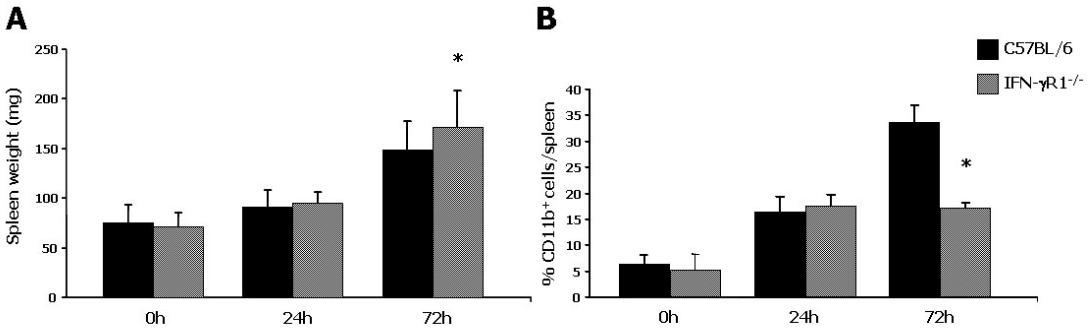

Figure 3.21 Influx of inflammatory cells in the spleen of *Yersinia*-infected IFN-γR1$^{-/-}$ mice. Fig.A The weight of the spleens was measured to evaluate the influx of inflammatory cells in the organs after infection. The bars represent mean values ±SD of three independent experiments. Fig.B The relative number of CD11b^{+} cells within the total spleen cells from IFN-γR1$^{-/-}$ and C57BL/6 mice (5 per group) intravenously infected with 5x10^{4} CFU of *Y. enterocolitica* pYV^{+} was assessed. The splenocytes were stained with an anti-CD11b allophycocyanin-conjugated antibody. The percentage of cells expressing the CD11b molecules was analysed by flow cytometry. The bars represent mean values ±SD of three independent experiments. Statistically significant differences comparing IFN-γR1$^{-/-}$ versus wild type mice are indicated with an asterisk ($p \leq 0.05$).

These finding was in line with the histological analyses of the spleen in the *Yersinia*-infected IFN-γR1$^{-/-}$ mice. The defect in the antimicrobial capacity of the interferon-γ receptor deficient mice leads to a significantly increase of the lesion in the spleens. As shown in figure 3.22, the amount and the extension of the abscesses lead to a complete disorganization of the spleen in these mice.

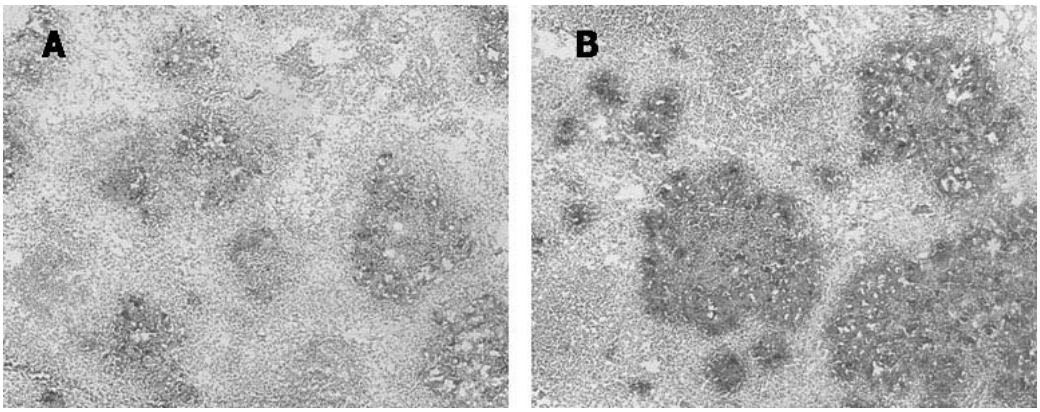

Figure 3.22 **Spleen lesions in *Y. enterocolitica*-infected IFN-γR1$^{-/-}$ mice.** C57BL/6 and IFN-γR1$^{-/-}$ mice were infected intravenously with 5x10^4 CFU of a *Y. enterocolitica* wild type strain (pYV$^+$) (Fig. A and B respectively). The spleens were removed 72 h post infection. Tissue sections were stained with an anti-*Y. enterocolitica* monoclonal antibody and with hematoxylin. The bacteria aggregates appeared brown and the nuclei blue. The pictures were taken at the same magnification.

As consequence, of the misregulation of *Yersinia* infection in IFN-γR deficient mice upon, mRNAs encoding the IL-1R2 and the IL-1RAP were strongly induced. These proteins are known to be essential regulatory factors of the inflammatory responses, acting as a decoy receptor for IL-1 (50, 87, 97, 151). The dramatic induction of these factors might represent the last move of the innate response to protect tissue from damage.

As showed in the table 3.3 more then 100 probe sets were lower expressed in the splenic CD11b$^+$ cells lacking IFN-γ signaling cascade compared to wild type mice. A detailed analysis of this group revealed the presence of two clusters with different expression profiles. The first cluster represents genes that were induced in IFN-γR1$^{-/-}$ mice upon *Yersinia* infection but with a significantly lower extend compare to wild type mice (as example: SOCS1, IFIT1, IFIT2, IFIT3, GBP2 and GPB3). This suggests that IFN-γ signaling is not essential for the induction of these factors but act more as reinforcement of the expression.

A second group comprised factors that were absolutely not induced in the *Y. enterocolitica*-infected IFN-γR1$^{-/-}$ mice. Thus, we can assume that the highly susceptibly of the interferon-γ receptor deficient mice to *Yersinia* infection is a consequence of the lack of these factors.

As already mentioned, for effective control of *Yersinia* infection, the host must mount an adaptative immune response that depends primarily on cytotoxic lymphocytes. These cells are specifically guided to infected tissue by local expression of chemokines. Intriguingly, several of these chemokines (CCL5, CXCL9 and CXCL10) are directly regulated via the interferon gamma receptor signaling. In agreement with this evidence these factors were not induced in CD11b^{+} cells from *Y. enterocolitica*-infected-IFN-γR1$^{-/-}$ mice. Therefore, taking into consideration that the mRNA encoding for CCL5, CXCL9 and CXCL10 was strongly induced in wild type mice, we can conclude that these are key modulator of the host immune response to *Yersinia.* Furthermore, recent reports provide strong evidence that CXCL9 and CXCL10 act as agonists for CXCR3 and, moreover, as antagonists for CCR3. Because CXCR3 and CCR3 are differentially expressed in Th1 and Th2 cells, our data suggest that these chemokines might be responsible of the Th1-type immune response polarization in yersiniosis.

Surprisingly, out of the group of the not induced genes, the newly identified IFN-inducible GTPase family was significantly represented (IFI1, IFI47, IIGP1, IIGP2, TGTP, IGTP and MX1). Recently, several studies have showed that some of these genes are essential to control intracellular pathogens (39, 96, 153). In deed, it had been proved that IIGP1 and IFI1 are involved in phagosome remodelling and in the vesicular trafficking that led to the formation of the phago-lysosome, and consequently to inhibition of the bacteria replication.

Taking into consideration that *Y. enterocolitica* expresses a sophisticated type III secretion mechanism that allow the bacteria to successfully inhibit the phagocytosis process, the up regulation by the host cells of factors that can only play a role when the bacteria are internalized seem to be an apparent contradiction. However, if one consider that almost all of the studies in which had been proved that the injection of the Yops can efficiently interfered with the phagocytosis, were performed with a high multiplicity of infection (MOI 50) that, most likely, does not correspond with the real occurrence *in vivo*, this contradiction it is self explaining (129, 130, 135). Furthermore, we demonstrated, with a phagocytosis assay using bone marrow derived macrophages, that the effects of the Yops

are strictly dose dependent. Infection of macrophages, with an MOI of less then 50 of a wild type *Y. enterocolitica* strain, led to an incomplete inhibition of the phagocytosis. Moreover, if the infection experiments were performed with ten bacteria per cell, the *Y. enterocolitica* were almost completely internalized by the macrophages (Fig. 3.23). This could mean that at lest at the early stage of *Y. enterocolitica* infection, when only a small number of bacteria are in contact with phagocytes, some bacteria can be efficiently internalized. Thus, in concert with the evidence that yersiniae can proliferate in naïve macrophages (118, 119,), it is likely that these cells can provide a replicative niche in which the bacterium can increase its numbers, while protected from neutrophils that are recruited to the site of infection. Further studies are required to finally address these finding and to clarify the role of intracellular located bacteria in the pathogenesis of the yersiniosis.

These findings can explain the key role of IFN-γ and the necessity of a T-cell mediated immune response to successful clear *Yersinia spp.* infection. Moreover, this studies indicated that IFN-γ-activated macrophages are most likely the effector cell to ihibith Y. enterocolitica proliferation in murine model.

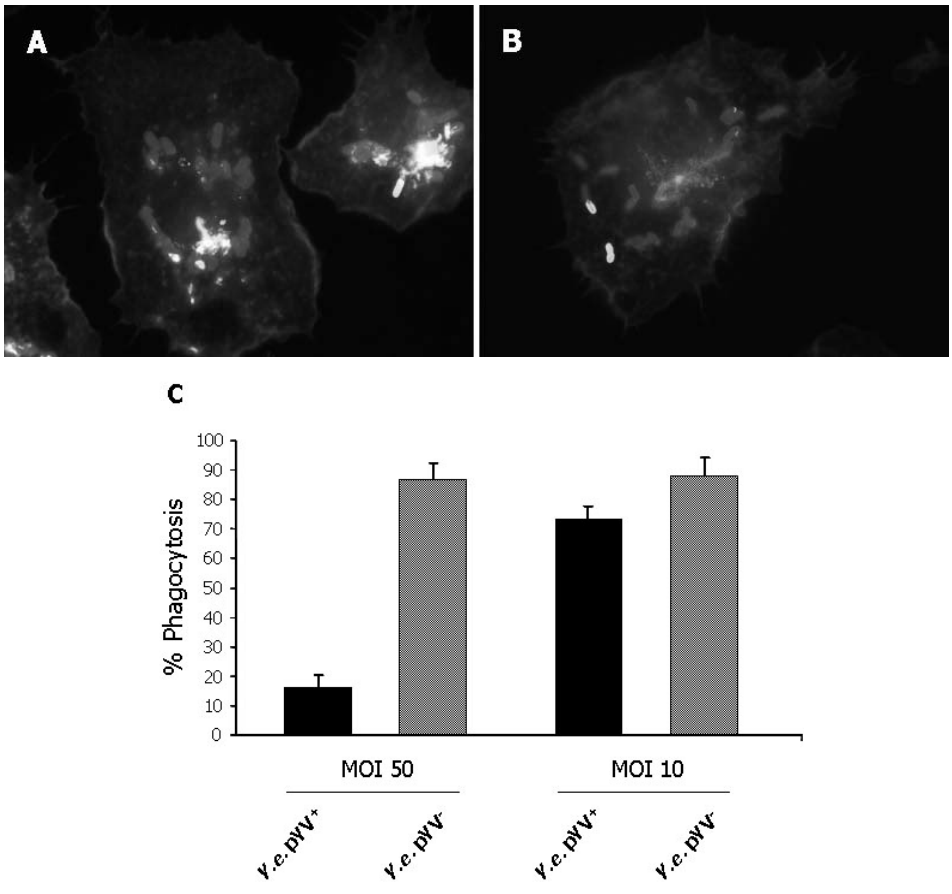

Figure 3.23 ***Y. enterocolitica*** **inhibits macrophage phagocytosis in a dose dependent manner.** Bone marrow-derived macrophages from C57BL/6 mice were infected with MOI 10:1 of the wild type *Y. enterocolitica* strains pYV^+ (A) or with the plasmid cured strain pYV^- (B) cultivated at 37°C. The number of adherent bacteria and intracellular bacteria were determined by the double-immunofluorescence technique. The extracellular bacteria appear green and the intracellular blue in the figure. Fig.C Phagocytosis results are given as percentages of phagocytosed bacteria relative to the total number of cell-associated bacteria. The values are the mean plus the standard error of three independent experiments. For each experiment, at least 100 cells were counted.

In order to verify the confidence of the microarray data, quantitative Real-time PCR was performed. Total mRNA was extracted from $CD11b^+$ cells isolated from IFN-γ-receptor deficient mice and their wild type mice controls from independent experiments. As shown in figure 3.24, the induction of IRF1, IIGP1, CXCL9 and IFI1 that normally occurs in *Y. enterocolitica* infected mice was significantly attenuated in the IFN-$\gamma R1^{-/-}$ mice, indicating that IFN-γ signaling cascade is required for the increase in expression of these genes in the spleen.

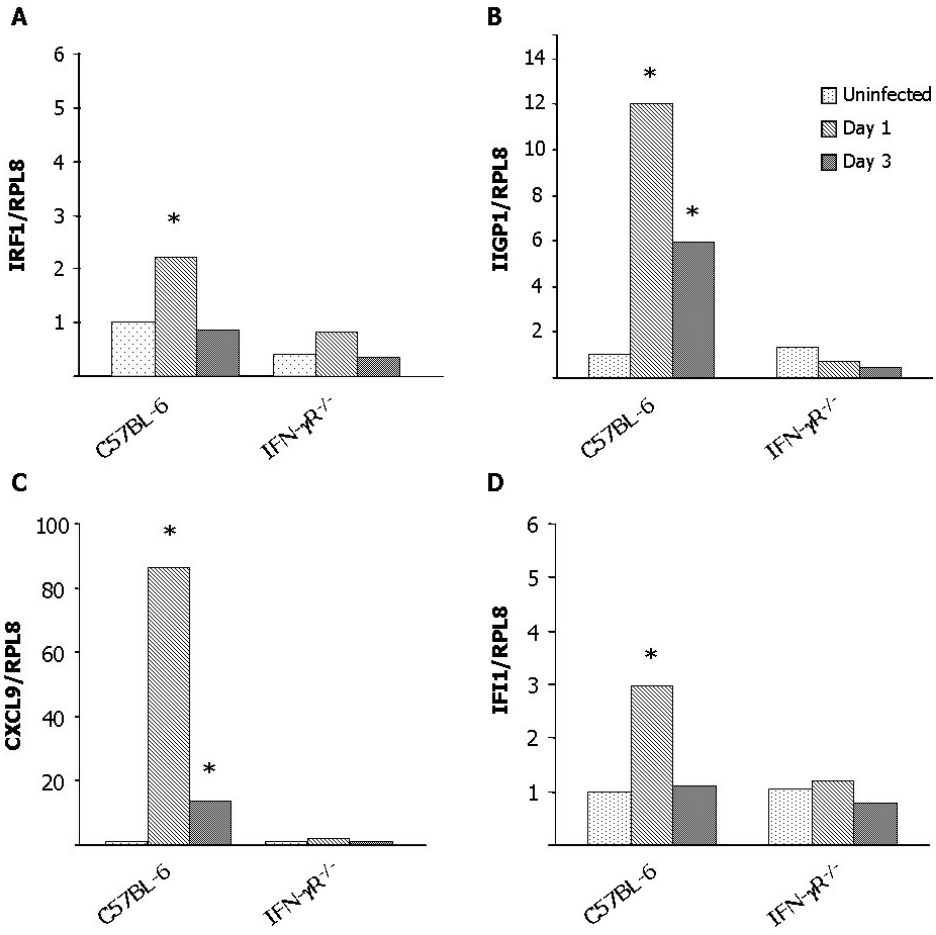

Figure 3.24 **Quantification of mRNA expression of interferon-γ induced genes.** The mRNA expression of IRF1, IIGP1, CXCL9 and IFI1 in splenic $CD11b^+$ cells isolated from C57BL/6 and IFN-$\gamma R1^{-/-}$ mice upon intravenous infection with $5x10^4$ CFU of *Y. enterocolitica* pYV^+ at

the indicated time points was analyzed by semiquantitative RT-PCR. The bars represent mean values of fold difference between infected and control mice normalized to the expression level of the control gene RPL8. Asterisks indicate significant differences when compared mRNA expression in C57BL/6 vs IFN-γR1$^{-/-}$ mice ($p \leq 0.05$).

4 Conclusions

The innate immune system supplies the first line of defense against pathogens and is essential to activate the adaptive immune system to mount an appropriate response for the particular pathogen. Not surprisingly, the innate immune system is a primary target of several pathogens that had evolutes different mechanisms to overcome the host response. Some of the most efficient bacteria in silencing the innate immune response are members of the genera *Yersinia*.

Yersinia spp. have evolved a sophisticated mechanisms called type III secretion system, encoded by a virulence plasmid (pYV), that lead the bacteria to inject directly in the cells host cytoplasm some virulence factors called *Yersinia outer proteins* (Yops H, P, E, M, T and O). By means of these mechanisms, bacteria can elude many aspects of the innate immune system by evading phagocytic cells, suppressing production of pro-inflammatory cytokines and chemokines, inducing apoptosis, and moreover inhibiting the activation of the adaptive immune response.

Our data prove that YopH is the most important virulence factor during the course of *Y. enterocolitica* infection. Several recent *in vitro* studies have showed that YopH affects phagocytosis by dephosphorylation of p130Cas, focal adhesion kinase (FAk), paxillin and the Fyn-binding protein (FBP) which leads to the disruption of focal adhesion complexes. The inhibition of the phagocitosis efficiently, protects bacteria from the host cells response, and it allows them to successfully proliferate in the host tissue. Consequently, mechanisms involving helper ($CD4^+$) and cytotoxic ($CD8^+$) T cell responses, particularly interferon-γ–producing CD4 T helper 1 (Th1) cells, are essential in cooperation with activated macrophages, to control *Yersinia* infections. Notably, we demonstrate that IFN-γ plays a key role in reprogramming the transcriptome response in cells of the innate immunity in the yersiniosis. The expression of newly discovered IFN-inducible genes, the family of the large GTPase, never associated with *Y. enterocolitica* infection was described. The induction of these genes was strictly regulated by IFN-γ and most likely accountable of its antimicrobial activity in cells of innate immunity during *Yersinia spp.* infection.

The present studies should prompt further research to definitely address the role of these newly discovered IFN-γ-inducible genes induced by and Yersinia spp. Moreover, it will be

of interest to study the course of *Yersinia spp.* infection in mice in which members of the GTPase family are disrupted.

Genome-wide expression profiling of cells directly isolated from infected host may provide new insight into the key pathways involved in gene regulation, modulation and subversion of host responses upon bacterial infection.
The development of DNA-microarray technologies, together with the sequencing of genomes from different species, has provided an opportunity to monitor and investigate the complex interactions that regulate biological processes.
The development of these sophisticated methods had allowed researchers to gain insight some of the most important features of the immune system.
However, one of the most challenging aspects of gene expression analysis is making sense of the vast quantities of data and extracting conclusions and hypotheses that are biologically meaningful. The collection of hundreds of analyses of immune-system gene expression using a wide representation of the microbial world as stimuli should allow the generation of expression databases that will provide immunologists with a powerful key to interpret the complexity of the host response and identify specific gene-expression programmes. These will increases our understanding of the function and regulation of genes and proteins, and their role in infectious diseases, in order to improve human health and well-being.

5 Summary

Yersinia enterocolitica causes acute and chronic enteric infections and complications such as septicaemia or reactive arthritis. The survival strategy of *Y. enterocolitica* in hosts is to silence the innate immune as well as the adaptive immune response. For this purpose *Y. enterocolitica* has developed a Type III secretion system which allows to directly translocate six effectors proteins Yops (*Yersinia outer protein* H, T, O, P, M and E) into host cells.

Aim of this work was the characterization of the molecular mechanisms by which the Yops affect gene expression in cells of the innate immune response, *in vivo*. For this purpose, $CD11b^+$ cells, including macrophages, granulocytes, dendritic cells and NK, were selected from the spleen of *Y. enterocolitica* infected mice and gene expression profiles were analyzed by oligonucleotide microarray. Three groups of C57BL/6 mice were infected intravenous with the *Y .enterocolitica* pYV^+, or the Δ*yopP* and or the Δ*yopH* mutants, respectively. It was demonstrated that while the infection with the Δ*yopP* showed a similar colonization of the spleen to the wild type pYV^+ strain, the Δ*yopH* mutant was highly attenuated. Furthermore, the microarray data revealed a significant difference between the gene expression profiles obtained with Δ*yopH* strain compared to the wild type pYV^+ or with the Δ*yopP* strain. Intriguingly, the majority of the differentially regulated genes were functionally involved in the immune response, indicating that YopH plays a crucial role in the yersiniosis. Analysis of the transcriptional regulation of this group of genes revealed the presence of a major group of IFNγ-regulated genes, suggesting that in the early stage of infection the activation via interferon gamma of cells of the innate immunity is essential to overcome the inhibitory effects of YopH. In fact, we could prove that IFN-γ priming of macrophages can enhance significantly their *Yersinia*-antimicrobial activity. In order to characterize the molecular mechanisms involved in this process, we performed gene expression analysis of $CD11b^+$ cells isolated from *Y. enterocolitica*-infected-interferon-γ receptor deficient mice. The data clearly revealed a panel newly IFN-γ-regulated genes plausibly related to the pathogenesis of *Yersinia* infection. Further studies will be of interest to characterize the course of yersiniosis in mice in which these genes are disrupted.

Moreover, this study shows that analyses of transcriptional response in host cells directly isolated from *in vivo* infection can reveal interesting insights into host cell functions and immune responses.

6 References

1 **Aili, M., M. Telepnev, B. Hallberg, H. Wolf-Watz, and R. Rosqvist**. 2003. *In vitro* GAP activity towards RhoA, Rac1 and Cdc42 is not a prerequisite for YopE induced HeLa cell cytotoxicity. Microb. Pathog. **34**:297-308.

2 **Aliprantis, A. O., R. B. Yang, M. R. Mark, S. Suggett, B. Devaux, J. D. Radolf, G. R. Klimpel, P. Godowski, and A. Zychlinsky**. 1999. Cell activation and apoptosis by bacterial lipoproteins through toll-like receptor-2. Science **285**:736-739.

3 **Amyere, M., M. Mettlen, S. P. Van Der, A. Platek, B. Payrastre, A. Veithen, and P. J. Courtoy**. 2002. Origin, originality, functions, subversions and molecular signalling of macropinocytosis. Int. J. Med. Microbiol. **291**:487-494.

4 **Anderson, D. M. and O. Schneewind**. 1997. A mRNA signal for the type III secretion of Yop proteins by *Yersinia enterocolitica*. Science **278**:1140-1143.

5 **Ardavin, C., L. Wu, C. L. Li, and K. Shortman**. 1993. Thymic dendritic cells and T cells develop simultaneously in the thymus from a common precursor population. Nature **362**:761-763.

6 **Arencibia, I., N. C. Suarez, H. Wolf-Watz, and K. G. Sundqvist**. 1997. *Yersinia* invasin, a bacterial beta1-integrin ligand, is a potent inducer of lymphocyte motility and migration to collagen type IV and fibronectin. J. Immunol. **159**:1853-1859.

7 **Arnold-Schild, D., D. Hanau, D. Spehner, C. Schmid, H. G. Rammensee, S. H. de la, and H. Schild**. 1999. Cutting edge: receptor-mediated endocytosis of heat shock proteins by professional antigen-presenting cells. J. Immunol. **162**:3757-3760.

8 **Arredouani M., Z.Yang, Y.Y.Ning, G. Qin, R. Soininen, K. Tryggvason, and L. Kobzik.** 2004. The scavenger receptor MARCO is required for lung defense against pneumococcal pneumonia and inhaled particles. J. Exp. Med. **200**: 267–272

9 **Ashburner M., Ball C.A.., Blake J.A., Botstein D., Butler H., Cherry J.M., Davis A.P., Dolinski K., Dwight S.S., Eppig J.T., Harris M.A., Hill D.P., Issel-Tarver L., Kasarskis A., Lewis S., Matese J.C., Richardson J.E., Ringwald M., Rubin G.M., Sherlock G.** 2000. Gene ontology: tool for the unification of biology. The Gene Ontology Consortium. Nat Genet. **25**:25-29.

10 **Austyn, J. M., J. W. Kupiec-Weglinski, D. F. Hankins, and P. J. Morris**. 1988. Migration patterns of dendritic cells in the mouse. Homing to T cell-dependent areas of spleen, and binding within marginal zone. J. Exp. Med. **167**:646-651.

11 **Autenrieth, I. B., and J. Heesemann.** 1992. In vivo neutralization of tumor necrosis factor alpha and interferon-gamma abrogates resistance to *Yersinia enterocolitica* in mice. Med. Microbiol. Immunol. **181:**333–338.

12 **Autenrieth, I. B., U. Vogel, S. Preger, B. Heymer, and J. Heesemann.** 1993. Experimental *Yersinia enterocolitica* infection in euthymic and T-cell-deficient athymic nude C57BL/6 mice: comparison of time course, histomorphology, and immune response. Infect. Immun. **61:**2585–2595.

13 **Autenrieth, I. B., M. Beer, E. Bohn, S. H. Kaufmann, and J. Heesemann**. 1994. Immune responses to *Yersinia enterocolitica* in susceptible BALB/c and resistant C57BL/6 mice: an essential role for gamma interferon. Infect. Immun. **62**:2590-2599.

14 **Autenrieth, I. B. and R. Firsching**. 1996. Penetration of M cells and destruction of Peyer's patches by *Yersinia enterocolitica*: an ultrastructural and histological study. J. Med. Microbiol. **44**:285-294.

15 **Autenrieth, I. B., P. Hantschmann, B. Heymer, and J. Heesemann**. 1993. Immunohistological characterization of the cellular immune response against *Yersinia enterocolitica* in mice: evidence for the involvement of T lymphocytes. Immunobiology **187**:1-16.

16 **Autenrieth, I. B., V. Kempf, T. Sprinz, S. Preger, and A. Schnell**. 1996. Defense mechanisms in Peyer's patches and mesenteric lymph nodes against *Yersinia enterocolitica* involve integrins and cytokines. Infect. Immun. **64**:1357-1368.

17 **Autenrieth, I. B., R. Reissbrodt, E. Saken, R. Berner, U. Vogel, W. Rabsch, and J. Heesemann**. 1994. Desferrioxamine-promoted virulence of *Yersinia enterocolitica* in mice depends on both desferrioxamine type and mouse strain. J. Infect. Dis. **169**:562-567.

18 **Autenrieth, I. B., A. Tingle, A. Reske-Kunz, and J. Heesemann**. 1992. T lymphocytes mediate protection against *Yersinia enterocolitica* in mice: characterization of murine T-cell clones specific for *Y. enterocolitica*. Infect. Immun. **60**:1140-1149.

19 **Banchereau, J., F. Briere, C. Caux, J. Davoust, S. Lebecque, Y. J. Liu, B. Pulendran, and K. Palucka**. 2000. Immunobiology of dendritic cells. Annu. Rev. Immunol. **18**:767-811.

20 **Banchereau, J. and R. M. Steinman**. 1998. Dendritic cells and the control of immunity. Nature **392**:245-252.

21 **Baran-Marszak F., J. Feuillard, I. Najjar, C. Le Clorennec, J.M. Bechet, I. Dusanter-Fourt, G. W. Bornkamm, M. Raphael and R. Fagard.** 2004 Differential roles of STAT1α and STAT1β in fludarabine-induced cell cycle arrest and apoptosis in human B cells. Blood **104**:2475-2483

22 **Bell, D., J. W. Young, and J. Banchereau**. 1999. Dendritic cells. Adv. Immunol. **72**:255-324.

23 **Black, D. S. and J. B. Bliska**. 1997. Identification of p130Cas as a substrate of *Yersinia* YopH (Yop51), a bacterial protein tyrosine phosphatase that translocates into mammalian cells and targets focal adhesions. EMBO J. **16**:2730-2744.

24 **Black, D. S. and J. B. Bliska**. 2000. The RhoGAP activity of the *Yersinia pseudotuberculosis* cytotoxin YopE is required for antiphagocytic function and virulence. Mol. Microbiol. **37**:515-527.

25 **Bliska, J. B. and D. S. Black**. 1995. Inhibition of the Fc receptor-mediated oxidative burst in macrophages by the *Yersinia pseudotuberculosis* tyrosine phosphatase. Infect. Immun. **63**:681-685.

26 **Bliska, J. B. and S. Falkow**. 1992. Bacterial resistance to complement killing mediated by the Ail protein of *Yersinia enterocolitica*. Proc. Natl. Acad. Sci. U. S. A **89**:3561-3565.

27 **Bohn, E. and I. B. Autenrieth**. 1996. IL-12 is essential for resistance against *Yersinia enterocolitica* by triggering IFN-gamma production in NK cells and CD4+ T cells. J. Immunol. **156**:1458-1468.

28 **Bohn, E., J. Heesemann, S. Ehlers, and I. B. Autenrieth**. 1994. Early gamma interferon mRNA expression is associated with resistance of mice against *Yersinia enterocolitica*. Infect. Immun. **62**:3027-3032.

29 **Bohn, E., E. Schmitt, C. Bielfeldt, A. Noll, R. Schulte, and I. B. Autenrieth**. 1998. Ambiguous role of interleukin-12 in *Yersinia enterocolitica* infection in susceptible and resistant mouse strains. Infect. Immun. **66**:2213-2220.

30 **Bohn, E., A. Sing, R. Zumbihl, C. Bielfeldt, H. Okamura, M. Kurimoto, J. Heesemann, and I. B. Autenrieth**. 1998. IL-18 (IFN-gamma-inducing factor) regulates early cytokine production in, and promotes resolution of, bacterial infection in mice. J. Immunol. **160**:299-307.

31 **Boland, A. and G. R. Cornelis**. 1998. Role of YopP in suppression of tumor necrosis factor alpha release by macrophages during *Yersinia* infection. Infect. Immun. **66**:1878-1884.

32 **Brett, S. J., A. V. Mazurov, I. G. Charles, and J. P. Tite**. 1993. The invasin protein of *Yersinia* spp. provides co-stimulatory activity to human T cells through interaction with beta 1 integrins. Eur. J. Immunol. **23**:1608-1614.

33 **Brightbill, H. D., D. H. Libraty, S. R. Krutzik, R. B. Yang, J. T. Belisle, J. R. Bleharski, M. Maitland, M. V. Norgard, S. E. Plevy, S. T. Smale, P. J. Brennan, B. R. Bloom, P. J. Godowski, and R. L. Modlin**. 1999. Host defense mechanisms triggered by microbial lipoproteins through toll-like receptors. Science **285**:732-736.

34 **Brocker, T., M. Riedinger, and K. Karjalainen**. 1997. Targeted expression of major histocompatibility complex (MHC) class II molecules demonstrates that dendritic cells can induce negative but not positive selection of thymocytes *in vivo*. J. Exp. Med. **185**:541-550.

35 **Brzostek K., A. Raczkowska, A. Zasada.** 2003. The osmotic regulator OmpR is involved in the response of *Yersinia enterocolitica* O:9 to environmental stresses and survival within macrophages, FEMS Microbiol. Lett. **228**: 265–271.

36 **Cella, M., A. Engering, V. Pinet, J. Pieters, and A. Lanzavecchia**. 1997. Inflammatory stimuli induce accumulation of MHC class II complexes on dendritic cells. Nature **388**:782-787.

37 **China, B., M. P. Sory, B. T. N'Guyen, B. M. De, and G. R. Cornelis**. 1993. Role of the YadA protein in prevention of opsonization of *Yersinia enterocolitica* by C3b molecules. Infect. Immun. **61**:3129-3136.

38 **Clark, M. A., B. H. Hirst, and M. A. Jepson**. 1998. M-cell surface beta1 integrin expression and invasin-mediated targeting of *Yersinia pseudotuberculosis* to mouse Peyer's patch M cells. Infect. Immun. **66**:1237-1243.

39 **Collazo, C.M. et al.** 2001 Inactivation of LRG-47 and IRG-47 reveals a family of interferon-γ-inducible genes with essential, pathogen specific roles in resistance to infection. J. Exp. Med. **194**: 181–187

40 **Cornelis, G. R.** 1998. The *Yersinia* deadly kiss. J. Bacteriol. **180**:5495-5504.

41 **Cornelis, G. R.** 2002. The *Yersinia* Ysc-Yop 'type III' weaponry. Nat. Rev. Mol. Cell Biol. **3**:742-752.

42 **Cornelis, G. R., A. Boland, A. P. Boyd, C. Geuijen, M. Iriarte, C. Neyt, M. P. Sory, and I. Stainier**. 1998. The virulence plasmid of *Yersinia*, an antihost genome. Microbiol. Mol. Biol. Rev. **62**:1315-1352.

43 **Cover, T. L. and R. C. Aber**. 1989. *Yersinia enterocolitica*. N. Engl. J. Med. **321**:16-24.

44 NK 3. **Davis DM, Chiu I, Fassett M, Cohen GB, Mandelboim O, Strominger JL.** 1999. The human natural killer cell immune synapse.Proc. Natl. Acad. Sci. USA **96**:15062–67

45 **Delor, I. and G. R. Cornelis**. 1992. Role of *Yersinia enterocolitica* Yst toxin in experimental infection of young rabbits. Infect. Immun. **60**:4269-4277.

46 **Denecker, G., W. Declercq, C. A. Geuijen, A. Boland, R. Benabdillah, G. M. van, M. P. Sory, P. Vandenabeele, and G. R. Cornelis**. 2001. *Yersinia enterocolitica* YopP-induced apoptosis of macrophages involves the apoptotic signaling cascade upstream of bid. J. Biol. Chem. **276**:19706-19714.

47 **Denecker, G., S. Totemeyer, L. J. Mota, P. Troisfontaines, I. Lambermont, C. Youta, I. Stainier, M. Ackermann, and G. R. Cornelis**. 2002. Effect of low-

and high-virulence *Yersinia enterocolitica* strains on the inflammatory response of human umbilical vein endothelial cells. Infect. Immun. **70**:3510-3520.

48 **Devenish, J. A. and D. A. Schiemann**. 1981. HeLa cell infection by *Yersinia enterocolitica*: evidence for lack of intracellular multiplication and development of a new procedure for quantitative expression of infectivity. Infect. Immun. **32**:48-55.

49 **Diebold, S. S., T. Kaisho, H. Hemmi, S. Akira, and Reis e Sousa**. 2004. Innate antiviral responses by means of TLR7-mediated recognition of single-stranded RNA. Science **303**:1529-1531.

50 **Dube P.H., S. A. Handley, J. Lewis and V. L. Miller.** 2004. Protective role of interleukin-6 during *Yersinia enterocolitica* infection is mediated through the modulation of inflammatory cytokines. Infect. Immun.**72**:3561–3570

51 **Tabrizi S.N., R.M. Robins-Browne.** 1992. Influence of a 70 kilobase virulence plasmid on the ability of *Yersinia enterocolitica* to survive phagocytosis in vitro, Microb. Pathog. **13**:171– 179.

52 **Falgarone, G., H. S. Blanchard, B. Riot, M. Simonet, and M. Breban**. 1999. Cytotoxic T-cell-mediated response against *Yersinia pseudotuberculosis* in HLA-B27 transgenic rat. Infect. Immun. **67**:3773-3779.

53 **Falgarone, G., H. S. Blanchard, F. Virecoulon, M. Simonet, and M. Breban**. 1999. Coordinate involvement of invasin and Yop proteins in a *Yersinia pseudotuberculosis*-specific class I-restricted cytotoxic T cell-mediated response. J. Immunol. **162**:2875-2883.

54 **Fallman, M., K. Andersson, S. Hakansson, K. E. Magnusson, O. Stendahl, and H. Wolf-Watz**. 1995. *Yersinia pseudotuberculosis* inhibits Fc receptor-mediated phagocytosis in J774 cells. Infect. Immun. **63**:3117-3124.

55 **Fearon, D. T. and R. M. Locksley**. 1996. The instructive role of innate immunity in the acquired immune response. Science **272**:50-53.

56 **Feng, C.G. et al.** 2004 Mice deficient in LRG-47 display increases susceptibility to mycobacterial infection associated with the induction of lymphopenia. J. Immunol. **172:** 1163–1168

57 **Galan, J. E. and A. Collmer**. 1999. Type III secretion machines: bacterial devices for protein delivery into host cells. Science **284**:1322-1328.

58 **Gallucci, S. and P. Matzinger**. 2001. Danger signals: SOS to the immune system. Curr. Opin. Immunol. **13**:114-119.

59 **Galyov, E. E., S. Hakansson, and H. Wolf-Watz**. 1994. Characterization of the operon encoding the YpkA Ser/Thr protein kinase and the YopJ protein of *Yersinia pseudotuberculosis*. J. Bacteriol. **176**:4543-4548.

60 **Garrett, W. S., L. M. Chen, R. Kroschewski, M. Ebersold, S. Turley, S. Trombetta, J. E. Galan, and I. Mellman**. 2000. Developmental control of endocytosis in dendritic cells by Cdc42. Cell **102**:325-334.

61 **Grant T., V. Bennett-Wood, R.M. Robins-Browne.** 1999. Characterization of the interaction between *Yersinia enterocolitica* biotype 1A and phagocytes and epithelial cells in vitro, Infect. Immun. **67**: 4367– 4375.

62 **Grutzkau, A., C. Hanski, H. Hahn, and E. O. Riecken**. 1990. Involvement of M cells in the bacterial invasion of Peyer's patches: a common mechanism shared by *Yersinia enterocolitica* and other enteroinvasive bacteria. Gut **31**:1011-1015.

63 **Guan, K. L. and J. E. Dixon**. 1990. Protein tyrosine phosphatase activity of an essential virulence determinant in *Yersinia*. Science **249**:553-556.

64 **Guarner, J., W. J. Shieh, P. W. Greer, J. M. Gabastou, M. Chu, E. Hayes, K. B. Nolte, and S. R. Zaki.** 2002. Immunohistochemical detection of *Yersinia pestis* in formalin-fixed, paraffin-embedded tissue. Am. J. Clin. Pathol. **117:** 205–209.

65 **Guermonprez, P., J. Valladeau, L. Zitvogel, C. Thery, and S. Amigorena**. 2002. Antigen presentation and T cell stimulation by dendritic cells. Annu. Rev. Immunol. **20**:621-667.

66 **Haag, H., K. Hantke, H. Drechsel, I. Stojiljkovic, G. Jung, and H. Zahner**. 1993. Purification of yersiniabactin: a siderophore and possible virulence factor of *Yersinia enterocolitica*. J. Gen. Microbiol. **139**:2159-2165.

67 **Halonen, S.K. et al.** 2001 Interferon-induced inhibition of Toxoplasma gondii in astrocytes mediated by IGTP. Infect. Immun. **69**:5573–5576

68 **Hanski, C., U. Kutschka, H. P. Schmoranzer, M. Naumann, A. Stallmach, H. Hahn, H. Menge, and E. O. Riecken**. 1989. Immunohistochemical and electron microscopic study of interaction of *Yersinia enterocolitica* serotype O8 with intestinal mucosa during experimental enteritis. Infect. Immun. **57**:673-678.

69 **Hart, D. N.** 1997. Dendritic cells: unique leukocyte populations which control the primary immune response. Blood **90**:3245-3287.

70 **Heesemann, J., and R. Laufs.** 1985. Double immunofluorescence microscopic technique for accurate differentiation of extracellularly and intracellularly located bacteria in cell culture. J. Clin. Microbiol. **22**:168–175.

71 **Heesemann, J. and R. Laufs**. 1983. Construction of a mobilizable *Yersinia enterocolitica* virulence plasmid. J. Bacteriol. **155**:761-767.

72 **Heil, F., H. Hemmi, H. Hochrein, F. Ampenberger, C. Kirschning, S. Akira, G. Lipford, H. Wagner, and S. Bauer**. 2004. Species-specific recognition of single-stranded RNA via toll-like receptor 7 and 8. Science **303**:1526-1529.

73 **Hein, J., V. A. Kempf, J. Diebold, N. Bucheler, S. Preger, I. Horak, A. Sing, U. Kramer, and I. B. Autenrieth**. 2000. Interferon consensus sequence binding protein confers resistance against *Yersinia enterocolitica*. Infect. Immun. **68**:1408-1417.

74 **Henderson, R. A., S. C. Watkins, and J. L. Flynn**. 1997. Activation of human dendritic cells following infection with *Mycobacterium tuberculosis*. J. Immunol. **159**:635-643.

75 **Hoffmann, J. A., F. C. Kafatos, C. A. Janeway, and R. A. Ezekowitz**. 1999. Phylogenetic perspectives in innate immunity. Science **284**:1313-1318.

76 **Hu, P., J. Elliott, P. McCready, E. Skowronski, J. Garnes, A. Kobayashi, R. R. Brubaker, and E. Garcia**. 1998. Structural organization of virulence-associated plasmids of Yersinia pestis. J. Bacteriol. **180**:5192-5202.

77 **Iriarte, M. and G. R. Cornelis**. 1998. YopT, a new *Yersinia* Yop effector protein, affects the cytoskeleton of host cells. Mol. Microbiol. **29**:915-929.

78 **Iriarte, M., J. C. Vanooteghem, I. Delor, R. Diaz, S. Knutton, and G. R. Cornelis**. 1993. The Myf fibrillae of *Yersinia enterocolitica*. Mol. Microbiol. **9**:507-520.

79 **Isberg, R. R. and J. M. Leong**. 1990. Multiple beta 1 chain integrins are receptors for invasin, a protein that promotes bacterial penetration into mammalian cells. Cell **60**:861-871.

80 **Janeway, C. A., P. Travers, M. Walport, Shlomchik**. 2001. Immunobiology.

81 **Jiang, W., W. J. Swiggard, C. Heufler, M. Peng, A. Mirza, R. M. Steinman, and M. C. Nussenzweig**. 1995. The receptor DEC-205 expressed by dendritic cells and thymic epithelial cells is involved in antigen processing. Nature **375**:151-155.

82 **Juris, S. J., A. E. Rudolph, D. Huddler, K. Orth, and J. E. Dixon**. 2000. A distinctive role for the *Yersinia* protein kinase: actin binding, kinase activation, and cytoskeleton disruption. Proc. Natl. Acad. Sci. U. S. A **97**:9431-9436.

83 **Kampik, D., R. Schulte, and I. B. Autenrieth**. 2000. *Yersinia enterocolitica* invasin protein triggers differential production of interleukin-1, interleukin-8, monocyte chemoattractant protein 1, granulocyte-macrophage colony-stimulating factor, and tumor necrosis factor alpha in epithelial cells: implications for understanding the early cytokine network in *Yersinia* infections. Infect. Immun. **68**:2484-2492.

84 **Kim S, Iizuka K, Aguila HL, Weissman IL, Yokoyama WM**. 2000. In vivo natural killer cell activities revealed by natural killer cell-deficient mice. PNAS USA **97**:2731-6.

85 **Koeberle, M., B. Manncke, J. Krejci, G. Grassl, P. Gaentzsch, K. Reinecke, S. Mueller, M. Asselin-Labat, M. Pallardy, I. Sorg, G. Cornelis, H. Wolf-**

Watz, R. Zumbihl, I. B. Autenrieth, and E. Bohn. 2005. Targeting of Rho GTPases by YopT leads to induction of GILZ which contributes to inhibition of NF-κB in epithelial cells. J. Biol. Chem., in press.

86 **Koster, M. and W. Bitter**. 1997. The outer membrane component, YscC, of the Yop secretion machinery of *Yersinia enterocolitica* forms a ring-shaped multimeric complex. **26**:789-797.

87 IL1 **Lang D, Knop J, Wesche H, et al.** 1998. The type II IL-1 receptor interacts with the IL-1 receptor accessory protein: a novel mechanism of regulation of IL-1 responsiveness. J Immunol. **161**:6871–7.

88 NK 11. **Lanier LL.** 2000. Turning on natural killer cells. J Exp Med. **191**:1259-62.

89 **Leung, K. Y., B. S. Reisner, and S. C. Straley**. 1990. YopM inhibits platelet aggregation and is necessary for virulence of *Yersinia pestis* in mice. Infect. Immun. **58**:3262-3271.

90 **Leung, K. Y. and S. C. Straley**. 1989. The yopM gene of *Yersinia pestis* encodes a released protein having homology with the human platelet surface protein GPIb alpha. J. Bacteriol. **171**:4623-4632.

91 **Loetscher P, Pellegrino A, Gong JH, Mattioli I, Loetscher M, Bardi G, et al.** 2001. The ligands of CXC chemokine receptor 3, I-TAC, Mig, and IP10, are natural antagonists for CCR3. J Biol Chem **276**:2986–2991.

92 NK 5. **Long E. O.** 1999. Regulation of immune responses through inhibitory receptors. Annu Rev Immunol. **17**:875-904.

93 **Lukaszewski R. A., D. J. Kenny, R. Taylor, D. G. Cerys Rees, M. Gill Hartley, and P. C. F. Oyston** 2005. Pathogenesis of *Yersinia pestis* Infection in BALB/c Mice: Effects on Host Macrophages and Neutrophils Infect. Immun. **73**:7142–7150

94 **Lund, J. M., L. Alexopoulou, A. Sato, M. Karow, N. C. Adams, N. W. Gale, A. Iwasaki, and R. A. Flavell**. 2004. Recognition of single-stranded RNA viruses by Toll-like receptor 7. Proc. Natl. Acad. Sci. U. S. A **101**:5598-5603.

95 **Lundgren, E., N. Carballeira, R. Vazquez, E. Dubinina, H. Branden, H. Persson, and H. Wolf-Watz**. 1996. Invasin of *Yersinia pseudotuberculosis* activates human peripheral B cells. Infect. Immun. **64**:829-835.

96 **MacMicking J. D., G. A. Taylor, J. D. McKinney.** 2003. Immune control of tuberculosis by IFN-γ–Inducible LRG-47. Science **302**: 654-659

97 IL1 **Malinowsky D, Lundkvist J, Laye S, Bartfai T.** 1998. Interleukin-1 receptor accessory protein interacts with the type II interleukin-1 receptor. FEBS Lett;429:299–302.

98 **Munder M, Mallo M, Eichmann K, Modolell M.** 1998. Murine macrophages secrete interferon gamma upon combined stimulation with interleukin (IL)-12 and

IL-18: A novel pathway of autocrine macrophage activation. J Exp Med. **187**:2103-2108.

99 **Matsumoto, M., K. Funami, M. Tanabe, H. Oshiumi, M. Shingai, Y. Seto, A. Yamamoto, and T. Seya**. 2003. Subcellular localization of Toll-like receptor 3 in human dendritic cells. J. Immunol. **171**:3154-3162.

100 **Matzinger, P.** 1994. Tolerance, danger, and the extended family. Annu. Rev. Immunol. **12**:991-1045.

101 **Medzhitov, R. and C. A. Janeway, Jr.** 1997. Innate immunity: impact on the adaptive immune response. Curr. Opin. Immunol. **9**:4-9.

102 **Michiels, T., P. Wattiau, R. Brasseur, J. M. Ruysschaert, and G. Cornelis**. 1990. Secretion of Yop proteins by *Yersiniae*. Infect. Immun. **58**:2840-2849.

103 **Miller, V. L. and S. Falkow**. 1988. Evidence for two genetic loci in *Yersinia enterocolitica* that can promote invasion of epithelial cells. Infect. Immun. **56**:1242-1248.

104 **Minamino, T. and R. M. Macnab**. 1999. Components of the *Salmonella* flagellar export apparatus and classification of export substrates. J. Bacteriol. **181**:1388-1394.

105 **Muzio, M., G. Natoli, S. Saccani, M. Levrero, and A. Mantovani**. 1998. The human toll signaling pathway: divergence of nuclear factor kappaB and JNK/SAPK activation upstream of tumor necrosis factor receptor-associated factor 6 (TRAF6). J. Exp. Med. **187**:2097-2101.

106 **Nakajima, R., V. L. Motin, and R. R. Brubaker**. 1995. Suppression of cytokines in mice by protein A-V antigen fusion peptide and restoration of synthesis by active immunization. Infect. Immun. **63**:3021-3029.

107 **Nathan, C. F., H. W. Murray, M. E. Wiebe, and B. Y. Rubin.** 1983. Identification of interferon-gamma as the lymphokine that activates human macrophage oxidative metabolism and antimicrobial activity. J. Exp. Med. **158:** 670–689.

108 **Noll, A. and AutenriethIB**. 1996. Immunity against *Yersinia enterocolitica* by vaccination with *Yersinia* HSP60 immunostimulating complexes or *Yersinia* HSP60 plus interleukin-12. Infect. Immun. **64**:2955-2961.

109 **Ohteki, T., T. Fukao, K. Suzue, C. Maki, M. Ito, M. Nakamura, and S. Koyasu**. 1999. Interleukin 12-dependent interferon gamma production by CD8alpha$^+$ lymphoid dendritic cells. J. Exp. Med. **189**:1981-1986.

110 **Orth, K., Z. Xu, M. B. Mudgett, Z. Q. Bao, L. E. Palmer, J. B. Bliska, W. F. Mangel, B. Staskawicz, and J. E. Dixon**. 2000. Disruption of signaling by *Yersinia* effector YopJ, a ubiquitin-like protein protease. Science **290**:1594-1597.

111 **Palecanda, A., J. Paulauskis, E. Al-Mutairi, A. Imrich, G. Qin, H. Suzuki, T. Kodama, K. Tryggvason, H. Koziel, and L. Kobzik.** 1999. Role of the scavenger

receptor MARCO in alveolar macrophage binding of unopsonized environmental particles. J. Exp. Med. **189**:1497–1506.

112 **Palmer, L. E., S. Hobbie, J. E. Galan, and J. B. Bliska**. 1998. YopJ of *Yersinia pseudotuberculosis* is required for the inhibition of macrophage TNF-alpha production and downregulation of the MAP kinases p38 and JNK. Mol. Microbiol. **27**:953-965.

113 **Pepe, J. C. and V. L. Miller**. 1993. The biological role of invasin during a *Yersinia enterocolitica* infection. Infect. Agents Dis. **2**:236-241.

114 **Perry, R. D., S. C. Straley, J. D. Fetherston, D. J. Rose, J. Gregor, and F. R. Blattner**. 1998. DNA sequencing and analysis of the low-$Ca2^{+}$-response plasmid pCD1 of Yersinia pestis KIM5. Infect. Immun. **66**:4611-4623.

115 **Persson, C., R. Nordfelth, K. Andersson, A. Forsberg, H. Wolf-Watz, and M. Fallman**. 1999. Localization of the *Yersinia* PTPase to focal complexes is an important virulence mechanism. Mol. Microbiol. **33**:828-838.

116 **Pierson, D. E. and S. Falkow**. 1993. The ail gene of *Yersinia enterocolitica* has a role in the ability of the organism to survive serum killing. Infect. Immun. **61**:1846-1852.

117 **Platt, N., R. P. da Silva, and S. Gordon**. 1998. Recognizing death: the phagocytosis of apoptotic cells. Trends Cell Biol. **8**:365-372.

118 **Pujol C. and J. B. Bliska** The ability to replicate in macrophages is conserved between *Yersinia pestis* and *Yersinia pseudotuberculosis.* 2003 Infect. Immun. **71**:5892–5899

119 **Pujol C. and J. B. Bliska** 2005. Turning *Yersinia* pathogenesis outside in: subversion of macrophage function by intracellular yersiniae. Clin. Immun. **114**:216– 226

120 **Ramamurthy, T., K. Yoshino, X. Huang, N. G. Balakrish, E. Carniel, T. Maruyama, H. Fukushima, and T. Takeda**. 1997. The novel heat-stable enterotoxin subtype gene (ystB) of *Yersinia enterocolitica*: nucleotide sequence and distribution of the yst genes. Microb. Pathog. **23**:189-200.

121 **Regnault, A., D. Lankar, V. Lacabanne, A. Rodriguez, C. Thery, M. Rescigno, T. Saito, S. Verbeek, C. Bonnerot, P. Ricciardi-Castagnoli, and S. Amigorena**. 1999. Fcgamma receptor-mediated induction of dendritic cell maturation and major histocompatibility complex class I-restricted antigen presentation after immune complex internalization. J. Exp. Med. **189**:371-380.

122 **Reis e Sousa, P. D. Stahl, and J. M. Austyn**. 1993. Phagocytosis of antigens by Langerhans cells *in vitro*. J. Exp. Med. **178**:509-519.

123 **Rescigno, M., S. Citterio, C. Thery, M. Rittig, D. Medaglini, G. Pozzi, S. Amigorena, and P. Ricciardi-Castagnoli**. 1998. Bacteria-induced neo-biosynthesis, stabilization, and surface expression of functional class I molecules in mouse dendritic cells. Proc. Natl. Acad. Sci. U. S. A **95**:5229-5234.

124 **Revell, P. A. and V. L. Miller**. 2001. *Yersinia* virulence: more than a plasmid. FEMS Microbiol. Lett. **205**:159-164.

125 **Ridge, J. P., R. F. Di, and P. Matzinger**. 1998. A conditioned dendritic cell can be a temporal bridge between a $CD4^+$ T-helper and a T-killer cell. Nature **393**:474-478.

126 **Roggenkamp, A., T. Bittner, L. Leitritz, A. Sing, and J. Heesemann**. 1997. Contribution of the Mn-cofactored superoxide dismutase (SodA) to the virulence of *Yersinia enterocolitica* serotype O8. Infect. Immun. **65**:4705-4710.

127 **Roggenkamp, A., H. R. Neuberger, A. Flugel, T. Schmoll, and J. Heesemann**. 1995. Substitution of two histidine residues in YadA protein of *Yersinia enterocolitica* abrogates collagen binding, cell adherence and mouse virulence. Mol. Microbiol. **16**:1207-1219.

128 **Roggenkamp, A., K. Ruckdeschel, L. Leitritz, R. Schmitt, and J. Heesemann**. 1996. Deletion of amino acids 29 to 81 in adhesion protein YadA of *Yersinia enterocolitica* serotype O:8 results in selective abrogation of adherence to neutrophils. Infect. Immun. **64**:2506-2514.

129 **Rosqvist, R., I. Bolin, and H. Wolf-Watz**. 1988. Inhibition of phagocytosis in *Yersinia pseudotuberculosis*: a virulence plasmid-encoded ability involving the Yop2b protein. Infect. Immun. **56**:2139-2143.

130 **Rosqvist, R., A. Forsberg, and H. Wolf-Watz**. 1991. Intracellular targeting of the *Yersinia* YopE cytotoxin in mammalian cells induces actin microfilament disruption. Infect. Immun. **59**:4562-4569.

131 **Ruckdeschel, K., S. Harb, A. Roggenkamp, M. Hornef, R. Zumbihl, S. Kohler, J. Heesemann, and B. Rouot**. 1998. *Yersinia enterocolitica* impairs activation of transcription factor NF-kappaB: involvement in the induction of programmed cell death and in the suppression of the macrophage tumor necrosis factor alpha production. J. Exp. Med. **187**:1069-1079.

132 **Ruckdeschel, K., O. Mannel, K. Richter, C. A. Jacobi, K. Trulzsch, B. Rouot, and J. Heesemann**. 2001. *Yersinia* outer protein P of *Yersinia enterocolitica* simultaneously blocks the nuclear factor-kappa B pathway and exploits lipopolysaccharide signaling to trigger apoptosis in macrophages. J. Immunol. **166**:1823-1831.

133 **Ruckdeschel, K., K. Richter, O. Mannel, and J. Heesemann**. 2001. Arginine-143 of *Yersinia enterocolitica* YopP crucially determines isotype-related NF-kappaB suppression and apoptosis induction in macrophages. Infect. Immun. **69**:7652-7662.

134 **Ruckdeschel, K., A. Roggenkamp, V. Lafont, P. Mangeat, J. Heesemann, and B. Rouot**. 1997. Interaction of *Yersinia enterocolitica* with macrophages leads to macrophage cell death through apoptosis. Infect. Immun. **65**:4813-4821.

135 **Ruckdeschel, K., A. Roggenkamp, S. Schubert, and J. Heesemann**. 1996. Differential contribution of *Yersinia enterocolitica* virulence factors to evasion of microbicidal action of neutrophils. Infect. Immun. **64**:724-733.

136 **Sallusto, F., M. Cella, C. Danieli, and A. Lanzavecchia**. 1995. Dendritic cells use macropinocytosis and the mannose receptor to concentrate macromolecules in the major histocompatibility complex class II compartment: downregulation by cytokines and bacterial products. J. Exp. Med. **182**:389-400.

137 **Sallusto, F. and A. Lanzavecchia**. 2000. Understanding dendritic cell and T-lymphocyte traffic through the analysis of chemokine receptor expression. Immunol. Rev. **177**:134-140.

138 **Sauvonnet, N., I. Lambermont, B. P. van der, and G. R. Cornelis**. 2002. YopH prevents monocyte chemoattractant protein 1 expression in macrophages and T-cell proliferation through inactivation of the phosphatidylinositol 3-kinase pathway. Mol. Microbiol. **45**:805-815.

139 **Schulte, R., G. A. Grassl, S. Preger, S. Fessele, C. A. Jacobi, M. Schaller, P. J. Nelson, and I. B. Autenrieth**. 2000. *Yersinia enterocolitica* invasin protein triggers IL-8 production in epithelial cells via activation of Rel p65-p65 homodimers. FASEB J. **14**:1471-1484.

140 **Schulte, R., R. Zumbihl, D. Kampik, A. Fauconnier, and I. B. Autenrieth**. 1998. Wortmannin blocks *Yersinia* invasin-triggered internalization, but not interleukin-8 production by epithelial cells. Med. Microbiol. Immunol. (Berl) **187**:53-60.

141 **Schulze A. and J. Downward.** 2001. Navigating gene expression using microarrays—a technology review. Nature Cell Biology **3**:190-195

142 **Shepel, M., J. Boyd, J. Luider, and A. P. Gibb**. 2001. Interaction of *Yersinia enterocolitica* and *Y. pseudotuberculosis* with platelets. J. Med. Microbiol. **50**:1030-1038.

143 **Simonet, M., S. Richard, and P. Berche**. 1990. Electron microscopic evidence for *in vivo* extracellular localization of *Yersinia pseudotuberculosis* harboring the pYV plasmid. Infect. Immun. **58**:841-845.

144 **Sing, A., A. Roggenkamp, A. M. Geiger, and J. Heesemann**. 2002. *Yersinia enterocolitica* evasion of the host innate immune response by V antigen-induced IL-10 production of macrophages is abrogated in IL-10-deficient mice. J. Immunol. **168**:1315-1321.

145 **Slepnev, V. I. and C. P. De**. 2000. Accessory factors in clathrin-dependent synaptic vesicle endocytosis. Nat. Rev. Neurosci. **1**:161-172.

146 **Snellings, N. J., M. Popek, and L. E. Lindler**. 2001. Complete DNA sequence of *Yersinia enterocolitica* serotype 0:8 low-calcium-response plasmid reveals a new virulence plasmid-associated replicon. Infect. Immun. **69**:4627-4638.

147 **Srivastava, P. K., H. Udono, N. E. Blachere, and Z. Li**. 1994. Heat shock proteins transfer peptides during antigen processing and CTL priming. Immunogenetics 93-98.

148 **Steinman, R. M.** 1991. The dendritic cell system and its role in immunogenicity. Annu. Rev. Immunol. **9**:271-296.

149 NK 8. **Stetson DB, Mohrs M, Reinhardt RL, Baron JL,Wang ZE, et al.** 2003. Constitutive cytokine mRNAs mark natural killer (NK) and NK T cells poised for rapid effector function. J. Exp. Med. **198**:1069–76

150 **Straley, S. P. H.** 1984. *Yersinia pestis* grows within phagolysosomes in mouse peritoneal macrophages. Infect. Immun. **45:**655–659.

151 IL1 **Symons JA, Young PR, Duff GW.** 1995. Soluble type II interleukin 1 (IL-1) receptor binds and blocks processing of IL-1 beta precursor and loses affinity for IL-1 receptor antagonist. Proc Natl Acad Sci USA;**92**:1714–8.

152 **Takeda, K., T. Kaisho, and S. Akira**. 2003. Toll-like receptors. Annu. Rev. Immunol. **21**:335-376.

153 **Taylor, G.A. et al.** .2000. Pathogen specific loss of host resistance in lacking the interferon-g-inducible gene IGTP. Proc. Natl. Acad. Sci. U. S. A. **97**: 751–755

154 **Teyton, L., D. O'Sullivan, P. W. Dickson, V. Lotteau, A. Sette, P. Fink, and P. A. Peterson**. 1990. Invariant chain distinguishes between the exogenous and endogenous antigen presentation pathways. Nature **348**:39-44.

155 **Thery, C. and S. Amigorena**. 2001. The cell biology of antigen presentation in dendritic cells. Curr. Opin. Immunol. **13**:45-51.

156 NK 1. **Trinchieri G.** 1989. Biology of natural killer cells. Adv Immunol **47**:187-376.

157 **Trulzsch, K., G. Geginat, T. Sporleder, K. Ruckdeschel, R. Hoffmann, J. Heesemann, and H. Russmann**. 2005. *Yersinia* outer protein P inhibits CD8 T cell priming in the mouse infection model. J. Immunol. **174**:4244-4251.

158 **Trulzsch, K., T. Sporleder, E. I. Igwe, H. Russmann, and J. Heesemann**. 2004. Contribution of the major secreted yops of *Yersinia enterocolitica* O:8 to pathogenicity in the mouse infection model. Infect. Immun. **72**:5227-5234.

159 **Valladeau, J., O. Ravel, C. zutter-Dambuyant, K. Moore, M. Kleijmeer, Y. Liu, V. Duvert-Frances, C. Vincent, D. Schmitt, J. Davoust, C. Caux, S. Lebecque, and S. Saeland**. 2000. Langerin, a novel C-type lectin specific to Langerhans cells, is an endocytic receptor that induces the formation of Birbeck granules. Immunity. **12**:71-81.

160 **van der Laan, L.J., E.A. Dopp, R. Haworth, T. Pikkarainen, M. Kangas, O. Elomaa, C.D. Dijkstra, S. Gordon, K. Tryggvason, and G. Kraal.** 1999. Regulation and functional involvement of macrophage scavenger receptor MARCO in clearance of bacteria in vivo. J. Immunol. **162**:939–947.

161 **Visser, L. G., A. Annema, and F. R. van**. 1995. Role of Yops in inhibition of phagocytosis and killing of opsonized *Yersinia enterocolitica* by human granulocytes. Infect. Immun. **63**:2570-2575.

162 **Vogel, U., I. B. Autenrieth, R. Berner, and J. Heesemann**. 1993. Role of plasmid-encoded antigens of *Yersinia enterocolitica* in humoral immunity against secondary *Y. enterocolitica* infection in mice. Microb. Pathog. **15**:23-36.

163 **Von Pawel-Rammingen, U., M. V. Telepnev, G. Schmidt, K. Aktories, H. Wolf-Watz, and R. Rosqvist**. 2000. GAP activity of the *Yersinia* YopE cytotoxin specifically targets the Rho pathway: a mechanism for disruption of actin microfilament structure. Mol. Microbiol. **36**:737-748.

164 **Welkos, S., A. Friedlander, D. McDowell, J. Weeks, and S. Tobery**. 1998. V antigen of *Yersinia pestis* inhibits neutrophil chemotaxis. Microb. Pathog. **24**:185-196.

165 **West, M. A., A. R. Prescott, E. L. Eskelinen, A. J. Ridley, and C. Watts**. 2000. Rac is required for constitutive macropinocytosis by dendritic cells but does not control its downregulation. Curr. Biol. **10**:839-848.

166 **West, M. A., R. P. Wallin, S. P. Matthews, H. G. Svensson, R. Zaru, H. G. Ljunggren, A. R. Prescott, and C. Watts**. 2004. Enhanced dendritic cell antigen capture via toll-like receptor-induced actin remodeling. Science **305**:1153-1157.

167 **Xaus J.**, **M. Cardo**, **AF**. **Valledor, C. Soler, J. Lloberas, A. Celada.**1999. Interferon gamma induces the expression of p21waf-1 and arrests macrophage cell cycle, preventing induction of apoptosis. Immunity **11**:103-113

168 **Yamamoto T., T. Hanawa, S. Ogata, S. Kamiya.** 1996 Identification and characterization of the *Yersinia enterocolitica* gsrA gene, which protectively responds to intracellular stress induced by macrophage phagocytosis and to extracellular environmental stress, Infect. Immun. **64**: 2980–2987.

169 **Yao, T., J. Mecsas, J. I. Healy, S. Falkow, and Y. Chien**. 1999. Suppression of T and B lymphocyte activation by a *Yersinia pseudotuberculosis* virulence factor, yopH. J. Exp. Med. **190**:1343-1350.

170 **Zumbihl, R., M. Aepfelbacher, A. Andor, C. A. Jacobi, K. Ruckdeschel, B. Rouot, and J. Heesemann**. 1999. The cytotoxin YopT of *Yersinia enterocolitica* induces modification and cellular redistribution of the small GTP-binding protein RhoA. J. Biol. Chem. **274**:29289-29293.

7 Supplementary data

Supplementary table 1: Figure 3.4

Probe sets differentially regulated in splenic CD11b$^+$ cells isolated from C57BL/6 mice intravenously infected with *Y. enterocolitica* pYV$^+$ compared to uninfected control mice.

Cluster A					
Probe set ID	**Public ID**	**Gene Symbol**	**pYV$^+$ vs uninfected 24h**	**pYV$^+$ vs uninfected 72h**	**GO Biological Process**
97560_at	AF037437	---	4,23	4,2	---
99419_g_at	AF032459	Bcl2l11	4,57	4,26	apoptosis
93214_at	AF059029	Camk2d	3,7	4,71	c cell cycle
94146_at	X62502	Ccl4	5,4	4,34	chemotaxis
102719_f_at	X94151	Ccr5	3,85	4,97	chemotaxis
97546_at	AF072127	Cldn1	4,66	3,41	---
95348_at	J04596	Cxcl1	4,38	3,84	inflammatory response
93858_at	M33266	Cxcl10	5,54	4,12	chemotaxis
101160_at	X53798	Cxcl2	5,46	5,15	chemotaxis
97689_at	M26071	F3	4,42	3,6	blood coagulation
102341_at	L46651	Gla	3,78	4,13	carbohydrate metabolism
103963_f_at	AA914345	Iigp1	6,09	4,93	cytokine and chemokine mediated signaling pathway
96764_at	AJ007971	Iigp1	5,31	4,24	cytokine and chemokine mediated signaling pathway
94755_at	M14639	Il1a	6,92	5,97	inflammatory response
98773_s_at	AI323667	Irg1	4,64	3,86	---
98774_at	L38281	Irg1	4,56	3,64	---
101327_at	U82610	Lcp1	4,78	3,92	response to wounding
94688_at	X83106	Mad	7,24	4,83	transcription
160353_i_at	X76850	Mapkapk2	4,75	4,38	protein amino acid phosphorylation
104218_s_at	AI507524	MGI:1923998	4,19	4,03	cell cycle
98818_at	X04435	Nr3c1	4,88	4,14	transcription
102696_s_at	AI747899	Pitpnb	4,79	4,94	transport
160608_at	AI854462	Rab20	4,55	3,48	small GTPase mediated signal transduction
99876_at	U29056	Sla	4,99	4,81	intracellular signaling cascade
98299_s_at	AF099974	Slfn4	4,92	2,95	negative regulation of cell proliferation
99392_at	U19463	Tnfaip3	5,61	4,27	apoptosis
100030_at	D44464	Upp1	5,72	5,01	nucleoside metabolism

Cluster B1					
Probe set ID	**Public ID**	**Gene Symbol**	**pYV$^+$ vs uninfected 24h**	**pYV$^+$ vs uninfected 72h**	**GO Biological Process**

98283_at	X91617	---	1,62	0	---
104146_at	AI853551	---	2,09	0	---
103517_at	AA822898	---	1,84	0,14	---
97162_at	AI451676	---	1,56	0,1	---
98049_at	AI853458	1300018I05Rik	1,6	0,46	cytokinesis
104713_at	AA863717	2410002M20Rik	1,54	0,38	---
102741_at	AW046250	Adar	1,63	0,27	RNA processing
102965_at	AW121646	AI481105	2,28	0,43	---
160131_at	AI854404	Amotl2	1,9	0,59	---
93869_s_at	U23781	Bcl2a1a	1,99	0,35	apoptosis
160645_at	U88908	Birc3	1,53	0,42	apoptosis
95414_i_at	AI132585	C1r	2,05	0,28	complement activation, classical pathway
97783_at	AJ242587	Ccl17	3,45	0,14	chemotaxis
98406_at	AF065947	Ccl5	2,18	-0,29	immune response
97504_at	M83749	Ccnd2	3,51	0,3	cytokinesis
104443_at	L31580	Ccr7	2,12	-0,38	chemotaxis
104509_at	AF059213	Ch25h	1,9	-0,27	cholesterol metabolism
94255_g_at	AI845237	Clic4	2,08	0,56	transportt
160150_f_at	AW125626	Cnn3	3,17	0,29	smooth muscle contraction
101845_s_at	M55219	Csprs	1,79	0,48	---
102638_at	AB015224	Cst7	2,53	0,52	---
95349_g_at	J04596	Cxcl1	1,69	0,33	inflammatory response
96125_at	AF110520	Daxx	2,67	0,51	apoptosis
94271_at	U70017	Dmtf1	2,26	-0,51	regulation of transcription, DNA-dependent
94107_at	AF047355	Dnase1l3	1,53	0,47	apoptosis
161181_f_at	AV234570	Dusp16	1,56	-0,14	inactivation of MAPK
92758_at	U09268	Dusp2	1,55	-0,17	protein amino acid dephosphorylation
102737_at	U35233	Edn1	1,9	-0,65	regulation of pH
92441_at	Y10007	Fap	2,34	0,11	proteolysis and peptidolysis
102921_s_at	M83649	Fas	2,19	0,52	apoptosis
103259_at	U58972	Gfi1	1,69	0,56	transcription
102877_at	M12302	Gzmb	1,52	-1,12	apoptosis
97896_r_at	AW125218	Hat1	1,67	0,46	DNA packaging
100013_at	AW121732	Ifi35	1,74	0,16	immune response
103446_at	AA959954	Ifih1	2,7	0,55	DNA restriction
93956_at	U43086	Ifit3	3,21	-0,47	immune response
99334_at	K00083	Ifng	5,19	-0,73	immune response
161037_at	U14332	Il15	1,98	0,03	immune response
104669_at	U73037	Irf7	2,39	0,45	transcription
162202_f_at	AV373853	Irf7	1,51	0,06	transcription
103432_at	AW122677	Isg20	3,13	0,43	---
93678_s_at	AF054819	Klrk1	1,76	-0,9	---
103335_at	U55060	Lgals9	1,81	0,39	---
160517_at	M35153	Lmnb1	1,88	0,31	---
161576_f_at	AV281450	MGI:1923551	1,73	0,61	---
103254_at	AW049897	MGI:1923551	1,52	0,36	---
104742_at	AA919832	Mgst2	1,61	-0,16	---

103025_at	X52574	Mov10	1,58	0,4	---
98417_at	M21038	Mx1	2,71	0,37	immune response
101424_at	AF019249	Nmi	2,3	0,41	---
94505_at	AW124934	Peli1	1,75	0,02	---
160632_at	AW124627	Prkcn	1,67	0,16	---
99589_f_at	X07625	Prm1	4,55	0,19	nuclear organization and biogenesis
95539_at	AA798971	Rab3ip	1,8	0,46	---
104476_at	U27177	Rbl1	1,71	0,2	transcription
104177_at	AA204579	Rsad2	2,06	-0,09	---
98405_at	U96700	Serpinb9	3,09	0,38	---
93898_at	AB024921	Sgcb	1,86	0,12	cytoskeleton organization and biogenesis
101847_at	AF040242	Sp100	1,93	0,5	---
102873_at	U60091	Tap2	1,55	0	immune response
92962_at	M83312	Tnfrsf5	2,01	0,04	apoptosis
94112_at	U37522	Tnfsf10	1,57	0,02	apoptosis
96533_at	AI508931	Tor3a	1,72	0,04	protein folding
94186_at	L35302	Traf1	1,5	-0,41	apoptosis
98030_at	J03776	Trim30	1,53	0,14	transcription
103066_at	L32973	Tyki	3,42	0,16	nucleotide biosynthesis
92715_at	AL078630	Ubd	2,47	-0,09	protein modification
99964_at	AW061016	Vdr	2,7	-0,2	transcription

Cluster B2					
Probe set ID	**Public ID**	**Gene Symbol**	**pYV^+ vs uninfected 24h**	**pYV^+ vs uninfected 72h**	**GO Biological Process**
99416_at	AU042276	---	2,5	1,51	---
161299_r_at	AV049751	---	2,87	2,08	---
100584_at	U72941	---	1,96	0,69	---
100880_at	AA816121	---	3,18	1,93	---
100944_at	AA958903	---	1,67	1,36	---
161511_f_at	AV152244	---	4,34	1,64	---
101820_at	X70920	---	2,79	2,65	---
160925_at	X13664	---	3,02	3,08	---
93779_at	AA261092	---	1,75	1,22	---
160799_at	AW060549	---	3,45	1,39	---
94355_at	AW048394	---	3,43	3,22	---
103508_at	AA919750	0610009F02Rik	3,27	2,04	---
160228_at	AI838249	1110019C08Rik	1,61	1,48	---
95078_at	AI841400	1200015F23Rik	2,46	1,44	---
103562_f_at	M26005	1300007C21Rik	3,21	2,32	---
93462_at	AA168418	1810054D07Rik	2,52	1,07	---
102030_at	AF026032	4833408C14Rik	2,92	2,42	---
103748_at	AW125627	4933407C03Rik	2,03	1,9	---
98495_at	AI846906	5033414D02Rik	2,03	1,28	---

92993_r_at	AI324972	5730497N03Rik	3,02	0,91	---
96196_i_at	AI851708	5730589K01Rik	1,94	1,39	regulation of transcription, DNA-dependent
94995_at	AI854331	A030007L17Rik	1,81	0,69	---
92688_at	X57199	Acp2	1,85	1,51	---
104168_at	AA791742	Actr2	2,73	2,05	cell motility
96188_at	AF052506	Adar	3,31	2,16	RNA processing
103615_at	AA727023	AI447904	3,81	2,52	---
102330_at	D86382	Aif1	1,5	0,93	actin filament bundle formation
93464_at	AI561567	Akap9	1,85	1,24	---
93500_at	M63245	Alas1	2	1,76	heme biosynthesis
99838_at	AF018172	Aoah	1,87	1,08	xenobiotic metabolism
92288_at	X54424	Ap1g1	3,89	3,37	transport
103796_at	AF064071	Apaf1	1,52	1,02	apoptosis
98473_at	AF032466	Arg2	1,94	0,76	urea cycle
98924_at	Y08027	Art3	3,76	1,58	protein amino acid ADP-ribosylation
103899_at	AA690863	Atp11a	2,76	2,59	metabolism
161166_i_at	AV222721	B7h3	2,23	1,78	immune response
102913_at	AI324342	Bcl2a1a	3,45	1,13	apoptosis
103789_at	AI854614	Brd4	1,53	1,44	---
103759_at	D31788	Bst1	1,78	1,62	defense response
97693_at	C78513	C78513	3,55	1,86	---
93721_at	L12367	Cap1	1,52	1,06	actin cytoskeleton organization and biogenesis
102064_at	L28095	Casp1	2,11	1,11	apoptosis
102905_at	Y13089	Casp11	2,84	1,79	apoptosis
98498_at	D86353	Casp7	1,78	0,78	apoptosis
98499_s_at	U67321	Casp7	3,83	3,65	apoptosis
102328_at	AJ007749	Casp8	2,24	1,42	apoptosis
95094_g_at	AI035334	Ccar1	1,75	1,52	positive regulation of apoptosis
93717_at	U50712	Ccl12	4,17	1,76	chemotaxis
102736_at	M19681	Ccl2	4,54	2,16	chemotaxis
102424_at	J04491	Ccl3	3,84	3,32	chemotaxis
99413_at	U29678	Ccr1	2,17	1,58	chemotaxis
93617_at	AF030185	Ccrl2	3,29	0,9	G-protein coupled receptor protein signaling pathway
93909_f_at	X04120	Ccrn4l	1,56	0,84	rhythmic process
98446_s_at	U06834	Cct3	1,56	1,31	protein folding
98088_at	X13333	Cd14	2,77	2,47	inflammatory response
100778_at	L11332	Cd38	2,02	1,98	---
99434_at	AF001036	Cd83	4,06	1,82	---
102830_at	L25606	Cd86	1,88	1,1	immune response
102831_s_at	U39456	Cd86	2,49	1,37	immune response
94881_at	AW048937	Cdkn1a	3,34	2,53	regulation of cell cycle
98067_at	U09507	Cdkn1a	3,8	3,13	regulation of cell cycle
100278_at	U09968	Cdkn1b	2,72	2,67	cell cycle arrest
94971_at	AI317217	Cdkn3	3,1	2,88	cell cycle arrest
93994_at	AW212131	Chpt1	2,14	1,11	---
100022_at	D89613	Cish	2,13	1,4	immune response

104392_at	AI122121	Clcn7	1,76	1,17	transport
104391_s_at	AI850563	Clcn7	1,82	1,15	transport
160415_at	AI604314	Cldn1	2,83	0,93	---
96551_at	AB024717	Clec4e	1,63	0,93	immune response
94254_at	AI845237	Clic4	1,97	0,73	transport
94256_at	AI849533	Clic4	2,54	1,1	transport
101937_s_at	AF005423	Clk4	3,39	3,31	protein amino acid phosphorylation
100533_s_at	M60285	Crem	2,43	1,72	transcription
160526_s_at	M60285	Crem	3,46	3,11	transcription
94747_at	M34397	Csf2rb1	2,88	2,94	---
103210_at	M29855	Csf2rb2	2,55	2,6	---
94142_at	M13926	Csf3	3,04	2,48	immune response
101846_r_at	M55219	Csprs	2,36	0,83	---
101436_at	M34815	Cxcl9	3,94	2,83	immune response
100300_at	U43384	Cybb	3,58	2,98	transport
104371_at	AF078752	Dgat1	2,13	1,63	---
97740_at	AI642662	Dusp16	2,15	1,52	inactivation of MAPK
94246_at	J04103	Ets2	2,4	1,15	regulation of cell cycle
102879_s_at	M31314	Fcgr1	2,15	1,39	immune response
101793_at	X70980	Fcgr1	2,85	2,01	immune response
104419_at	AI132380	Fndc3a	1,68	0,81	---
101800_at	AF071180	Fpr-rs2	1,69	1,02	---
97531_at	X95280	G0s2	1,84	1,45	cell cycle
98822_at	X56602	G1p2	3,55	1,91	immune response
101294_g_at	Z84471	G6pd2	2,59	2,43	metabolism
161666_f_at	AV138783	Gadd45b	1,85	0,85	regulation of cell cycle
102779_at	X54149	Gadd45b	2,35	1,13	regulation of cell cycle
104597_at	AJ007970	Gbp2	3,92	3,05	immune response
103202_at	AW047476	Gbp4	3,07	2,26	immune response
102313_at	L09737	Gch1	2,46	1,2	tetrahydrobiopterin biosynthesis
94192_at	Y17860	Gdap10	3	1,22	---
92217_s_at	U05265	Gp49a	1,86	0,9	immune response
162262_f_at	AV357306	Gyg1	1,67	1,42	metabolism
100597_at	AW049730	Gyg1	1,93	1,69	metabolism
97525_at	U48403	Gyk	1,67	0,97	metabolism
101658_f_at	D90146	H2-Q8	2,57	2,06	immune response
93865_s_at	M35244	H2-T10, H2-T17, H2-T22, H2-T9	1,63	0,9	immune response
94746_at	L22338	H2-T24	2,67	1,25	immune response
93328_at	X57437	Hdc	1,88	0,82	---
160101_at	X56824	Hmox1	2,19	1,79	heme oxidation
99815_at	D50096	Hrh2	2,02	1,03	signal transduction
103563_at	AW125713	Ibrdc3	1,63	0,67	---
96752_at	M90551	Icam1	2,17	1,08	immune response
94384_at	X67644	Ier3	3,44	2,13	---
97409_at	U19119	Ifi1	2,9	1,3	immune response
94224_s_at	M74123	Ifi205	1,83	0,97	immune response

98465_f_at	M31419	Ifi204	1,9	0,71	immune response
104750_at	M63630	Ifi47	2,94	1,76	immune response
100981_at	U43084	Ifit1	3,88	1,25	immune response
103639_at	U43085	Ifit2	5	1,93	immune response
101641_at	M86751	Igk-V21	2,08	1,45	---
160933_at	U53219	Igtp	3,13	1,86	---
98410_at	AJ007972	Iigp2	2,09	1,07	---
92301_at	AB016589	Ikbke	2,96	2,39	protein amino acid phosphorylation
100773_at	M86672	Il12a	5,19	2	immune response
98240_at	U23922	Il12rb1	2,6	2	cell surface receptor linked signal transduction
161023_at	U22339	Il15ra	2,88	1,51	cell surface receptor linked signal transduction
92689_at	AB019505	Il18bp	4,01	1,95	---
161689_f_at	AV223216	Il1r2	1,93	1,49	inflammatory response
102658_at	X59769	Il1r2	2,2	2,03	inflammatory response
103769_at	X85999	Il1rap	4,01	3,35	immune response
93871_at	L32838	Il1rn	2,33	1,35	immune response
102218_at	X54542	Il6	4,99	1,58	immune response
100277_at	X69619	Inhba	2,23	1,97	growth
93942_at	U27295	Inpp1	4,22	1,68	---
93850_at	AI642553	Iqgap1	2,53	1,82	small GTPase mediated signal transduction
102401_at	M21065	Irf1	1,51	0,76	immune response
94764_at	M60778	Itgal	1,6	1,27	immune response
100010_at	U36340	Klf3	2,65	2,02	transcription
160618_at	AA760613	Lgals8	3,73	2,28	---
97173_f_at	M27134	LOC436489	2,36	1,91	---
97173_f_at	M27134	LOC436489	2,36	1,91	---
97420_at	AW230891	Lrg1	1,67	1,53	---
93078_at	X04653	Ly6a	2,66	2,44	---
101945_g_at	U89352	Lypla1	3,66	3,59	metabolism
104628_at	X61172	Man2a1	1,79	1,44	metabolism
99960_at	U18310	Map2k4	1,7	1,49	MAPKKK cascade
97106_at	D13759	Map3k8	2,67	1,62	regulation of cell cycle
99604_at	AI848713	March5	1,83	0,65	---
93997_at	AI853475	MGI:1929890	1,95	0,82	---
100484_at	X66473	Mmp13	2,83	1,79	proteolysis and peptidolysis
160118_at	AF022432	Mmp14	3,06	2,37	proteolysis and peptidolysis
94769_at	U96696	Mmp8	2,02	1,51	proteolysis and peptidolysis
97322_at	AI835093	Ms4a6b	1,55	1,22	signal transduction
102360_at	AW214225	Mthfr	2,75	1,08	methionine metabolism
102430_at	X51397	Myd88	1,51	0,89	inflammatory response
97763_at	AB002663	Ncf1	2,19	1,79	transport
101554_at	U57524	Nfkbia	1,71	0,93	regulation of cell proliferation
101727_at	AF030896	Nfkbie	2,22	0,81	regulation of transcription, DNA-dependent
98988_at	AA614971	Nfkbiz	2,6	1,72	inflammatory response
93831_at	AI316087	Nono	2,51	1,77	mRNA processing
104420_at	U43428	Nos2	1,93	1,75	defense response to bacteria
160189_at	AI843747	Nudt4	2,51	1,99	---

160189_at	AI843747	Nudt4	2,51	1,99	---
102717_at	X58077	Oas1g	3,21	1,7	immune response
160668_at	AI838195	Ogfr	1,93	0,7	regulation of cell growth
94461_at	AI852144	Pbef1	2,69	1,37	---
92810_at	AI842259	Pdk3	2,41	1,46	protein amino acid phosphorylation
102845_at	AI836034	Pdlim7	2,27	1,96	---
102845_at	AI836034	Pdlim7	2,27	1,96	---
97833_at	AI853802	Pfkp	2,01	1,52	glycolysis
92312_at	U55772	Pik3c2a	2,19	1,59	intracellular signaling cascade
99384_at	M13945	Pim1	2,83	1,03	protein amino acid phosphorylation
99513_at	M72394	Pla2g4a	1,64	1,18	lipid catabolism
102663_at	X62700	Plaur	1,81	1,28	cell surface receptor linked signal transduction
92310_at	M96163	Plk2	2,17	0,93	cell cycle
102839_at	D78354	Plscr1	2,47	2,17	---
93290_at	U35374	Pnp	2,24	1,51	---
98508_s_at	D84376	Ppap2a	1,53	0,66	signal transduction
93672_at	U09928	Prkr	2,6	1,06	immune response
98018_at	L39017	Procr	3,58	1,71	blood coagulation
94841_at	AW048997	Psma5	1,73	0,91	ubiquitin-dependent protein catabolism
101486_at	Y10875	Psmb10	1,7	0,86	ubiquitin-dependent protein catabolism
99433_at	Y18101	Pstpip2	4,01	3,23	---
94159_at	D50872	Ptafr	1,66	1,17	chemotaxis
94158_f_at	AF004858	Ptafr	3,75	2,37	chemotaxis
104406_at	AI060798	Ptges	1,81	1,54	prostaglandin metabolism
104647_at	M88242	Ptgs2	2,95	2,57	prostaglandin biosynthesis
101298_g_at	M23158	Ptprc	2,76	2,02	thymocyte differentiation
94643_at	U35836	Pvr	2,56	2,2	---
160314_at	AI839803	Pyp	2,75	1,35	metabolism
101933_at	AF035646	Rab10	1,95	1,68	small GTPase mediated signal transduction
95785_s_at	Y13361	Rab7	3,92	3,02	small GTPase mediated signal transduction
100530_at	L07924	Ralgds	2,43	1,4	small GTPase mediated signal transduction
92368_at	AJ250491	Ramp3	3,42	2,36	regulation of G-protein coupled receptor protein signaling pathway
94972_at	AB026569	Rbms1	1,59	0,73	regulation of translation
103231_at	AA739233	Rhoh	2,57	0,67	small GTPase mediated signal transduction
96747_at	AW121294	Rhou	1,68	1,27	small GTPase mediated signal transduction
97091_at	U25995	Ripk1	2,5	1,41	apoptosis
99127_at	X61506	Sca10	1,8	1,43	---
160708_at	AI840446	Schip1	4,06	1,98	---
102860_at	M64085	Serpina3g	2,42	1,27	---
92978_s_at	X16490	Serpinb2	1,93	1,88	---
94752_s_at	U10531	Skil	3,55	1,86	cell differentiation
93738_at	M22998	Slc2a1	1,92	1,66	transport
101877_at	AI854432	Slc31a1	2,18	1,88	transport
101713_at	AB022345	Slc7a11	1,71	1,63	transport
92736_at	L03290	Slc7a2	2,33	1,85	transport
94556_at	AI746846	Snx10	1,74	1,04	transport

96333_g_at	AW259199	Snx2	3,37	2,94	transport
92832_at	U88325	Socs1	4,38	2,39	immune response
162206_f_at	AV374868	Socs3	1,73	1,31	immune response
92232_at	U88328	Socs3	2,12	1,48	immune response
96042_at	L35528	Sod2	2,59	1,18	superoxide metabolism
97310_at	AW124318	St13	3,36	2,55	protein folding
99847_at	X73523	St3gal1	1,69	1,12	protein amino acid glycosylation
101465_at	U06924	Stat1	2,29	1,36	signal transduction
98775_at	U28726	Stk3	2,91	2,51	apoptosis
92648_at	U19521	Stxbp3	2,1	1,04	transport
103648_at	Y08830	Tacstd2	1,54	1,21	defense response
103328_at	U59864	Tank	1,68	0,66	I-kappaB kinase/NF-kappaB cascade
103035_at	U60020	Tap1	1,54	0,9	immune response
102689_at	AF110520	Tapbp	2,27	1,41	immune response
101551_s_at	X78989	Tes	2,36	1,67	---
101502_at	X89749	Tgif	1,66	1,23	transcription
102906_at	L38444	Tgtp	3,51	2,36	---
102629_at	D84196	Tnf	3,39	1,68	inflammatory response
160489_at	L24118	Tnfaip2	2,27	1,15	angiogenesis
98474_r_at	U83903	Tnfaip6	1,72	0,87	cell adhesion
95543_at	AI843046	Tpm4	2,23	1,55	muscle development
103032_at	AF038008	Tpst1	2,19	0,83	---
92942_at	AA138192	Trim21	2,25	0,85	protein ubiquitination
102678_at	L27990	Trim21	2,27	1,11	protein ubiquitination
99985_at	AB027565	Txnrd1	1,79	1,25	transport
102279_at	AW046479	Ube1l	2,48	0,76	---
98597_at	AW048912	Ube2l6	3,43	1,51	protein modification
94197_at	D89866	Ugcg	1,82	1,69	glucosylceramide biosynthesis
95024_at	AW047653	Usp18	3,6	0,98	ubiquitin-dependent protein catabolism
98605_at	AI851163	Wars	1,94	1,04	protein biosynthesis
98606_s_at	X69656	Wars	2,66	1,44	protein biosynthesis
97950_at	X75129	Xdh	1,78	1,06	transport
102259_at	AF058799	Ywhag	3,08	3,15	signal transduction
94109_at	AI850113	Zfp281	2,35	1,21	---
102293_at	L03547	Zfpn1a1	1,68	1,54	transcription

Cluster C1					
Probe set ID	**Public ID**	**Gene Symbol**	**pYV$^+$ vs uninfected 24h**	**pYV$^+$ vs uninfected 72h**	**GO Biological Process**
92763_at	U43892	Abcb7	0,28	1,58	transport
93097_at	U51805	Arg1	-0,42	2,5	urea cycle
103697_at	AW061234	AW061234	-0,92	1,61	---
104097_at	AF002823	Bub1	-1,44	1,56	cytokinesis
93454_at	AF081789	C1qr1	-0,12	2,1	defense response

99535_at	AW047630	Ccrn4l	0,85	2,25	rhythmic process
101963_at	X06086	Ctsl	0,12	2,57	proteolysis and peptidolysis
98045_s_at	U18869	Dab2	-0,24	1,69	cellular morphogenesis during differentiation
102337_s_at	M31312	Fcgr2b	0,64	1,51	immune response
160873_at	AV206059	Ghrl	0,06	1,67	regulation of physiological process
100911_at	AB002136	Gpaa1	0,87	1,51	GPI anchor biosynthesis
97444_at	AI844520	Ifi30	0,74	1,51	antigen processing, exogenous antigen via MHC class II
104659_g_at	D17444	Lifr	-0,28	1,83	---
104658_at	D17444	Lifr	-0,24	1,58	---
97871_at	AW120614	LOC434220	0,82	1,83	---
98440_at	AA596710	Ltb4dh	0,93	2,56	---
103022_at	U23470	Map3k1	-0,91	1,9	regulation of cell migration
93573_at	V00835	Mt1	-0,4	1,55	signal transduction
95506_at	U96723	Myo1c	0,84	1,94	transport
160091_at	AW125401	Pgam1	0,74	1,56	metabolism
92474_at	AF083497	Pld1	0,73	1,55	metabolism
104541_at	U43525	Prtn3	0,27	1,8	proteolysis and peptidolysis
96038_at	AI840339	Rnase4	-1,63	1,39	---
160795_at	AW123662	Scamp1	0,54	2,38	transport
100095_at	U37799	Scarb1	-0,13	2,02	cell adhesion
93918_at	AA673500	Taf9	0,51	1,77	transcription

Cluster C2					
Probe set ID	**Public ID**	**Gene Symbol**	**pYV$^+$ vs uninfected 24h**	**pYV$^+$ vs uninfected 72h**	**GO Biological Process**
161317_r_at	AV088715	---	2,56	2,68	---
100368_at	AB019601	---	2,13	2,6	---
102805_at	M77196	---	1,12	2,07	---
104400_at	AF076956	0610042I15Rik	1,75	1,84	---
96606_at	AB025217	1500003O03Rik	3,08	3,49	---
96124_at	AI835632	2310001H13Rik	1,44	2,08	---
98894_at	AA867655	2610016F04Rik	1,45	1,7	regulation of transcription, DNA-dependent
100464_at	AI840585	3110043O21Rik	1,07	1,59	---
99343_at	AA796133	4932441K18	2,24	2,5	---
94955_at	AW125433	5530600A18Rik	2,02	2,83	---
99329_at	AF022908	Abcc1	2,08	2,15	transport
96054_f_at	Y17345	Acp1	1,51	1,59	protein amino acid dephosphorylation
96738_at	U41765	Adam9	1,63	1,93	proteolysis and peptidolysis
98589_at	M93275	Adfp	1,28	1,62	long-chain fatty acid transport
97733_at	U05673	Adora2b	2,38	2,46	signal transduction
96501_at	AI506285	AI194738	1,39	1,72	---
98490_at	AA822412	Arl10c	1,44	1,83	transport
100315_at	U75321	Atp8a1	1,72	1,79	metabolism

94423_at	AW049551	BC004728	1,63	1,44	---
100405_at	X56683	Cbx3	1,48	2,11	transcription
161968_f_at	AV370035	Ccr5	2,46	3,26	chemotaxis
102718_at	AF022990	Ccr5	2,6	3,09	chemotaxis
97832_at	AA754887	Cd97	1,9	2,07	cell adhesion
94748_g_at	M34397	Csf2rb1, Csf2rb2	2,12	1,94	---
100019_at	D45889	Cspg2	2,21	2,97	cell adhesion
101020_at	AI842667	Ctsc	1,55	1,51	proteolysis and peptidolysis
93860_i_at	M17327	Ctse	1,5	1,43	proteolysis and peptidolysis
93861_f_at	M17327	Ctse	1,85	2,04	proteolysis and peptidolysis
103768_at	AW209561	D19Ertd678e	1,99	2,72	---
100037_at	AW213225	Ddx18	2,81	3,2	---
93722_at	AJ005985	Ensa	1,81	2,04	regulation of insulin secretion
103977_at	AF087644	F10	2,61	3,5	blood coagulation
103816_at	U89915	F11r	1,27	2,87	cell adhesion
93634_at	AW125157	Fbxw11	1,88	1,85	ubiquitin cycle
160714_at	AI046826	Gab1	1,62	4,46	response to oxidative stress
96336_at	AI844626	Gatm	1,24	2,03	transport
95392_at	U68182	Gcnt2	2,38	2,83	---
104222_f_at	C79210	Ggps1	1,57	2,2	isoprenoid biosynthesis
93231_at	AJ007511	Hic1	2,67	3,02	transcription
96696_at	AI837110	Hrmt1l2	2,17	2,51	protein amino acid methylation
103904_at	X81584	Igfbp6	2	3,98	regulation of cell growth
98828_at	X07640	Itgam	1,79	2,1	cell adhesion
99509_s_at	L40172	Jak3	1,73	1,46	protein amino acid phosphorylation
160617_at	AW125783	Klf13	1,1	1,59	transcription
93930_at	U58882	Lasp1	1,89	2,25	transport
97870_s_at	AA798624	LOC434220	1,1	1,87	---
101944_at	U89352	Lypla1	1,54	1,59	lipid metabolism
101946_at	AA840463	Lypla1	1,84	2,19	lipid metabolism
94549_at	AI315650	Mfsd1	1,19	1,5	transport
92703_at	AI325791	MGI:1923998	2,07	2,37	cell cycle
96249_at	AW122105	MGI:1927947	1,02	1,67	---
92464_at	Y11091	Mknk1	2,79	3,02	regulation of protein biosynthesis
102955_at	U83148	Nfil3	1,84	2,02	regulation of transcription, DNA-dependent
102780_at	Z31362	Npn3	2,27	3	---
94351_r_at	U12961	Nqo1	1,1	1,74	electron transport
103288_at	AF053062	Nrip1	2,2	2,29	negative regulation of transcription from RNA polymerase II promoter
102342_at	U10120	Nsf	1,22	1,67	transport
93167_f_at	AA104818	Olr1	1,74	2,09	---
102063_at	AF079535	Pdpk1	1,46	1,79	signal transduction
93619_at	AF022992	Per1	1,06	1,56	transcription
92390_at	U86587	Pik3cd	2,6	2,75	B-cell homeostasis
100951_at	AF014010	Pkd2	1,54	2,05	JAK-STAT cascade
160589_at	AI854234	Ppig	1,62	1,56	protein folding
100332_s_at	AF093853	Prdx6, Prdx6-rs1	1,54	1,72	response to reactive oxygen species

103885_at	AW049156	Prpf31	1,05	1,52	nuclear mRNA splicing, via spliceosome
101966_s_at	AF037206	Rnf13	1,55	1,79	proteolysis and peptidolysis
93164_at	Y12783	Rnf2	2,68	3,28	mitotic cell cycle
99350_at	C76102	Sec63	1,37	3,79	protein folding
160539_at	X66091	Sfrs1	2,1	1,97	nuclear mRNA splicing, via spliceosome
98766_at	AB016835	Sh3bp5	1,08	1,66	intracellular signaling cascade
100618_f_at	AA062013	Slc25a5	1,18	1,57	transport
92343_at	AF010138	Smarca3	1,52	1,51	transcription
97206_at	AW230369	Spint1	2,05	3,69	---
97519_at	X13986	Spp1	1,44	4,05	cell adhesion
104249_g_at	AW227650	Ssr3	2,71	3,98	---
100426_s_at	U36776	Syk	3,4	4	activation of MAPK
92427_at	D25540	Tgfbr1	3,27	3,47	protein amino acid phosphorylation
160469_at	M62470	Thbs1	1,21	1,64	cell adhesion
93985_at	AW120868	Tiparp	1,93	2,15	protein amino acid ADP-ribosylation
99501_at	AA882416	Tloc1	2,62	3,36	protein transport
101514_at	AF041433	Trappc3	1,74	2,01	transport
94209_g_at	AW045202	Txndc7	1,6	1,97	electron transport
94208_at	AW045202	Txndc7	1,89	2,08	electron transport
99799_at	X64361	Vav1	1,35	1,56	immune response
103520_at	M95200	Vegfa	2,71	3,87	angiogenesis
95800_s_at	X53250	Zfa, Zfx	2,15	2,38	transcription
95801_s_at	L36316	Zfp260	1,4	2,17	---

Cluster D					
Probe set ID	**Public ID**	**Gene Symbol**	**pYV$^+$ vs uninfected 24h**	**pYV$^+$ vs uninfected 72h**	**GO Biological Process**
98524_f_at	AI848479	---	-1,86	-1,36	---
161268_f_at	AV318100	---	-1,7	-1,46	---
101863_at	C78246	---	-1,82	-1,75	---
160272_at	AI849356	---	-1,8	-0,74	---
94916_at	AW122260	---	-1,96	-1,73	---
161132_at	AA727482	---	-1,92	-0,01	---
97102_at	AA276948	---	-2,32	-1,47	---
160642_at	AI853079	---	-2,15	-0,9	---
98767_at	AI842603	---	-1,6	-0,6	---
92202_g_at	AI553024	Zbtb16	-2,49	-2,18	apoptosis
95285_at	AI153315	---	-1,56	-1,37	---
95636_at	AW123628	0610010K14Rik	-1,72	-0,28	transcription
102969_at	AI847369	0610025P10Rik	-1,55	-0,71	---
94907_f_at	AW045632	1110001J03Rik	-1,66	-1,33	---
96862_at	AI848584	1110002B05Rik	-1,87	-0,85	---
160240_at	AI852051	1110003E01Rik	-1,55	-1,03	---
160378_at	AI853127	1110006I15Rik	-1,61	-0,37	---

103881_at	AA691185	1110013G13Rik	-1,59	-0,56	metabolism
104573_at	AA921069	1110025L05Rik	-1,61	-0,36	---
160245_at	AW045564	1110034O07Rik	-1,94	-1,36	---
95596_at	AW122957	1110054H05Rik	-1,67	-0,57	---
160787_at	AW124900	1500010J02Rik	-2,79	-0,5	---
97885_at	AB031386	1810009M01Rik	-1,57	-1,35	---
160955_at	AW124904	2010309E21Rik	-4,55	-1,23	---
99187_f_at	AI835662	2010315L10Rik	-1,62	-1,03	transport
92338_f_at	AI957030	2310001H12Rik	-1,6	-0,5	---
96122_at	AW049373	2310016A09Rik	-3,57	-0,87	---
101404_at	AI853654	2310061I09Rik	-1,62	-0,43	---
104513_at	AA688938	2410004N09Rik	-3,21	-1,25	---
96885_at	AW122271	2510015F01Rik	-3,9	0,76	---
103545_at	AA240695	2610019E17Rik	-1,55	-0,82	---
95514_at	AI846302	2610510H01Rik	-1,77	-0,25	---
100955_at	AA989957	2700084L22Rik	-2,39	-0,88	ubiquitin cycle
95150_at	AI852196	2810052M02Rik	-1,53	-0,83	---
160166_r_at	AI843495	2810409H07Rik	-2,02	-0,12	---
160235_at	AI843521	5033425B17Rik	-1,56	-0,24	---
161005_at	AI835776	5730420B22Rik	-1,92	-1,27	electron transport
95890_r_at	AA185884	5730488B01Rik	-1,65	-1,16	---
95021_at	AW124028	9430010O03Rik	-1,5	-1,02	---
103667_at	AA866655	A130034M23Rik	-2,08	-0,69	---
103689_at	AA833514	Abcc3	-2,02	-0,73	transport
92913_at	Z48670	Abcd2	-1,73	-0,31	fatty acid metabolism
103401_at	L11163	Acads	-1,83	-0,36	lipid metabolism
160921_at	AW125884	Acas2l	-3	-1,96	metabolism
161224_f_at	AV258262	Ace	-1,89	-1,37	proteolysis and peptidolysis
98976_at	AJ242912	Adamdec1	-1,73	-1,08	proteolysis and peptidolysis
160255_at	AA657044	Ahnak	-2,28	-1,29	---
160495_at	M94623	Ahr	-1,5	0,05	transcription
94459_at	AA681764	AI462493	-1,66	-0,67	---
95902_at	AW229127	AI465270	-1,56	-0,77	---
100970_at	X65687	Akt1	-1,81	-1,34	apoptosis
94290_at	AW124346	Akt1s1	-2,36	-0,71	Notch signaling pathway
104407_at	L25274	Alcam	-1,75	-1,29	cell adhesion
100948_at	AW049351	Ank	-1,72	-1,23	transport
93354_at	Z22661	Apoc1	-1,74	-1,09	transport
97887_at	Z22216	Apoc2	-2,31	0,18	lipid metabolism
95356_at	D00466	Apoe	-1,99	-1,17	transport
102704_at	U88623	Aqp4	-3,65	-0,7	transport
100575_at	AI841645	Ard1	-1,64	0,34	DNA packaging
98001_at	U58203	Arhgef1	-1,5	-0,94	intracellular signaling cascade
100473_at	AI851750	Arrb1	-2	-0,65	signal transduction
92375_at	AW211207	Ascc1	-1,59	-0,78	transcription
93798_at	AI839988	Atp1a1	-2,11	-1,46	transport
93797_g_at	AW123952	Atp1a1	-1,82	-1,19	transport

103935_at	AI504474	Atp2a3	-1,58	-1,02	transport
161331_r_at	AV114328	Atp5d	-2,67	-1,75	ATP biosynthesis
103497_at	AA592351	BC025546	-1,51	-1,13	---
103449_at	AA795923	BC040823	-2,37	-1,23	---
96035_at	L47335	Bckdha	-1,64	0,16	metabolism
99514_at	AI835443	Bmyc	-1,99	-1,42	regulation of cell cycle
96255_at	AF067395	Bnip3l	-1,51	-0,04	apoptosis
94815_at	X13586	Bpgm	-3,69	-1,14	metabolism
101078_at	Y16258	Bsg	-1,61	-0,34	---
95984_at	AI586160	C79468	-4,68	-0,78	---
104589_at	AF091096	C80913	-2,08	-1,49	protein folding
160479_at	M29394	Cat	-1,76	-0,64	response to oxidative stress
102397_at	AF038029	Cbfa2t3h	-1,9	-1,12	granulocyte differentiation
92849_at	M58004	Ccl6	-1,59	-1,45	chemotaxis
104388_at	U49513	Ccl9	-2,4	-0,25	chemotaxis
162384_f_at	AV252118	Ccrn4l	-1,61	0,12	rhythmic process
97828_at	AF033115	Cd27b	-1,53	-0,37	apoptosis
104023_at	AW060457	Cd300c, Cd300a	-1,75	-0,58	---
161012_at	J03857	Cd79b	-2,46	-2,25	cell surface receptor linked signal transduction
95063_at	AI606257	Cdca7	-1,95	-1,02	cytokinesis
98447_at	M62362	Cebpa	-1,68	-0,6	transcription
103900_at	AW124150	Centg3	-1,54	-0,72	transcription
101426_at	AW125333	Cerk	-2,79	-0,69	ceramide metabolism
102622_r_at	AJ011106	Clcn1	-3,61	-1,77	transport
97928_at	AW045278	Cln6	-1,59	-0,04	lysosome organization and biogenesis
93048_at	AJ005253	Clpp	-1,73	-0,67	proteolysis and peptidolysis
102966_at	AA934166	Cnot6l	-2,01	-1,37	---
98535_at	AF076156	Comt	-2,19	-0,52	catecholamine metabolism
160590_r_at	AI853323	Comtd1	-2,46	-1,45	catecholamine metabolism
160813_r_at	AI893329	Cox6b2	-2,29	-1,8	---
160383_at	X80899	Cox7a2l	-1,62	-0,17	electron transport
93550_at	D88792	Csrp2	-3,87	-0,87	development
161522_i_at	AV218205	Cst3	-1,63	-1,43	---
104045_at	AW122372	D10Bwg0791e	-3,48	-0,99	nucleosome assembly
95657_f_at	AW125164	D13Wsu177e	-1,68	-0,58	---
99828_at	AA673252	D3Ertd789e	-2,69	-1,05	---
97770_s_at	AA733372	D6Wsu176e	-1,71	-1,33	---
93821_at	AW046101	D8Ertd594e	-2,33	-1,14	---
161060_i_at	AV338120	Ddx51	-4,24	-1,16	---
98989_at	AF057368	Dhcr7	-4,47	-1,77	steroid biosynthesis
102797_at	X95281	Dhrs3	-1,82	0,05	metabolism
95620_at	AW120882	Dhrs7	-1,52	-1,08	metabolism
103225_at	AW018420	Dnase1l1	-1,83	0,17	DNA catabolism
97220_at	AW122732	Dscr2	-1,56	-0,49	---
93285_at	AI845584	Dusp6	-1,56	-1,08	protein amino acid dephosphorylation
100311_f_at	U72032	Ear1	-1,93	-1,25	---
95426_at	AW048512	Echs1	-2,03	0,25	fatty acid metabolism

103537_at	AF076681	Eif2ak3	-2,18	-1,07	electron transport
160554_at	AI839363	Eif3s6	-1,54	-0,51	protein biosynthesis
96344_at	X61600	Eno3	-1,62	-0,91	glycolysis
94332_at	AI882555	Ets1	-3,48	-1,21	---
100567_at	M20497	Fabp4	-2,53	-1,28	transport
94917_at	AI844932	Fbxo8	-1,86	-0,64	ubiquitin-dependent protein catabolism
97518_at	D29016	Fdft1	-1,54	-0,87	lipid biosynthesis
103699_i_at	AI646638	Frat2	-2,92	-1,93	Wnt receptor signaling pathway
102260_at	AF017275	Gfi1b	-1,52	-0,9	---
93268_at	AI852001	Glo1	-1,61	-0,49	carbohydrate metabolism
94897_at	D87896	Gpx4	-2,08	-1,1	response to oxidative stress
93750_at	J04953	Gsn	-1,92	-0,71	vesicle-mediated transport
97819_at	AI843119	Gsto1	-1,54	0,13	metabolism
96710_at	AI854262	H2afv	-2,09	-0,87	nucleosome assembly
95485_at	D29639	Hadhsc	-1,57	-0,36	lipid metabolism
92580_at	U39473	Hars	-1,95	-0,62	protein biosynthesis
104376_at	AF006602	Hdac5	-1,56	-0,29	transcription
104014_at	Y12650	Hfe	-1,83	-0,34	antigen presentation
94288_at	J03482	Hist1h1c	-2,05	-1,85	nucleosome assembly
94325_at	AW124932	Hmgcs1	-1,67	-1,38	metabolism
96048_at	U50631	Hrsp12	-3,31	0,23	---
100451_at	AF059275	Hsf1	-1,55	-0,06	transcription
99053_at	X65493	Icam2	-1,57	-0,56	cell adhesion
160571_at	AF020039	Idh1	-1,51	0,05	metabolism
100552_at	M28233	Ifngr1	-1,99	-0,48	intracellular signaling cascade
95546_g_at	X04480	Igf1	-1,84	-0,88	apoptosis
102824_g_at	X67210	Ighg	-1,56	-1,16	---
102823_at	X67210	Ighg	-2,19	-1,64	---
98500_at	D13695	Il1rl1	-1,61	-1,29	defense response
100601_at	AF022110	Itgb5	-3,69	0,45	cell adhesion
97302_at	AI854285	Ivns1abp	-1,89	-1,27	---
103310_at	AA220427	Jarid1b	-3,2	-0,87	transcription
102892_at	U65592	Kcnab2	-1,51	0,03	transport
95490_at	AW120891	Kdelr1	-1,51	-0,63	transport
96168_at	AI591702	Kif23	-2	-1,63	---
99622_at	U20344	Klf4	-1,95	-1,08	transcription
94477_at	AW123796	LOC434498	-2,39	-1,46	---
101083_s_at	AF109905	Lsm2	-2,6	-0,05	---
160553_at	X63782	Ly6d	-5,02	-4,24	defense response
100468_g_at	X57687	Lyl1	-2,15	-1,55	transcription
100467_at	X57687	Lyl1	-1,92	-0,91	transcription
104677_at	AI852008	Man1b1	-1,79	-0,86	ER-associated protein catabolism
103020_s_at	AI317205	Map3k1	-1,83	-1,16	protein amino acid phosphorylation
98036_at	AA870525	Marveld1	-2,19	-1,82	---
96012_f_at	AI835367	Matr3	-2,02	-1,34	---
96013_r_at	AI835367	Matr3	-2,01	-1,07	---
97451_at	AI837599	Mcfd2	-1,64	-0,42	transport

103599_at	M20824	Mdm1	-2,21	-1,31	---
97357_at	AI426400	Mef2c	-2,88	-2,05	regulation of transcription, DNA-dependent
93039_at	AF009513	MGI:1889205	-3,62	-1,71	---
102340_at	AA833077	Mina	-1,64	-0,77	regulation of cell proliferation
101007_at	AI845732	Mknk2	-1,71	-0,15	regulation of protein biosynthesis
95338_s_at	M82831	Mmp12	-2,17	-1,19	proteolysis and peptidolysis
95339_r_at	M82831	Mmp12	-2,26	-1,68	proteolysis and peptidolysis
103226_at	Z11974	Mrc1	-3,54	-1,7	endocytosis
160431_at	AW124432	Mrpl12	-1,91	-0,7	protein biosynthesis
96864_at	AI848770	Mrps26	-1,65	-0,86	ribosome biogenesis
162009_f_at	AV246753	Msh2	-2,52	-1,1	DNA metabolism
99024_at	U32395	Mxd4	-1,81	-0,41	transcription
98586_at	AW107230	Nap1l1	-2,01	-1,46	nucleosome assembly
95961_at	AW122131	Nbeal2	-1,74	-1,39	---
95129_at	AW121057	Ncor2	-1,53	-0,65	transcription
94982_f_at	AI852470	Nme3	-2,44	-1,12	nucleotide metabolism
94981_i_at	AI852470	Nme3	-2,39	-1,02	nucleotide metabolism
98604_at	U79774	Nnp1	-1,6	-0,98	rRNA processing
160732_at	AA726383	Npepl1	-3,94	-1,8	---
103922_f_at	AI839690	Nqo3a2	-1,54	-0,86	lipid biosynthesis
100125_at	U43918	Pa2g4	-1,62	-0,64	transcription
92775_at	AA656757	Pabpc4	-1,55	-1,01	---
95470_at	AI846025	Pak1ip1	-1,58	-1,18	---
101957_f_at	X14206	Parp1	-2,76	-0,98	DNA metabolism
93615_at	AF020200	Pbx3	-1,72	-0,49	transcription
103029_at	D86344	Pdcd4	-2,9	-1,61	---
101042_f_at	U51014	Pep4	-1,61	-0,68	proteolysis and peptidolysis
93421_at	AF033655	Pftk1	-2,29	-0,99	transport
160419_r_at	AA866869	Phgdhl1	-1,52	-1,12	---
160615_at	AI835963	Pias3	-1,77	-1,59	transcription
100607_at	AF026124	Pld3	-1,87	-0,77	metabolism
100927_at	U28960	Pltp	-2,86	-1,12	transport
160439_at	U53584	Polg	-2,38	-0,26	DNA replication
97926_s_at	U10374	Pparg	-2,09	-0,34	transcription
93116_at	J02626	Prkacb	-2,03	-1,29	protein amino acid phosphorylation
160204_at	AI838470	Prr6	-2,54	-1,14	---
160328_at	AI838015	Prss15	-3,77	-1,2	---
104030_at	AI848841	Ptch1	-1,65	-0,78	organogenesis
161694_f_at	AV230409	Ptgs1	-1,87	-0,57	lipid biosynthesis
99600_at	AI838337	Ptov1	-1,84	-0,8	---
92356_at	M90388	Ptpn22	-1,5	-0,47	protein amino acid dephosphorylation
94998_at	AI838452	Rala	-1,68	-0,63	small GTPase mediated signal transduction
104680_at	AJ250489	Ramp1	-2,06	-1,01	transport
161757_f_at	AV298789	Ranbp5	-3,07	-1,35	transport
93070_at	AI847564	Ranbp5	-1,57	-0,42	transport
102419_at	M34476	Rarg	-2,86	-1,14	transcription
93319_at	U20238	Rasa3	-1,77	-0,81	intracellular signaling cascade

103457_at	AF083464	Rev3l	-1,64	-0,93	DNA replication
97844_at	U67187	Rgs2	-1,79	-1,51	cell cycle
98057_at	AW121162	Rnf166	-2	-1,09	---
161327_f_at	AV104703	Rpl10a	-2,29	-1,46	protein biosynthesis
92834_at	X51528	Rpl13a	-1,87	-0,61	protein biosynthesis
92857_at	AI853960	Rpl22	-2,02	-0,36	protein biosynthesis
101680_at	X05021	Rpl27a	-1,83	-0,96	protein biosynthesis
161480_i_at	AV055186	Rplp1	-1,62	-1,03	protein biosynthesis
99093_at	AI852864	Rps10	-1,66	-1,01	transcription
100003_at	D38216	Ryr1	-2,21	-0,75	transport
95453_f_at	AF087687	S100a1	-1,9	-0,08	---
160388_at	AI848668	Sc4mol	-1,83	-1,2	lipid biosynthesis
94057_g_at	M21285	Scd1	-3,6	-1,95	lipid biosynthesis
95758_at	M26270	Scd2	-1,73	-0,55	lipid biosynthesis
96060_at	U25844	Serpinb6a	-2,09	-1,2	---
160869_at	AI849490	Sirt3	-1,66	-0,46	transcription
99500_at	U13174	Slc12a2	-3,38	-2,18	transport
95060_at	AF058054	Slc16a7	-1,57	-1,04	transport
95733_at	AI838274	Slc29a1	-1,58	-0,43	transport
104380_at	Z71268	Slc35a1	-1,58	-0,49	transport
103877_at	AW060485	Slc35c2	-1,94	-0,8	transport
103527_at	AW124360	Slc35e4	-1,96	-1,09	---
102384_at	AI842968	Smarca2	-1,73	-1,09	transcription
104408_s_at	L35032	Sox18	-2,46	-1,65	transcription
96192_at	AF062567	Sp3	-1,76	-1,34	transcription
94432_at	AI117157	St6gal1	-2,25	-1,39	protein amino acid glycosylation
102318_at	X86000	St8sia4	-2,06	-1,61	protein amino acid glycosylation
95513_at	AW124310	Statip1	-1,94	-1,04	ubiquitin cycle
103330_at	AI838709	Strbp	-2,58	-1,95	transcription
160428_at	AF058956	Suclg2	-1,65	-1,09	metabolism
93728_at	X62940	Tgfb1i4	-1,81	-0,66	transcription
104601_at	X14432	Thbd	-2,94	-0,13	blood coagulation
162023_f_at	AV364086	Thbd	-2,23	-1,02	blood coagulation
93780_at	AW060827	Them2	-1,86	-0,57	---
99603_g_at	AF064088	Tieg1	-1,66	-0,73	transcription
96708_at	AW120643	Tmed3	-1,68	-0,6	intracellular protein transport
99462_at	D38046	Top2b	-1,85	-1,05	DNA metabolism
94554_at	AW120965	Trappc5	-2,22	-1,56	---
103092_at	AW124316	Trim37	-4,14	-0,53	---
95939_i_at	AW047237	Trio	-1,73	-0,76	---
95940_f_at	AW047237	Trio	-1,63	-0,61	---
97473_at	AW124470	Tspan4	-2,61	-0,96	---
102423_at	AI649125	Uxs1	-2,19	-1,13	carbohydrate metabolism
92558_at	M84487	Vcam1	-1,97	-1,69	cell adhesion
95709_at	AW012491	Vkorc1	-1,56	-0,29	vitamin K biosynthesis
100523_r_at	U92454	Wbp5	-1,51	-0,92	---
96836_r_at	AI447619	Zfp161	-1,59	-0,98	transcription

104604_at	U62908	Zfp96	-2,21	-0,56	transcription

Cluster E1					
Probe set ID	**Public ID**	**Gene Symbol**	**pYV+ vs uninfected 24h**	**pYV+ vs uninfected 72h**	**GO Biological Process**
162412_r_at	AV317927	---	-2,08	-2,09	---
162198_f_at	AV373027	---	-1,78	-1,7	---
101179_at	D50494	---	-1,64	-1,99	---
95184_f_at	AA419684	---	-1,39	-1,79	---
101363_at	AI644801	---	-0,95	-1,89	---
161356_at	AV207158	---	-1,46	-1,74	---
104429_at	AF027865	---	-0,68	-1,54	---
96791_at	AW047875	1500005K14Rik	-1,09	-1,93	---
92316_f_at	J00592	2010309G21Rik	-2,33	-2,65	---
97425_at	AI840191	2210409B22Rik	-1,43	-1,56	---
161018_at	AI661590	2310010J17Rik	-1,28	-2,05	---
93568_i_at	AI853444	2610042L04Rik	-0,67	-1,53	---
160934_s_at	X05546	3110007P09Rik	-1,47	-2,01	---
161735_r_at	AV281129	5730469M10Rik	-1,6	-1,85	---
93465_at	AA711915	9130211I03Rik	-1,13	-1,56	transcription
98346_at	AI593759	9530051K01Rik	-1,64	-1,81	---
160236_at	AI835624	9630044O09Rik	-0,56	-3,88	---
93193_at	X15643	Adrb2	-1,49	-1,69	signal transduction
98758_at	L34570	Alox15	-1,18	-1,77	metabolism
97524_f_at	X02578	Amy2	-1,36	-1,92	metabolism
161467_f_at	AV348528	Atp1b1	-0,96	-1,75	transport
95284_at	AI662509	BB219290	-1,3	-1,99	---
95893_at	AA204265	Blk	-1,68	-1,74	intracellular signaling cascade
100772_g_at	AF068182	Blnk	-1,49	-1,67	intracellular signaling cascade
94689_at	C79248	C79248	-1,44	-1,97	---
92322_at	X94353	Camp	-2,17	-2,62	defense response
99856_r_at	AI852919	Catnd2	-1,88	-1,87	cell adhesion
94232_at	AI849928	Ccnd1	-0,94	-1,97	regulation of cell cycle
99945_at	M28240	Cd19	-1,14	-1,6	---
92683_at	X02339	Cd3d	-1,57	-2,99	cell surface receptor linked signal transduction
102778_at	X13450	Cd79a	-1,59	-2,5	cell surface receptor linked signal transduction
103040_at	AI837100	Cd83	-0,33	-2,29	---
99820_f_at	AA204255	Cecr5	-1,61	-1,55	metabolism
93284_at	D78135	Cirbp	-1,11	-1,52	---
102794_at	Z80112	Cxcr4	-1,36	-1,83	chemotaxis
95701_at	AW124069	Cxxc5	-0,06	-3,04	---
98072_r_at	X77731	Dck	-0,32	-1,52	nucleobase, nucleoside, nucleotide and nucleic acid metabolism
100155_at	L57509	Ddr1	-1,82	-2,3	cell adhesion

161788_f_at	AV347228	Edg1	-1,44	-3,46	signal transduction
161802_i_at	AV369921	Egr1	-0,41	-3,06	transcription
98575_at	X13135	Fasn	-2,02	-2,37	lipid biosynthesis
94141_at	X64224	Fcer2a	-0,87	-3,13	defense response
102065_at	AB007813	Fcna	-1,83	-1,57	transport
95295_s_at	X59398	Flt3	-1,98	-2,6	protein amino acid phosphorylation
96172_at	AA795946	Gimap4	-0,45	-1,54	---
102995_s_at	M13226	Gzma	0,22	-2,25	apoptosis
102274_at	M95514	H2-Oa	-1,57	-2,41	antigen processing
92833_at	L07645	Hal	-1,08	-2,5	metabolism
97318_at	AI846197	Hars2	-0,74	-2,06	D-amino acid catabolism
162457_f_at	AV003378	Hba-a1	-1,15	-1,6	transport
101869_s_at	J00413	Hbb, Hbb-b1, Hbb-b2	-1,5	-2,37	transport
103534_at	V00722	Hbb-b2	-1,95	-2,89	transport
93067_f_at	U62674	Hist2h2aa1, Hist2h2aa2	-1,17	-1,93	---
96269_at	AA716963	Idi1	-1,84	-2,4	lipid biosynthesis
98974_at	AI183084	Igh-5	-1,39	-1,9	humoral defense mechanism
93584_at	V00821	Igh-6	-1,99	-2,41	humoral immune response
99420_at	X94418	Igh-V7183	-1,76	-2,33	---
102372_at	M90766	Igj	-1,43	-2,18	humoral immune response
102156_f_at	M80423	Igk-C	-1,75	-2,6	---
93086_at	M18237	Igk-C	-1,2	-1,93	---
101656_f_at	U60442	IgM	-0,63	-1,55	---
93605_r_at	AF061260	Igsf4a	-1,06	-1,83	cell adhesion
92286_g_at	AA967539	Il4	-1,81	-3,27	immune response
95511_at	X69902	Itga6	-1,47	-1,63	cell adhesion
93894_f_at	U49866	Klra3	-1,06	-2,93	defense response
93893_f_at	U56404	Klra3	-0,74	-1,59	defense response
101331_f_at	U55641	LOC243467, LOC384419, LOC434044	-1,86	-2,42	---
98776_at	AF035203	LOC380800	-0,91	-1,91	---
100299_f_at	U55576	LOC381783	-0,8	-2,41	---
160083_at	M63335	Lpl	-1,15	-2,67	lipid metabolism
95611_at	AA726364	Lpl	-0,62	-1,59	lipid metabolism
102940_at	U16985	Ltb	-0,93	-2,46	immune response
99855_at	AB006787	Map3k5	-1,14	-1,51	apoptosis
104591_g_at	L13171	Mef2c	-1,08	-2,92	transcription
93195_at	AI957146	Mfhas1	-1,45	-2,19	---
94259_at	AB024935	MGI:1929282	-1,63	-1,83	---
161107_r_at	AA529901	Mogat2	-0,26	-1,57	lipid metabolism
104173_at	AA797989	Ms4a1	-1,76	-2,17	defense response
99446_at	M62541	Ms4a1	-1,13	-1,71	defense response
103491_at	AA968123	Nav1	-1,99	-1,99	microtubule bundle formation
98118_at	Y07708	Ndufa1	-1,95	-3,06	---

162172_f_at	AV365271	Nedd4	-1,58	-3	protein modification
93101_s_at	U96635	Nedd4	-1,41	-2,03	protein modification
92271_at	X63963	Pax6	-0,5	-1,56	transcription
93694_at	AF036893	Per2	-0,69	-3,4	transcription
95073_at	Y09046	Pex19	-0,82	-1,54	peroxisome organization and biogenesis
160105_r_at	AI847033	Pigk	-0,91	-1,62	proteolysis and peptidolysis
162252_f_at	AV335799	Plekha1	-0,91	-1,59	---
161590_r_at	AV290437	Plf, Mrpplf4	-1,08	-3,89	---
93915_at	Z54283	Pou2af1	-1,22	-1,59	transcription
162129_f_at	AV378129	Ppfibp2	-1,72	-1,81	DNA integration
160862_at	AF035645	Ptp4a3	-1,52	-1,55	protein amino acid dephosphorylation
98511_at	L17076	Raly	-1,67	-1,94	---
94545_at	AW123115	Rtn1	-1,72	-1,8	nucleosome assembly
97126_at	D38218	Ryr3	-0,46	-1,92	transport
99665_at	U05252	Satb1	-1,65	-1,72	transcription
94056_at	M21285	Scd1	-1,32	-1,82	lipid biosynthesis
93557_at	U43285	Sephs2	-1,85	-1,72	---
98550_at	AI854006	Set	-1,65	-1,46	DNA replication
103918_at	AI846682	Slc15a2	-0,8	-1,72	transport
100009_r_at	X94127	Sox2	-0,57	-1,58	transcription
93657_at	U87620	Spib	-0,62	-1,6	transcription
97994_at	AI019193	Tcf7	-0,1	-2,23	transcription
104526_at	U36393	Tcfeb	-1,59	-1,63	transcription
161516_r_at	AV157222	Vapa	-0,68	-1,64	---
97484_at	AI852704	Zmynd11	-1,56	-1,71	transcription

Cluster E2					
Probe set ID	**Public ID**	**Gene Symbol**	**pYV+ vs uninfected 24h**	**pYV+ vs uninfected 72h**	**GO Biological Process**
93372_at	U73478	Anp32a	-2,83	-3,4	---
92406_at	D31956	Cd7	-2,68	-2,78	immune response
160906_i_at	AA184423	E430003D02Rik	-3,58	-3,95	---
160857_at	U30244	Efnb2	-3,04	-3,27	organogenesis
97509_f_at	U22324	Fgfr1	-4,51	-4,96	organogenesis
94781_at	V00714	Hba-a1	-2,46	-3,24	transport
93351_at	U44389	Hpgd	-3,48	-2,77	prostaglandin metabolism
161486_f_at	AV080003	Igh-VJ558	-2,21	-3,25	---
100583_at	J00475	Igh-VJ558	-2,69	-3,71	---
96964_at	L14554	Igk-C , Igk-V28	-1,67	-5,05	---
93638_s_at	J00579	Igl-V1	-4,19	-4,52	humoral immune response
92737_at	U20949	Irf4	-3,67	-4,56	transcription
93677_at	AF030311	Klrd1	-2,71	-2,75	---
102235_at	X13945	Lmyc1	-3,55	-4,33	transcription
93106_i_at	M20878	LOC381765	-3,86	-4,38	---

104592_i_at	AI595996	Mef2c	-4,8	-4,72	transcription
96588_at	D10204	Ptger3	-4,81	-6,46	signal transduction
93855_at	U91601	Rem1	-2,98	-3,06	small GTPase mediated signal transduction
95387_f_at	AA266467	Sema4b	-3,2	-2,6	cell differentiation

Supplementary table 2

Probe sets differentially regulated in splenic CD11b$^+$ cells isolated from C57BL/6 mice intravenously infected with *Y. enterocolitica* pYV$^+$ Δ*yopP* strain compared to mice infected with the *Y. enterocolitica* pYV$^+$ strain.

Cluster A					
Probe set ID	**Public ID**	**Gene Symbol**	**Δ*yopP* vs pYV$^+$ 24h**	**Δ*yopP* vs pYV$^+$ 72h**	**GO Biological Process**
101826_at	X58216	---	2,54	-0,63	transcription
162149_i_at	AV325777	---	1,8	0,37	transcription
161060_i_at	AV338120	2310061O04Rik	2	0,14	---
96748_i_at	AA619554	9130011B11Rik	-0,13	1,68	regulation of cell cycle
92432_at	AI844359	A630056B21Rik	2,14	0,41	ubiquitin-dependent protein catabolism
95705_s_at	J04181	Actb	1,37	2,79	transcription
96260_at	AB021491	AL033314	1,75	1,58	actin cytoskeleton organization and biogenesis
93372_at	U73478	Anp32a	2,16	2,83	cell communication
93798_at	AI839988	Atp1a1	1,81	1,25	proteolysis and peptidolysis
93797_g_at	AW123952	Atp1a1	2,3	1,74	proteolysis and peptidolysis
95466_at	AI837006	Cotl1	2,59	1,83	electron transport
93285_at	AI845584	Dusp6	1,9	1,24	immune response
94941_at	AJ243533	Eif2ak4	2,15	0,48	transport
94332_at	AI882555	Ets1	2,63	1,28	---
94781_at	V00714	Hba-a1	1,79	0,07	cell adhesion
101869_s_at	J00413	Hbb-b1	1,66	-0,31	cell adhesion
103534_at	V00722	Hbb-b1	1,83	-0,28	cell adhesion
160601_at	AF015768	Lfng	1,86	0,78	glycogen metabolism
160732_at	AA726383	Npepl1	3,29	0,15	kidney development
95357_at	AI325802	Nvl	2,78	1,89	intracellular signaling cascade
93694_at	AF036893	Per2	-0,18	2,35	transcription
93039_at	AF009513	Pgcp	3,3	0,47	defense response
160439_at	U53584	Polg	1,56	-0,23	---
99916_at	D90242	Prkch	1,79	0,93	---
97548_at	AI155120	Prpf39	2,94	0,68	---
96554_r_at	AW107462	Taf15	0,58	2,61	---
162430_at	AV294852	Tor1b	2,33	0,09	activation of MAPK

94964_at	L18880	Vcl	1,24	1,52	cell adhesion
102277_at	M36514	Zfp26	1,61	0,86	---

Cluster B					
Probe set ID	**Public ID**	**Gene Symbol**	**Δ*yopP* vs pYV$^+$ 24h**	**Δ*yopP* vs pYV$^+$ 72h**	**GO Biological Process**
95858_at	C76988	---	-1,68	-0,9	---
161411_i_at	AV315398	---	-1,85	0,47	development
94113_at	AA163908	---	-0,95	-3,89	exocytosis
160934_s_at	X05546	---	-3,79	-3,38	DNA repair
92703_at	AI325791	2310032M22Rik	-1,19	-1,98	---
97749_at	AI836270	9130415E20Rik	-2,23	-1,76	ubiquitin-dependent protein catabolism
160993_at	AI854813	A630053O10	-2	-0,54	transforming growth factor beta receptor signaling pathway
96188_at	AF052506	Adar	-1,73	-0,79	apoptosis
93464_at	AI561567	Akap9	-3,02	-4	protein amino acid phosphorylation
103789_at	AI854614	Brd4	-2,03	-2,54	regulation of cell cycle
162366_r_at	AV233144	C2	-1,82	-0,5	---
93721_at	L12367	Cap1	-2,06	-1,93	transport
100405_at	X56683	Cbx3	-1,21	-2,01	electron transport
98067_at	U09507	Cdkn1a	-1,66	-0,83	regulation of cell cycle
100278_at	U09968	Cdkn1b	-2,32	-3,41	regulation of cell cycle
161825_f_at	AV381191	Ceacam10	-1,88	-0,05	---
160511_at	L12029	Cxcl12	-0,96	-1,95	immune response
93965_r_at	AF038995	Ddx6	-1,58	-1,54	transcription
93964_s_at	AF038995	Ddx6	-1,56	-1,57	transcription
103926_at	AV380793	Eif4g1	-2,1	-1,31	G-protein coupled receptor protein signaling pathway
102341_at	L46651	Gla	-3,67	-1,01	chemotaxis
102995_s_at	M13226	Gzma	-2,05	0,73	fatty acid biosynthesis
160101_at	X56824	Hmox1	-2,46	-0,35	---
96696_at	AI837110	Hrmt1l2	-1,88	-0,93	cytokine and chemokine mediated signaling pathway
99334_at	K00083	Ifng	-2,43	-0,13	---
97574_f_at	AF036736	Igh-VJ558	-2	0,29	---
93927_f_at	L33954	Igh-VJ558	-1,9	0,56	---
104268_at	X51975	Il6ra	-1,63	-1,75	---
103022_at	U23470	Map3k1	-0,46	-1,55	---
100484_at	X66473	Mmp13	-1,97	0,64	receptor mediated endocytosis
95351_at	AA414339	Ncoa6	-0,6	-2,52	regulation of cell cycle
160949_at	AI848924	Parg	-0,96	-2,66	transport
97808_at	AI844532	Sf3b1	-1,28	-1,55	cellular morphogenesis
104158_at	AW046671	Skiip	-1,14	-2,1	regulation of transcription, DNA-dependent

99607_at	Z47088	Skp1a	-1,21	-1,83	transcription
100947_at	AI847906	Tcf20	-3,57	-0,69	---
99126_at	L04961	Xist	-1,83	-1,98	---

Supplementary table 3: Figure 3.11

Probe sets differentially regulated in splenic CD11b$^+$ cells isolated from C57BL/6 mice intravenously infected with *Y. enterocolitica* pYV$^+$ Δ*yopH* strain compared to mice infected with the *Y. enterocolitica* pYV$^+$ strain.

Cluster A			
Probe set ID	**Public ID**	**Gene Symbol**	**GO Biological Process**
161299_r_at	AV049751	---	---
161511_f_at	AV152244	---	---
104400_at	AF076956	0610042I15Rik	---
97733_at	U05673	Adora2b	signal transduction
96501_at	AI506285	AI194738	---
93500_at	M63245	Alas1	heme biosynthesishesis
103899_at	AA690863	Atp11a	metabolism
102064_at	L28095	Casp1	apoptosis
102905_at	Y13089	Casp11	apoptosis
102736_at	M19681	Ccl2	chemotaxis
102424_at	J04491	Ccl3	chemotaxis
94146_at	X62502	Ccl4	chemotaxis
99413_at	U29678	Ccr1	inflammatory response
161968_f_at	AV370035	Ccr5	chemotaxis
102718_at	AF022990	Ccr5	chemotaxis
104443_at	L31580	Ccr7	chemotaxis
98088_at	X13333	Cd14	inflammatory response
94881_at	AW048937	Cdkn1a	regulation of cell cycle
100022_at	D89613	Cish	immune response
160415_at	AI604314	Cldn1	---
97546_at	AF072127	Cldn1	---
160526_s_at	M60285	Crem	transcription
100533_s_at	M60285	Crem	transcription
102638_at	AB015224	Cst7	---
95348_at	J04596	Cxcl1	inflammatory response
101160_at	X53798	Cxcl2	chemotaxis
104371_at	AF078752	Dgat1	---
94246_at	J04103	Ets2	regulation of cell cycle
103977_at	AF087644	F10	blood coagulation

102921_s_at	M83649	Fas	apoptosis
102779_at	X54149	Gadd45b	activation of MAPKK activity
161666_f_at	AV138783	Gadd45b	activation of MAPKK activity
92217_s_at	U05265	Gp49a, Lilrb4	immune response
93328_at	X57437	Hdc	---
96696_at	AI837110	Hrmt1l2	protein amino acid methylation
94384_at	X67644	Ier3	---
100981_at	U43084	Ifit1	immune response
103639_at	U43085	Ifit2	immune response
92301_at	AB016589	Ikbke	protein amino acid phosphorylation
161023_at	U22339	Il15ra	cell surface receptor linked signal transduction
92689_at	AB019505	Il18bp	---
94755_at	M14639	Il1a	inflammatory response
93871_at	L32838	Il1rn	inflammatory response
98774_at	L38281	Irg1	---
103432_at	AW122677	Isg20	---
101820_at	X70920	LOC546644	---
94688_at	X83106	Mad	transcription
160118_at	AF022432	Mmp14	proteolysis and peptidolysis
102955_at	U83148	Nfil3	regulation of transcription, DNA-dependent
101554_at	U57524	Nfkbia	regulation of cell proliferation
98988_at	AA614971	Nfkbiz	inflammatory response
94461_at	AI852144	Pbef1	pyridine nucleotide biosynthesis
103508_at	AA919750	Pcgf5	---
102696_s_at	AI747899	Pitpnb	transport
102839_at	D78354	Plscr1	---
98018_at	L39017	Procr	blood coagulation
94158_f_at	AF004858	Ptafr	inflammatory response
94159_at	D50872	Ptafr	inflammatory response
104406_at	AI060798	Ptges	prostaglandin metabolism
160608_at	AI854462	Rab20	transport
95785_s_at	Y13361	Rab7	transport
160708_at	AI840446	Schip1	---
92978_s_at	X16490	Serpinb2	---
98405_at	U96700	Serpinb9	---
101877_at	AI854432	Slc31a1	transport
94556_at	AI746846	Snx10	transport
96042_at	L35528	Sod2	superoxide metabolism
101551_s_at	X78989	Tes	---
102629_at	D84196	Tnf	inflammatory response
99392_at	U19463	Tnfaip3	apoptosis
103066_at	L32973	Tyki	dTDP biosynthesis
98597_at	AW048912	Ube2l6	protein modification
100030_at	D44464	Upp1	nucleoside metabolism
95024_at	AW047653	Usp18	ubiquitin-dependent protein catabolism

Cluster B

Probe set ID	Public ID	Gene Symbol	GO Biological Process
104419_at	AI132380	---	---
102969_at	AI847369	0610025P10Rik	---
103748_at	AW125627	4933407C03Rik	---
104168_at	AA791742	Actr2	cell motility
96188_at	AF052506	Adar	RNA processing
100584_at	U72941	Anxa4	kidney development
98473_at	AF032466	Arg2	urea cycle
98924_at	Y08027	Art3	protein amino acid ADP-ribosylation
97693_at	C78513	C78513	---
98406_at	AF065947	Ccl5	immune response
102719_f_at	X94151	Ccr5	immune response
93617_at	AF030185	Ccrl2	G-protein coupled receptor protein signaling pathway
93908_f_at	X16670	Ccrn4l	rhythmic process
93909_f_at	X04120	Ccrn4l	rhythmic process
102831_s_at	U39456	Cd86	defense response
98067_at	U09507	Cdkn1a	regulation of cell cycle
104509_at	AF059213	Ch25h	metabolism
93994_at	AW212131	Chpt1	---
96551_at	AB024717	Clec4e	immune response
94256_at	AI849533	Clic4	transport
100019_at	D45889	Cspg2	cell adhesion
101845_s_at	M55219	Csprs, Sp100-rs	---
95349_g_at	J04596	Cxcl1	inflammatory response
92758_at	U09268	Dusp2	protein amino acid dephosphorylation
102737_at	U35233	Edn1	regulation of pH
97689_at	M26071	F3	blood coagulation
92441_at	Y10007	Fap	proteolysis and peptidolysis
101793_at	X70980	Fcgr1	immune response
102313_at	L09737	Gch1	tetrahydrobiopterin biosynthesis
102341_at	L46651	Gla	carbohydrate metabolism
97525_at	U48403	Gyk	carbohydrate metabolism
100013_at	AW121732	Ifi35	immune response
99334_at	K00083	Ifng	immune response
103963_f_at	AA914345	Iigp1	cytokine and chemokine mediated signaling pathway
100773_at	M86672	Il12a	immune response
161037_at	U14332	Il15	immune response
102218_at	X54542	Il6	immune response
100277_at	X69619	Inhba	growth
101327_at	U82610	Lcp1	response to wounding
160618_at	AA760613	Lgals8	---
160517_at	M35153	Lmnb1	---
93997_at	AI853475	MGI:1929890	---
104742_at	AA919832	Mgst2	---
102360_at	AW214225	Mthfr	methionine metabolism

101727_at	AF030896	Nfkbie	regulation of transcription, DNA-dependent
104420_at	U43428	Nos2	defense response to bacteria
94505_at	AW124934	Peli1	---
102663_at	X62700	Plaur	cell surface receptor linked signal transduction
93672_at	U09928	Prkr	immune response
99589_f_at	X07625	Prm1	nuclear organization and biogenesis
104647_at	M88242	Ptgs2	prostaglandin biosynthesis
95803_at	D85785	Ptpns1	phagocytosis
160314_at	AI839803	Pyp	metabolism
92901_at	M60909	Rara	transcription
104146_at	AI853551	Rasip1	positive regulation of cell proliferation
94972_at	AB026569	Rbms1	DNA replication
103231_at	AA739233	Rhoh	small GTPase mediated signal transduction
93738_at	M22998	Slc2a1	transport
162206_f_at	AV374868	Socs3	immune response
97206_at	AW230369	Spint1	---
99847_at	X73523	St3gal1	protein amino acid glycosylation
103328_at	U59864	Tank	I-kappaB kinase/NF-kappaB cascade
101502_at	X89749	Tgif	transcription
99144_s_at	D50031	Tgoln1	---
93985_at	AW120868	Tiparp	protein amino acid ADP-ribosylation
102959_at	U61363	Tle4	transcription
160489_at	L24118	Tnfaip2	angiogenesis
98474_r_at	U83903	Tnfaip6	cell adhesion
92962_at	M83312	Tnfrsf5	apoptosis
94112_at	U37522	Tnfsf10	apoptosis
95543_at	AI843046	Tpm4	muscle development
104582_g_at	AI845438	Zdhhc6	---
94109_at	AI850113	Zfp281	---

Cluster C			
Probe set ID	**Public ID**	**Gene Symbol**	**GO Biological Process**
101912_at	AI019679	1100001G20Rik	---
95740_at	AA727291	2300003P22Rik	proteolysis and peptidolysis
103024_at	X13335	Adam8	cell-cell adhesion
103759_at	D31788	Bst1	defense response
161825_f_at	AV381191	Ceacam10	---
99952_at	X93035	Chi3l1	carbohydrate metabolism
99387_at	L22181	Fpr1	chemotaxis
101800_at	AF071180	Fpr-rs2	---
97531_at	X95280	G0s2	cell cycle
98111_at	L40406	Hsp105	protein folding
102658_at	X59769	Il1r2	inflammatory response
161689_f_at	AV223216	Il1r2	inflammatory response
94171_at	AF051367	Itgb2l	cell-matrix adhesion

160564_at	X81627	Lcn2	transport
97420_at	AW230891	Lrg1	---
102974_at	U18424	Marco	defense response
94769_at	U96696	Mmp8	proteolysis and peptidolysis
96603_at	AW123556	Qscn6	---
96747_at	AW121294	Rhou	small GTPase mediated signal transduction
102712_at	X03505	Saa3	acute-phase response
104692_at	M72332	Selp	cell adhesion
94752_s_at	U10531	Skil	cell differentiation
101713_at	AB022345	Slc7a11	transport
97519_at	X13986	Spp1	cell adhesion
160469_at	M62470	Thbs1	cell adhesion

Cluster D			
Probe set ID	**Public ID**	**Gene Symbol**	**GO Biological Process**
97102_at	AA276948	---	---
160272_at	AI849356	---	---
102969_at	AI847369	0610025P10Rik	---
160378_at	AI853127	1110006I15Rik	---
160245_at	AW045564	1110034O07Rik	---
160787_at	AW124900	1500010J02Rik	---
92338_f_at	AI957030	2310001H12Rik	---
101404_at	AI853654	2310061I09Rik	---
160166_r_at	AI843495	2810409H07Rik	---
103667_at	AA866655	A130034M23Rik	---
103689_at	AA833514	Abcc3	canalicular bile acid transport
93193_at	X15643	Adrb2	signal transduction
100970_at	X65687	Akt1	apoptosis
100473_at	AI851750	Arrb1	signal transduction
93797_g_at	AW123952	Atp1a1	cation transport
103449_at	AA795923	BC040823	---
96255_at	AF067395	Bnip3l	apoptosis
104023_at	AW060457	Cd300c,Cd300a	---
98447_at	M62362	Cebpa	transcription
101426_at	AW125333	Cerk	protein kinase C activation
102966_at	AA934166	Cnot6l	---
95466_at	AI837006	Cotl1	---
94916_at	AW122260	Cyp51	electron transport
93821_at	AW046101	D8Ertd594e	---
102797_at	X95281	Dhrs3	metabolism
93285_at	AI845584	Dusp6	protein amino acid dephosphorylation
94332_at	AI882555	Ets1	---
100567_at	M20497	Fabp4	transport
98575_at	X13135	Fasn	lipid biosynthesis
95596_at	AW122957	Foxk2	---

93268_at	AI852001	Glo1	carbohydrate metabolism
93750_at	J04953	Gsn	vesicle-mediated transport
92580_at	U39473	Hars	protein biosynthesis
94781_at	V00714	Hba-a1	transport
103534_at	V00722	Hbb-b2	transport
104376_at	AF006602	Hdac5	transcription
160571_at	AF020039	Idh1	metabolism
102892_at	U65592	Kcnab2	transport
99603_g_at	AF064088	Klf10	transcription
102123_at	Z31689	Lip1	lipid metabolism
100467_at	X57687	Lyl1	transcription
101007_at	AI845732	Mknk2	regulation of protein biosynthesis
98524_f_at	AI848479	Mtm1	protein amino acid dephosphorylation
99024_at	U32395	Mxd4	transcription
98586_at	AW107230	Nap1l1	nucleosome assembly
95961_at	AW122131	Nbeal2	---
103922_f_at	AI839690	Nqo3a2	electron transport
100125_at	U43918	Pa2g4	proteolysis and peptidolysis
160615_at	AI835963	Pias3	transcription
100607_at	AF026124	Pld3	metabolism
100927_at	U28960	Pltp	transport
97926_s_at	U10374	Pparg	transcription
101836_at	D45859	Ppm1b	protein amino acid dephosphorylation
93116_at	J02626	Prkacb	protein amino acid phosphorylation
95597_at	M34141	Ptgs1	prostaglandin biosynthesis
92356_at	M90388	Ptpn22	protein amino acid dephosphorylation
94998_at	AI838452	Rala	small GTPase mediated signal transduction
104680_at	AJ250489	Ramp1	transport
93070_at	AI847564	Ranbp5	protein-nucleus import, docking
93319_at	U20238	Rasa3	intracellular signaling cascade
96038_at	AI840339	Rnase4	---
160388_at	AI848668	Sc4mol	lipid biosynthesis
93557_at	U43285	Sephs2	---
96060_at	U25844	Serpinb6a	---
95733_at	AI838274	Slc29a1	transport
103877_at	AW060485	Slc35c2	transport
102384_at	AI842968	Smarca2	nucleosome assembly
95513_at	AW124310	Statip1	---
160428_at	AF058956	Suclg2	metabolism
104526_at	U36393	Tcfeb	transcription
104601_at	X14432	Thbd	blood coagulation
160642_at	AI853079	Tmem5	---
99462_at	D38046	Top2b	neuron migration
94554_at	AW120965	Trappc5	transport
97473_at	AW124470	Tspan4	---
100955_at	AA989957	Ube2t	ubiquitin cycle
92558_at	M84487	Vcam1	cell adhesion

Cluster E			
Probe set ID	**Public ID**	**Gene Symbol**	**GO Biological Process**
160955_at	AW124904	2010309E21Rik	---
96122_at	AW049373	2310016A09Rik	---
104513_at	AA688938	2410004N09Rik	---
104640_f_at	AI464596	4930553M18Rik	---
160921_at	AW125884	Acas2l	acetyl-CoA biosynthesis
160927_at	J04946	Ace	proteolysis and peptidolysis
161224_f_at	AV258262	Ace	proteolysis and peptidolysis
98976_at	AJ242912	Adamdec1	proteolysis and peptidolysis
160255_at	AA657044	Ahnak	intracellular signaling cascade
160495_at	M94623	Ahr	transcription
96260_at	AB021491	AL033314	transcription
93372_at	U73478	Anp32a	---
104215_at	AA592069	Atf6	regulation of cell cycle
93798_at	AI839988	Atp1a1	cation transport
161331_r_at	AV114328	Atp5d	ATP biosynthesis
96035_at	L47335	Bckdha	metabolism
99514_at	AI835443	Bmyc	regulation of cell cycle
103789_at	AI854614	Brd4	---
95984_at	AI586160	C79468	---
104589_at	AF091096	C80913	protein folding
103682_at	AA122571	C80913	protein folding
160479_at	M29394	Cat	response to oxidative stress
102397_at	AF038029	Cbfa2t3h	granulocyte differentiation
162384_f_at	AV252118	Ccrn4l	rhythmic process
92406_at	D31956	Cd7	immune response
101908_s_at	AF101164	Ceacam1, Ceacam2	---
94465_g_at	AF029347	Clcn3	transport
97928_at	AW045278	Cln6	lysosome organization and biogenesis
93550_at	D88792	Csrp2	cell differentiation
102794_at	Z80112	Cxcr4	chemotaxis
104045_at	AW122372	D10Bwg0791e	nucleosome assembly
99828_at	AA673252	D3Ertd789e	---
103460_at	AI849939	Ddit4	---
161060_i_at	AV338120	Ddx51	---
93964_s_at	AF038995	Ddx6	---
93965_r_at	AF038995	Ddx6	---
98989_at	AF057368	Dhcr7	steroid biosynthesis
100311_f_at	U72032	Ear1	---
103537_at	AF076681	Eif2ak3	protein biosynthesis
96344_at	X61600	Eno3	glycolysis
102065_at	AB007813	Fcna	phosphate transport

97509_f_at	U22324	Fgfr1	organogenesis
103699_i_at	AI646638	Frat2	Wnt receptor signaling pathway
97819_at	AI843119	Gsto1	metabolism
104014_at	Y12650	Hfe	immune response
94288_at	J03482	Hist1h1c	nucleosome assembly
94325_at	AW124932	Hmgcs1	acetyl-CoA metabolism
93351_at	U44389	Hpgd	prostaglandin metabolism
96048_at	U50631	Hrsp12	---
96269_at	AA716963	Idi1	lipid biosynthesis
100552_at	M28233	Ifngr1	---
95546_g_at	X04480	Igf1	apoptosis
102823_at	X67210	Ighg	---
93605_r_at	AF061260	Igsf4a	cell adhesion
98500_at	D13695	Il1rl1	defense response
104268_at	X51975	Il6ra	cell surface receptor linked signal transduction
92737_at	U20949	Irf4	transcription
100601_at	AF022110	Itgb5	cell adhesion
97302_at	AI854285	Ivns1abp	---
96168_at	AI591702	Kif23	---
102235_at	X13945	Lmyc1	regulation of cell cycle
160934_s_at	X05546	LOC435551	---
93568_i_at	AI853444	LOC544991	---
160553_at	X63782	Ly6d	defense response
99855_at	AB006787	Map3k5	apoptosis
103599_at	M20824	Mdm1	---
93852_at	AW045443	Mef2a	transcription
97357_at	AI426400	Mef2c	transcription
93039_at	AF009513	MGI:1889205	---
103226_at	Z11974	Mrc1	endocytosis
162009_f_at	AV246753	Msh2	DNA metabolism
93246_at	AW260482	Narg1	angiogenesis
103491_at	AA968123	Nav1	microtubule bundle formation
95129_at	AW121057	Ncor2	transcription
96153_at	L37297	Ngp	defense response
100120_at	L17324	Nid1	cell adhesion
160732_at	AA726383	Npepl1	proteolysis and peptidolysis
103508_at	AA919750	Pcgf5	---
160412_at	U10903	Pdcd2	apoptosis
103029_at	D86344	Pdcd4	---
93421_at	AF033655	Pftk1	electron transport
160105_r_at	AI847033	Pigk	proteolysis and peptidolysis
160204_at	AI838470	Prr6	---
161757_f_at	AV298789	Ranbp5	transport
102419_at	M34476	Rarg	transcription
98057_at	AW121162	Rnf166	---
100732_at	X73829	Rps8	ribosome biogenesis
94394_at	M21019	Rras	regulation of cell cycle

94545_at	AW123115	Rtn1	nucleosome assembly
100003_at	D38216	Ryr1	transport
94057_g_at	M21285	Scd1	lipid biosynthesis
95387_f_at	AA266467	Sema4b	cell differentiation
160869_at	AI849490	Sirt3	transcription
104158_at	AW046671	Skiip	transcription
99500_at	U13174	Slc12a2	transport
95060_at	AF058054	Slc16a7	transport
162333_r_at	AV093322	Slpi	---
94432_at	AI117157	St6gal1	protein amino acid glycosylation
93106_i_at	M20878	Tcrb-J	cellular defense response
102425_at	U61362	Tle1	transcription
103092_at	AW124316	Trim37	protein ubiquitination
102423_at	AI649125	Uxs1	---
92202_g_at	AI553024	Zbtb16	apoptosis
104418_at	AA796868	Znrf2	---

Supplementary table 4

Probe sets differentially regulated in splenic $CD11b^{+}$ cells isolated from uninfected IFN-$\gamma R1^{-/-}$ mice compared to uninfected C57BL/6 mice.

Cluster A				
Probe set ID	**Public ID**	**Gene Symbol**	**IFN-$\gamma R1^{-/-}$ vs C57BL/6**	**GO Biological Process**
101617_s_at	U59758	---	1,63	---
98974_at	AI183084	---	1,79	---
104429_at	AF027865	---	1,97	---
102805_at	M77196	---	2,32	---
160799_at	AW060549	---	2,78	---
92740_at	J00475	---	4,23	---
94355_at	AW048394	---	4,34	---
92741_g_at	J00475	---	4,57	---
104314_r_at	AI851206	1110032A03Rik	2,23	---
95031_at	AW060212	1110059H15Rik	1,85	---
98894_at	AA867655	2610016F04Rik	1,59	transcription
93441_at	AI595322	2700099C18Rik	2,27	---
101998_at	AW125086	4833420G17Rik	1,74	---
160191_at	AW122058	4931433E08Rik	2,15	---
96196_i_at	AI851708	5730589K01Rik	1,83	transcription
102870_at	AW125272	5930418K15Rik	1,99	---
161114_i_at	AV330064	6330509M23Rik	1,52	---

160905_s_at	AI840713	A030009H04Rik	1,94	---
102910_at	M24417	Abcb1a	1,75	transport
103615_at	AA727023	AI447904	2,25	---
96069_at	AI840094	Akr7a5	1,55	metabolism
92288_at	X54424	Ap1g1	3,86	protein complex assembly
94512_f_at	AI843210	Arcn1	2,41	---
93235_at	AI020029	BB128963	1,79	---
102913_at	AI324342	Bcl2a1a	3,16	apoptosis
99405_at	U30241	bd2, bj2	1,8	---
94363_at	AI840815	Bms1l	1,55	---
95094_g_at	AI035334	Ccar1	2,1	positive regulation of apoptosis
98446_s_at	U06834	Cct3	2,44	protein folding
99434_at	AF001036	Cd83	4,05	---
102831_s_at	U39456	Cd86	1,56	defense response
102806_g_at	M77196	Ceacam1	1,55	---
160330_at	AW122453	Chordc1	1,52	---
101937_s_at	AF005423	Clk4	3,94	protein amino acid dephosphorylation
93861_f_at	M17327	Ctse	1,72	proteolysis and peptidolysis
100300_at	U43384	Cybb	3,04	transport
98952_at	AW120971	D8Ertd325e	3,31	---
92198_s_at	L41365	Daf1, Daf2	2,75	immune response
160935_at	AI036466	Ddhd1	1,5	lipid catabolism
93309_at	U42386	Ddx3x	2	---
160286_at	AA733594	Dek	1,51	transcription
160153_at	AI835917	Dnajc7	1,58	protein folding
94941_at	AJ243533	Eif2ak4	1,54	protein amino acid phosphorylation
94253_at	AW061243	Eif2s1	1,59	protein biosynthesis
93722_at	AJ005985	Ensa	1,94	regulation of insulin secretion
101587_at	U89491	Ephx1	2,71	proteolysis and peptidolysis
102427_at	AI849991	Fyttd1	1,93	---
99011_at	U70538	Galnt3	1,93	---
95974_at	M55544	Gbp1	2,2	immune response
95392_at	U68182	Gcnt2	2,78	---
92449_at	AF002701	Gfra2	2,05	neurogenesis
104402_at	AA030469	Gtf3c4	1,77	transcription
101868_i_at	X90807	H2-DMb2	2,37	antigen processing
160101_at	X56824	Hmox1	2,38	response to stimulus
96696_at	AI837110	Hrmt1l2	3,71	protein amino acid methylation
93226_i_at	Z70661	Igh-1a	4,16	antibody-dependent cellular cytotoxicity
96973_f_at	X02468	Igh-V	1,91	---
97008_f_at	L33943	Igh-V	1,99	antibody-dependent cellular cytotoxicity
100721_f_at	U10410	Igh-VJ558	1,66	---
101641_at	M86751	Igk-V21	1,7	---
93638_s_at	J00579	Igl-V1	1,91	humoral immune response
98828_at	X07640	Itgam	1,6	cell adhesion
101327_at	U82610	Lcp1	2,61	response to wounding
97563_f_at	AF042798	LOC211331	1,54	---

93904_f_at	AF059706	LOC238418	1,59	---
94389_at	AA915720	Lsm5	2,2	transcription
101946_at	AA840463	Lypla1	2,11	lipid metabolism
101945_g_at	U89352	Lypla1	3,58	lipid metabolism
160353_i_at	X76850	Mapkapk2	2,08	protein amino acid dephosphorylation
96011_at	AB009275	Matr3	2,04	---
95338_s_at	M82831	Mmp12	2,02	proteolysis and peptidolysis
92644_s_at	M12848	Myb	2,39	regulation of cell cycle
103791_at	AW048763	Narg1	2,24	angiogenesis
93101_s_at	U96635	Nedd4	1,79	protein modification
93563_s_at	AB017202	Nid2	1,58	cell adhesion
93831_at	AI316087	Nono	2,06	transcription
99076_at	U09504	Nr1d2	3,33	transcription
160925_at	X13664	Nras	2,49	regulation of cell cycle
160189_at	AI843747	Nudt4	2,06	---
95075_at	AW229141	Nup35	1,77	---
160970_at	AI848335	Odf2	1,63	---
103508_at	AA919750	Pcgf5	1,51	---
101732_at	M12039	Phxr5	1,58	---
101865_at	AB009615	Pip5k2a	2	---
102696_s_at	AI747899	Pitpnb	4,44	transport
99916_at	D90242	Prkch	1,75	protein amino acid dephosphorylation
97919_at	AI837467	Prpf38b	1,65	---
97560_at	AF037437	Psap	3,66	lipid metabolism
99433_at	Y18101	Pstpip2	2,83	---
97363_at	M95408	Ptk2	1,54	cell motility
95803_at	D85785	Ptpns1	1,59	phagocytosis
101298_g_at	M23158	Ptprc	3,03	protein amino acid dephosphorylation
95785_s_at	Y13361	Rab7	1,94	transport
99032_at	AF009246	Rasd1	3,44	small GTPase mediated signal transduction
160192_at	AF031568	Rbmxrt	1,71	RNA processing
101902_at	X17459	Rbpsuh	1,63	angiogenesis
101966_s_at	AF037206	Rnf13	2,21	proteolysis and peptidolysis
93164_at	Y12783	Rnf2	4,69	transcription
100980_at	U58512	Rock1	1,7	apoptosis
100612_at	K02927	Rrm1	2,72	DNA replication
160795_at	AW123662	Scamp1	1,84	transport
94057_g_at	M21285	Scd1	1,92	lipid biosynthesis
160373_i_at	AI839175	Sdpr	2,06	---
99621_s_at	AA690583	Sfpq	1,79	transcription
160539_at	X66091	Sfrs1	2,49	transcription
98299_s_at	AF099974	Slfn3, Slfn4	1,64	negative regulation of cell proliferation
92343_at	AF010138	Smarca3	2,19	transcription
96333_g_at	AW259199	Snx2	2,19	transport
97160_at	X04017	Sparc	1,61	---
101684_r_at	X67863	Srst	1,58	transcription
104249_g_at	AW227650	Ssr3	4,78	cotranslational protein-membrane targeting

97310_at	AW124318	St13	4,4	protein folding
98775_at	U28726	Stk3	3,95	apoptosis
100426_s_at	U36776	Syk	3,35	activation of MAPK activity
93918_at	AA673500	Taf9	2,29	transcription
94262_at	AI172920	Thrap3	2,17	transcription
95543_at	AI843046	Tpm4	1,61	muscle development
99149_at	AI851230	Trim59	1,56	---
97486_at	AA693246	U2af1	1,82	transcription
92560_g_at	U12884	Vcam1	2,02	cell adhesion
160583_at	AA880988	Xlkd1	2,98	cell adhesion
101883_s_at	L22977	Xlr3a	2,48	---
104582_g_at	AI845438	Zdhhc6	2,08	---

Cluster B				
Probe set ID	**Public ID**	**Gene Symbol**	**INF-γR1$^{-/-}$ vs C57BL/6**	**GO Biological Process**
161476_at	AV011715	---	-1,72	---
162496_r_at	AV153195	---	-1,69	---
162379_r_at	AV245272	---	-1,52	---
96791_at	AW047875	1500005K14Rik	-1,81	---
95740_at	AA727291	2300003P22Rik	-1,89	proteolysis and peptidolysis
161462_r_at	AV346841	2610005L07Rik	-3,56	---
161387_i_at	AV253622	5730555F13Rik	-2,88	---
104206_at	AA815845	5730557B15Rik	-2,31	---
104035_at	AW123795	9130404D08Rik	-2,29	---
92913_at	Z48670	Abcd2	-1,69	transport
93100_at	X13297	Acta2	-2,32	cytoskeleton organization and biogenesis
161629_i_at	AV037200	Afp	-2,41	transport
161088_r_at	AV171460	Akap8	-1,99	mitotic chromosome condensation
162034_r_at	AV369210	Antxr2	-1,73	---
102815_at	U65986	Anxa11	-1,78	---
98473_at	AF032466	Arg2	-1,51	arginine metabolism
102854_s_at	U03434	Atp7a	-1,54	transport
93142_at	D86603	Bach1	-2,57	transcription
101217_at	D18865	BC023892	-1,82	---
161214_r_at	AV265258	BC037034	-2,01	---
162221_i_at	AV112892	Blmh	-2,17	proteolysis and peptidolysis
103789_at	AI854614	Brd4	-2,48	---
96037_at	X61454	Bri3	-1,58	---
103759_at	D31788	Bst1	-1,79	defense response
100932_at	AF084459	Capn1	-2,03	proteolysis and peptidolysis
161825_f_at	AV381191	Ceacam10	-2,47	---
103217_at	Y14041	Cflar	-2,05	proteolysis and peptidolysis
99952_at	X93035	Chi3l1	-1,93	metabolism

160655_at	D85391	Cpd	-2,33	proteolysis and peptidolysis
97925_at	AB028241	Csnk1e	-1,88	protein amino acid dephosphorylation
101436_at	M34815	Cxcl9	-1,96	immune response
99463_at	X63023	Cyp3a13	-2,47	transport
102224_at	AF056187	D930020L01	-1,87	---
93965_r_at	AF038995	Ddx6	-2,77	---
93964_s_at	AF038995	Ddx6	-2,58	---
95944_at	AV299153	Dhx36	-1,65	---
103994_at	AI152867	Eif2c2	-2,16	protein biosynthesis
92231_at	D28818	Epb4.1l4a	-3,02	---
160901_at	V00727	Fos	-2,78	regulation of cell cycle
160850_at	U32197	Fpgs	-1,68	folic acid and derivative biosynthesis
160873_at	AV206059	Ghrl	-1,86	regulation of physiological process
100514_at	M63660	Gna13	-1,92	angiogenesis
103215_g_at	AW048883	Hspb2	-2,18	protein folding
100552_at	M28233	Ifngr1	-1,7	---
98776_at	AF035203	Igh-6	-2,4	humoral defense mechanism
96764_at	AJ007971	Iigp1	-2,82	cytokine and chemokine mediated signaling pathway
102658_at	X59769	Il1r2	-1,58	inflammatory response
104268_at	X51975	Il6ra	-2,22	cell surface receptor linked signal transduction
94137_at	L13239	Il8rb	-2,45	chemotaxis
161407_i_at	AV312395	Inpp1	-1,55	---
162193_f_at	AV371872	Itgb7	-2,05	cell adhesion
102362_i_at	U20735	Junb	-2,56	regulation of cell cycle
102364_at	J04509	Jund1	-1,86	regulation of cell cycle
161796_r_at	AV367240	Kcnq1	-1,54	transport
96109_at	U25096	Klf2	-1,55	transcription
161301_f_at	AV049898	Lgals9	-2,81	---
97420_at	AW230891	Lrg1	-1,61	---
104592_i_at	AI595996	Mef2c	-4,55	transcription
97510_at	AJ001118	Mgll-rs1	-2,85	---
94769_at	U96696	Mmp8	-1,5	proteolysis and peptidolysis
162369_f_at	AV239570	Mmp9	-1,57	proteolysis and peptidolysis
98010_at	L09600	Nfe2	-1,59	transcription
161912_r_at	AV377244	Numb	-1,6	development
102583_at	AJ132195	Olfr138	-2,02	G-protein coupled receptor protein signaling pathway
104648_at	AI844597	Pacs1	-1,77	protein-Golgi targeting
162475_f_at	AV092014	Pglyrp1	-1,81	apoptosis
104099_at	AF076482	Pglyrp1	-1,78	apoptosis
103387_at	AB011550	Phf1	-1,57	transcription
160829_at	U44088	Phlda1	-2,66	FasL biosynthesis
161270_i_at	AV319920	Prkwnk1	-1,97	protein amino acid dephosphorylation
160739_at	AI835081	Prkwnk1	-1,72	protein amino acid dephosphorylation
104647_at	M88242	Ptgs2	-2,23	prostaglandin biosynthesis

94929_at	M97590	Ptpn1	-1,94	protein amino acid dephosphorylation
92303_at	D31898	Ptprr	-2,37	protein amino acid dephosphorylation
103067_at	Z48587	Rala	-1,55	small GTPase mediated signal transduction
102131_f_at	AU014874	Rnf20	-1,93	---
161480_i_at	AV055186	Rplp1	-1,76	protein biosynthesis
104177_at	AA204579	Rsad2	-1,53	---
104106_at	AI837830	Sbno1	-2,02	---
94181_at	AJ223206	Scrg1	-1,76	---
161935_r_at	AV329249	Sh3bgr	-2,44	---
162007_i_at	AV337065	Sipa1	-1,7	regulation of cell cycle
161650_at	AV090497	Slpi	-1,87	---
103680_at	AA683850	Srpr	-1,76	protein targeting
94104_at	AF051911	Tert	-1,97	telomere maintenance
161385_r_at	AV250738	Tph1	-2,86	metabolism
100348_at	AW214136	X83313	-1,98	---
100897_f_at	AF100956	Zfp297	-3,17	---

Supplementary table 5

Probe sets differentially regulated in splenic CD11b^{+} cells isolated from IFN-γR1$^{-/-}$ mice intravenously infected with *Y. enterocolitica* pYV^{+} strain compared to C57BL/6 infected mice.

	Public ID	**Gene Symbol**	**INF-γR1$^{-/-}$ vs C57BL/6 24 h**	**INF-γR1$^{-/-}$ vs C57BL/6 72 h**	**GO Biological Process**
100880_at	AA816121	---	-0,42	-1,79	---
100944_at	AA958903	---	-2,14	-1,67	---
101223_r_at	C77112	---	2,96	-0,57	---
102254_f_at	AA289585	---	-0,94	-2,49	---
160799_at	AW060549	---	0,15	2,72	---
160906_i_at	AA184423	---	-0,66	1,73	---
161317_r_at	AV088715	---	1,71	0	---
161369_r_at	AV239611	---	2,13	-0,47	---
161448_f_at	AV355612	---	-0,91	-1,54	---
161511_f_at	AV152244	---	-0,01	-1,99	---
162393_at	AV266447	---	3,07	-0,12	---
92320_f_at	AA415783	---	0,97	2,86	---
95184_f_at	AA419684	---	-0,28	2,05	---
96215_f_at	AI153421	---	-1,18	-2,11	---
104314_r_at	AI851206	1110032A03Rik	0,06	1,64	---
160359_at	AI854358	1190002H23Rik	0,46	1,69	cell cycle
160184_at	AA815795	1200007D18Rik	0,7	1,52	transport
96791_at	AW047875	1500005K14Rik	0,07	1,87	---
104000_at	AI181346	2210023G05Rik	-0,19	4,74	---

95740_at	AA727291	2300003P22Rik	-0,04	2,55	proteolysis and peptidolysis
92338_f_at	AI957030	2310001H12Rik	0,53	-1,59	---
93138_at	AI853219	2410012H22Rik	1,73	-0,05	---
97247_at	AW124778	2610034N03Rik	-0,41	-1,55	metabolism
93568_i_at	AI853444	2610042L04Rik	-0,61	2,08	---
93569_f_at	AI853444	2610042L04Rik	-1,08	1,83	---
99080_at	AI853930	2810012H18Rik	-0,01	-1,79	---
102910_at	M24417	Abcb1a	0,75	-2,55	transport
101578_f_at	M12481	Actb	-0,91	2,02	---
104578_f_at	AI195392	Actn1	0,39	1,63	---
104579_r_at	AI195392	Actn1	0,86	1,57	---
92280_at	AA867778	Actn1	0,72	3,4	---
100450_r_at	L48015	Acvrl1	0,33	1,61	protein amino acid phosphorylation
98632_at	M10319	Ada	0,33	2,01	immune response
100751_at	AF011379	Adam10	2	-0,11	proteolysis and peptidolysis
104326_at	AI838951	Adpgk	0,61	3,01	carbohydrate metabolism
103615_at	AA727023	LOC545384	0,49	-1,71	---
102330_at	D86382	Aif1	-0,54	-2,09	actin filament bundle formation
93464_at	AI561567	Akap9	-0,48	-2,73	---
97111_at	AA290180	Als2cr3	1,1	2,08	---
93037_i_at	M69260	Anxa1	0,76	1,78	cell cycle
102815_at	U65986	Anxa11	0,14	1,92	---
101393_at	AJ001633	Anxa3	0,75	1,5	---
92288_at	X54424	Ap1g1	1,64	-0,76	transport
99915_at	L41352	Areg	2,63	3,7	---
93097_at	U51805	Arg1	2,54	1,24	arginine metabolism
98084_at	AI849834	Arl2bp	0,58	2,07	---
104155_f_at	U19118	Atf3	-1,47	-1,63	transcription
93142_at	D86603	Bach1	-1,58	-1,54	transcription
95247_at	AA517754	BB001228	2,66	0,11	---
100949_at	AI461767	BC004044	0,45	1,88	---
102913_at	AI324342	Bcl2a1a	1,1	-1,79	apoptosis
99018_at	AA874446	Bclaf1	1,8	0,04	transcription
103707_at	U77461	C3ar1	1,56	-0,29	chemotaxis
97710_f_at	AI425990	C530046L02Rik	1,01	1,56	---
101728_at	S46665	C5r1	1,61	0,84	chemotaxis
92322_at	X94353	Camp	-0,13	2,4	defense response
102424_at	J04491	Ccl3	1,73	-1,29	chemotaxis
98406_at	AF065947	Ccl5	-1,09	-2,82	immune response
102719_f_at	X94151	Ccr5	1,55	-1,16	chemotaxis
93617_at	AF030185	Ccrl2	-0,52	-1,64	G-protein coupled receptor protein signaling pathway
103281_at	AF077003	Cd2ap	-0,4	-2,16	---
98980_at	U18372	Cd37	0,11	1,5	---
160493_at	D16432	Cd63	0,5	2,15	---
100278_at	U09968	Cdkn1b	-0,92	-1,94	cell cycle
101637_at	L38422	Ceacam10	1,39	2,84	---
161825_f_at	AV381191	Ceacam10	1,15	3,32	---
99952_at	X93035	Chi3l1	0,57	1,86	metabolism
101956_at	AI834849	Ckap4	0,62	2,31	---
94255_g_at	AI845237	Clic4	-0,54	-1,5	transport
93688_at	D21826	Cmah	2,96	1,64	transport
160150_f_at	AW125626	Cnn3	-3,13	-1,27	smooth muscle contraction
94305_at	U03419	Col1a1	0,26	4,33	cell adhesion

101080_at	AB009993	Col5a1	0,38	4,34	cell adhesion
92851_at	U49430	Cp	0,06	2,48	transport
103581_at	Y14004	Cte1	0,14	1,66	lipid metabolism
96912_s_at	X15591	Ctla2a, Ctla2b	0,2	1,87	---
103518_at	X15592	Ctla2b	-0,32	3,18	---
95348_at	J04596	Cxcl1	1,9	0,61	inflammatory response
93858_at	M33266	Cxcl10	-0,09	-3,23	immune response
160511_at	L12029	Cxcl12	0,91	2,99	chemotaxis
102025_at	AF030636	Cxcl13	0,82	4,8	chemotaxis
101160_at	X53798	Cxcl2	1,78	0,56	chemotaxis
101436_at	M34815	Cxcl9	-5	-8,13	immune response
98045_s_at	U18869	Dab2	2,6	0,72	cellular morphogenesis during differentiation
103617_at	D63679	Daf1	1,15	1,57	immune response
92198_s_at	L41365	Daf1, Daf2	0,86	4,2	immune response
103460_at	AI849939	Ddit4	1,36	1,7	---
93964_s_at	AF038995	Ddx6	0,26	-1,56	---
160711_at	AI844846	Decr1	0,08	-2,63	metabolism
96679_at	AW120711	Dnajb9	1,77	1,53	protein folding
94492_at	AB025406	Dstn	0,68	1,55	---
104687_at	AJ006074	Edg6	0,1	1,86	signal transduction
97426_at	X98471	Emp1	2	1,01	cell growth
100472_at	D10727	Enah	2,03	4,8	development
97317_at	AW122933	Enpp2	0,79	2,57	nucleotide metabolism
97689_at	M26071	F3	-0,64	-1,99	blood coagulation
160231_at	AI851129	Farsla	-0,04	-1,7	protein biosynthesis
101793_at	X70980	Fcgr1	-0,36	-2,36	immune response
102879_s_at	M31314	Fcgr1	-0,27	-1,99	immune response
160424_f_at	AI846851	Fdps	-0,19	2,2	lipid biosynthesis
99098_at	AW045533	Fdps	-0,13	2,02	lipid biosynthesis
97509_f_at	U22324	Fgfr1	-1,51	1,89	protein amino acid phosphorylation
94297_at	U16959	Fkbp5	0,8	2,67	protein folding
92483_g_at	AF006466	Fmnl1	0,21	1,97	actin cytoskeleton organization and biogenesis
160088_at	U90535	Fmo5	-0,51	5,55	electron transport
99835_at	AF017128	Fosl1	2,75	1,78	regulation of transcription, DNA-dependent
95756_at	AI839681	Ftsj3	0,14	-1,61	---
97531_at	X95280	G0s2	1,74	0,91	cell cycle
98822_at	X56602	G1p2	-0,34	-1,72	immune response
160714_at	AI046826	Gab1	3,66	0,38	activation of MAPK activity
95974_at	M55544	Gbp1	2,85	1,79	immune response
104597_at	AJ007970	Gbp2	-1,73	-3,77	immune response
103202_at	AW047476	Gbp4	-1,33	-2,71	immune response
160335_at	U95053	Gclm	0,95	1,63	glutathione biosynthesis
94192_at	Y17860	Gdap10	-0,68	-1,78	---
92449_at	AF002701	Gfra2	3,73	-0,27	neurogenesis
100085_at	U30509	Ggt1	1,43	2,1	glutathione metabolism
160873_at	AV206059	Ghrl	0,77	2	regulation of physiological process
100064_f_at	M63801	Gja1	1,17	1,7	cell communication
100065_r_at	M63801	Gja1	2,35	0,12	cell communication
160893_at	AI882325	Gngt2	-0,64	-1,56	signal transduction
96337_at	AF033350	Gp1bb, Sept5	0,81	2,14	cell adhesion
99441_at	AW123852	Gphn	-0,02	-2,16	protein targeting

104227_at	AI504074	Gpr97	1,15	2,17	signal transduction
102995_s_at	M13226	Gzma	-1,93	-2,19	apoptosis
102877_at	M12302	Gzmb	-1,78	0,26	apoptosis
92866_at	X52643	H2-Aa	-0,5	-1,58	immune response
100998_at	M21932	H2-Ab1, Rmcs1	-0,52	-1,74	immune response
162346_f_at	AV153894	H2-DMa	-0,94	-2,6	immune response
93092_at	U35323	H2-DMa	-1,12	-1,89	immune response
98034_at	U35330	H2-DMb1	-0,56	-2,73	immune response
98035_g_at	U35330	H2-DMb2	-0,47	-1,86	immune response
94285_at	X00958	H2-Eb1	-0,57	-1,51	immune response
93865_s_at	M35244	H2-T10, H2-T17, H2-T22, H2-T9	-0,99	-1,88	defense response
101876_s_at	M35247	H2-T10, H2-T17, H2-T22, H2-T9	-0,71	-1,74	defense response
97551_at	AI846182	Hip1r	-0,94	1,69	receptor mediated endocytosis
93024_at	M32460	Hist1h3g	0,25	2,28	nucleosome assembly
96696_at	AI837110	Hrmt1l2	1,73	0,31	embryonic development
97867_at	X83202	Hsd11b1	0,42	1,9	lipid metabolism
101891_at	Y09517	Hsd17b2	0,32	1,76	lipid biosynthesis
98002_at	M32489	Icsbp1	-1,73	-1,85	transcription
100050_at	M31885	Id1	1,7	2,86	regulation of angiogenesis
97409_at	U19119	Ifi1	-0,8	-2,32	defense response
93321_at	AF022371	Ifi203	-0,25	-2,17	immune response
98465_f_at	M31419	Ifi204	-0,23	-1,52	transcription
94224_s_at	M74123	Ifi205	-0,22	-2,32	transcription
104750_at	M63630	Ifi47	-0,97	-3,21	defense response
100981_at	U43084	Ifit1	-0,07	-1,91	immune response
103639_at	U43085	Ifit2	-1,02	-3,8	immune response
93956_at	U43086	Ifit3	-0,23	-3,29	immune response
98776_at	AF035203	Igh-6	0,42	-2,15	immune response
102823_at	X67210	Ighg	-3,67	-2,63	---
102824_g_at	X67210	Ighg	-1,5	-0,28	---
160933_at	U53219	Igtp	-1,56	-2,53	---
103963_f_at	AA914345	Iigp1	-3,5	-4,38	cytokine and chemokine mediated signaling pathway
96764_at	AJ007971	Iigp1	-5,41	-7,25	cytokine and chemokine mediated signaling pathway
98410_at	AJ007972	Iigp2	-1,05	-1,88	---
102658_at	X59769	Il1r2	1,13	2,62	transport
161689_f_at	AV223216	Il1r2	1	2,61	transport
103769_at	X85999	Il1rap	2,08	2,41	cytokine and chemokine mediated signaling pathway
98349_at	X62646	Il6st	1,55	-0,22	signal transduction
102401_at	M21065	Irf1	-1,65	-1,41	immune response
94171_at	AF051367	Itgb2l	1,36	3,51	cell-matrix adhesion
162193_f_at	AV371872	Itgb7	-1,84	-2,41	cell adhesion
94977_at	X15373	Itpr1	-0,14	-1,51	transport
104121_at	M90365	Jup	0,77	2,71	cell adhesion
101624_at	AF008573	Kcns1	0,14	2,04	transport
97937_at	AA611766	Klf5	0,7	2,21	angiogenesis
93527_at	Y14296	Klf9	1,16	1,95	transcription
93679_at	AF030313	Klrk1	-2,25	0,54	---
101327_at	U82610	Lcp1	2,26	-0,24	response to wounding
160517_at	M35153	Lmnb1	0,69	1,81	---
94389_at	AA915720	Lsm5	-2,13	0,04	mRNA processing
101115_at	J03298	Ltf	1,15	3,8	transport

93078_at	X04653	Ly6a	-1,77	-1,87	---
103258_at	U19271	Ly75	-0,32	1,63	immune response
94425_at	AB007599	Ly86	-0,86	-2,13	immune response
97447_at	AI836718	Map1lc3a	0,12	1,76	ubiquitin cycle
99367_at	AA434661	Mapre1	1,55	0,02	cell cycle
102974_at	U18424	Marco	1,8	4,01	phosphate transport
104591_g_at	L13171	Mef2c	0,07	-2,02	transcription
104592_i_at	AI595996	Mef2c	-2,18	-3,03	muscle development
98312_at	AB016768	MGI:2183426	-3,87	-3,7	---
101159_at	Z23066	Mitf	0,04	-1,65	transcription
94769_at	U96696	Mmp8	1,4	1,83	proteolysis and peptidolysis
98373_at	AI462516	Ms4a4c	0	-1,59	---
93573_at	V00835	Mt1	0,91	1,96	nitric oxide mediated signal transduction
98417_at	M21038	Mx1	-0,24	-2,19	immune response
92644_s_at	M12848	Myb	0,03	4	regulation of cell cycle
93427_at	AW122310	Myo1d	0,67	1,57	cytoskeleton organization and biogenesis
93590_at	AI844370	Ndst1	0,54	1,58	polysaccharide biosynthesis
93101_s_at	U96635	Nedd4	0,58	2,89	protein modification
103234_at	M35131	Nefh	1,38	2,83	intermediate filament cytoskeleton organization and biogenesis
160846_at	AI846534	Nek6	0,82	2,12	protein amino acid phosphorylation
96153_at	L37297	Ngp	1,06	2,48	defense response
93563_s_at	AB017202	Nid2	2,53	0,29	cell adhesion
96259_at	U35646	Npepps	0,4	1,8	proteolysis and peptidolysis
94351_r_at	U12961	Nqo1	1,23	2,22	electron transport
98818_at	X04435	Nr3c1	1,62	0,19	transcription
92773_at	AF079528	Nrp1	-0,99	-1,87	angiogenesis
95016_at	D50086	Nrp1	-1,55	-2,17	angiogenesis
95075_at	AW229141	Nup35	0,08	1,75	---
100436_at	M27008	Orm1	0,04	3,79	transport
100437_g_at	M27008	Orm1, Orm2	0,19	4,64	transport
103278_at	AB013850	Padi4	-0,01	1,52	protein modification
160412_at	U10903	Pdcd2	-0,1	-1,88	apoptosis
95423_at	Y00884	Pdia4	1,8	0,6	electron transport
93619_at	AF022992	Per1	0,73	1,91	transcription
93694_at	AF036893	Per2	0,44	2,56	transcription
104099_at	AF076482	Pglyrp1	-0,13	2,56	apoptosis
162475_f_at	AV092014	Pglyrp1	0,08	2,86	apoptosis
160829_at	U44088	Phlda1	2,06	1,61	FasL biosynthesis
103299_at	AW123773	Pld4	-0,29	-1,66	---
102839_at	D78354	Plscr1	0,82	2,25	---
103943_at	AI838513	Ppfia4	-0,22	-3,71	---
100606_at	M18070	Prnp	0,36	3,05	response to oxidative stress
98018_at	L39017	Procr	-1,76	-1,6	blood coagulation
93389_at	AF039663	Prom1	0,91	2,27	phototransduction
93390_g_at	AF039663	Prom1	0,06	1,9	phototransduction
97560_at	AF037437	Psap	2,36	-0,16	lipid metabolism
101486_at	Y10875	Psmb10	-1,42	-1,62	ubiquitin-dependent protein catabolism
93085_at	D44456	Psmb9	-1,44	-1,53	immune response
95597_at	M34141	Ptgs1	0,51	1,93	lipid biosynthesis
104647_at	M88242	Ptgs2	0,94	-1,91	prostaglandin biosynthesis
97363_at	M95408	Ptk2	0,43	1,29	blood vessel development

100427_at	U37465	Ptpro	-0,85	-1,95	protein amino acid dephosphorylation
96602_g_at	AW045751	Qscn6	1,36	2,29	---
96603_at	AW123556	Qscn6	1,52	3,43	---
160965_at	AA163960	Rasa4	-1,22	-2,09	intracellular signaling cascade
99032_at	AF009246	Rasd1	0,1	5,16	small GTPase mediated signal transduction
103804_at	AB006960	Reck	0,91	2,64	cell cycle
99028_at	AI788534	Rnf8	0,11	2,18	protein ubiquitination
104177_at	AA204579	Rsad2	0,02	-1,97	---
95544_at	AI843150	Rusc1	0,27	1,6	---
160795_at	AW123662	Scamp1	1,96	1,67	transport
94057_g_at	M21285	Scd1	0,67	1,7	lipid biosynthesis
161132_at	AA727482	Scel	2,29	1,56	---
94181_at	AJ223206	Scrg1	0,16	3	---
160373_i_at	AI839175	Sdpr	1,37	3,05	---
104692_at	M72332	Selp	0,19	1,52	inflammatory response
102860_at	M64085	Serpina3g	-2,05	-1,74	apoptosis
92978_s_at	X16490	Serpinb2	2,68	0,71	---
94147_at	M33960	Serpine1	-1,65	4,12	regulation of angiogenesis
97487_at	X70296	Serpine2	1,55	4,37	development
161935_r_at	AV329249	Sh3bgr	0,75	1,77	---
99876_at	U29056	Sla	1,97	0,67	intracellular signaling cascade
102947_at	AJ006036	Slc22a2	1,84	-0,1	ion transport
97957_at	AF072759	Slc27a4	0,52	1,84	metabolism
92292_at	M75135	Slc2a3	2,23	0,83	transport
93471_at	AI594427	Slc4a7	-0,25	-1,5	anion transport
101713_at	AB022345	Slc7a11	2,15	0,15	transport
103830_at	M95604	Snai1	1,87	3,71	development
92832_at	U88325	Socs1	-2,06	-0,78	immune response
97160_at	X04017	Sparc	0,66	3,65	---
97519_at	X13986	Spp1	2,6	0,21	cell adhesion
103680_at	AA683850	Srpr	-0,35	-1,63	protein targeting
104249_g_at	AW227650	Ssr3	2,07	-0,49	cotranslational protein-membrane targeting
98596_s_at	Y15003	St3gal5	-2,79	2,87	protein amino acid glycosylation
101465_at	U06924	Stat1	-0,71	-1,92	transcription
100426_s_at	U36776	Syk	3,75	-0,33	activation of MAPK activity
103035_at	U60020	Tap1	-1,37	-1,84	immune response
102873_at	U60091	Tap2	-1,69	-0,91	immune response
93367_at	U86137	Tep1	-0,48	-1,56	telomere maintenance
101551_s_at	X78989	Tes	1,79	1,22	---
92427_at	D25540	Tgfbr1	1,79	-0,53	embryonic development
93882_f_at	D50032	Tgoln1, Tgoln2	1,57	-0,62	---
102906_at	L38444	Tgtp	-2,91	-5,96	---
160469_at	M62470	Thbs1	3,43	1,49	cell adhesion
160613_at	AW049768	Tinagl	0,58	1,81	proteolysis and peptidolysis
96748_i_at	AA619554	Tmem30b	2,23	-0,01	---
160817_at	AA727424	Tmem40	-0,09	1,82	---
99392_at	U19463	Tnfaip3	1,63	-0,73	apoptosis
92962_at	M83312	Tnfrsf5	-1,28	-1,68	apoptosis
161361_s_at	AV213431	Tnnt1	0,38	4,59	muscle development
161385_r_at	AV250738	Tph1	3,29	0,99	serotonin biosynthesis
160376_at	AW125508	Trp53inp2	0,34	2,42	---
160085_at	U35741	Tst	1,19	1,57	sulfate transport

92715_at	AL078630	Ubd	-2,96	-0,97	protein modification
94367_at	AI850362	Uck2	2,29	0,38	carbohydrate metabolism
95024_at	AW047653	Usp18	-0,3	-2	ubiquitin-dependent protein catabolism
93463_at	AW122517	Usp19	2,27	-0,37	ubiquitin-dependent protein catabolism
97960_at	AW125800	Usp22	1,57	0,58	---
94964_at	L18880	Vcl	1,63	0,13	cell adhesion
104181_at	AJ132103	Vnn3	-0,52	-1,6	nitrogen compound metabolism
161337_f_at	AV121930	Wars	-1,47	-1,51	protein biosynthesis
98605_at	AI851163	Wars	-1,83	-1,36	protein biosynthesis
98606_s_at	X69656	Wars	-1,48	-1,77	protein biosynthesis
160583_at	AA880988	Xlkd1	2,16	2,82	cell adhesion
101883_s_at	L22977	Xlr3a, Xlr3b	0,1	-1,5	---
102259_at	AF058799	Ywhag	2,52	-0,11	signal transduction

8 Acknowledgments

Part of my research work was performed at the Institute for Medical Microbiology of the University of Tuebingen (Germany), under the supervision of the Prof. Ingo B. Autenrieth and of the Dr. Erwin Bohn. My research project was supported by grants from the by the Marie Curie Association (European Union)and from the DAAD-Deutscher Akademischer Austauschdienst (Germany).

I thank Prof. Norma Staiano, Dr. Michele Trotta and Christian Eberharth for critical readings of the manuscript.

I am grateful to the Prof. Alessandro Fioretti and to the Prof. Francesca Menna, for the opportunity to begin this trilling adventure in the world of the research.